THE PROCESS OF SEASONAL AND VERTICAL DYNAMICS OF NUTRIENT CYCLE IN LAKE BIWA

March, 2021

LE TIEN HUU

Graduate School of Environmental and Life Science

(Doctor's Course)

OKAYAMA UNIVERSITY

ABSTRACT

Lake Biwa is the largest lake in Japan ranked 130th among the world's freshwater lakes. The lake is separated into two parts, the northern main and deeper basin and the southern small and shallower one. There are many rivers of various sizes flowing into the lake. However, only one outflow from the lake (the Seta River), apart from canals constructed during early modern times. The difference in the physical structure and nutrient status between the two basins have given rise to a valuable diversity of biological and chemical ecosystem in the lake. In the North basin, with the deep averaging 44 m, thermal stratification occurs from spring to autumn, typically monomictic with the turnover period between February and March, creating a specific ecosystem and biogeochemical processes.

Currently, Lake Biwa has undergone progressive eutrophication in the past few decades. It is facing the issues of toxic algal blooms and may be affected by eutrophication and global warming. Nutrients hold key roles in the water quality of lakes while Chlorophyll-a (Chl-a), on the other hand, is well-known as an indicator of phytoplankton biomass. Increasing nutrient loading to the aquatic eco-system results in an enhanced primary production that leads to undesirable changes in aquatic resources. Moreover, physical, chemical, and biological processes and water quality formation processes are closely affected by water currents. There are mainly currents caused by great gyres and periodic currents caused by internal waves in the lake. However, the effect of both biological and physical factors on the fluctuation of nutrients and Chl-a. Therefore, the overarching objective of this thesis was to improve understanding of the seasonal and vertical dynamic of nutrient cycle and phytoplankton change under the effect of biological and physical processes in Lake Biwa.

In the first study, the external loading process to Lake Biwa was described using a hydrological tank model and a loading-discharge curve. The model was applied to collective drainage basins of the lake's Imazu (northwest), Hikone (northeast), and Otsu (south) areas. The hourly model was conducted using particular discharges from the Kita (Ado) river, Takatoki (Ane) river, and the trunk of Yasu River to obtain loading curves for phosphate (PO_4) and silica (SiO_2) by assimilating the collected concentrations (2002-2003). The model was updated by adding an evapotranspiration routine and direct paths to lacustrine groundwater discharges of the lake floor.

The daily model was calibrated through an analysis of water budget among the basin, inflow, lake, and outflow (1991-1995), then validated. The daily tank model was established and combined into a loading-discharge curve to determine the long-term external nutrient loads entering the lake. However, the relationship between nutrient loading and nutrient concentration offshore station was still unclear and the role of seasonal fluctuation of loading on the lake nutrient was questioned.

The second study describes nutrient patterns using biochemical and physical measurements in Lake Biwa. Seasonal variation in profiles of water temperature, pH, silicate, total nitrogen, total phosphorus, dissolved oxygen, and Chl-a was compiled and analyzed. By using the flux profiles which were the monthly averaged flux profiles from 1980 to 2015 consisting of five successive periods of averaged for seven years each, temporal evolution could be elucidated, including decomposition in winter, blooming in spring, sustaining in summer, and settling in autumn. The downward flux value showed the sedimentation rate of biomass. It was inferred that nutrients and Chl-a fluxes in the North basin were influenced by the gyre in summer and internal seiches in autumn. On the other hand, the relationship of external loading and lake water quality showed that the flows affected the distribution of phosphorus and silicate concentrations in the epilimnion and metalimnion while strong sedimentation was observed in the hypolimnion. It is suggested that phytoplankton composition and reed biomass has been related to the fluctuation of nutrient supply from rivers surrounding Lake Biwa.

The final study focuses to analyze the physical transport including the gyres-internal wave effect on the distribution of Chl-a and nutrients. Water temperature profiles were recorded at stations, 17B-North and 12B-South in the north basin of Lake Biwa. Buoyancy fluxes at the stations were of opposite phases, and amplitude was higher at the South for which representative area is narrower than the North. The summer lake became stably stratified, and the internal seiches period was shortest at 46 hours in July to August before increasing to 54 hours in September, and 66 hours in October as the literature suggested. The stability at 17B is due to the first gyre, established in July to suppress internal seiches, while the third gyre at 12B was advective, causing vertical mixing. On the other hand, the surface data of Chl-a and nutrients in several inshore (A and C) and offshore stations (B) surrounding the Lake were compared. It found that phytoplankton was transported from inshore to offshore, south to north. The Chl-a was kept within the epilimnion by the gyre activity in summer. Then convective Chl-a fluxes downward were seen in the

thermocline in September to October when the stirring efficiency of water was highest in the deep lake with basin-scale internal waves, and destratification of the monomictic lake was shown with a frequency modulation due to a reduction in internal celerity.

Finally, we infer that the nutrient cycle and phytoplankton dynamics in Lake Biwa are complicated which be affected by not only internal processes (thermal mixing, gyres, internal waves, resuspension nutrient supply) but also long-term external process (nutrient loads and accumulation). From our results, we suggest the BSMS (Blooming – Sustaining (Gyre) – Mixing (Internal waves) – Sedimentation) processes with the concept as blooming in spring, sustaining in summer, mixing in autumn, and sedimentation in winter. This concept could partly explain the seasonal and vertical change of nutrient transport and biochemical succession in Lake Biwa.

LIST OF FIGURES

LIST OF TABLES

TABLE OF CONTENT

CHAPTER 1. GENERAL INTRODUCTION

1.1 Eutrophication status and nutrient loading in Lake Biwa

Lake Biwa is the largest lake in Japan ranked 130th among the world's freshwater lakes. The lake is separated into two parts, the northern main and deeper basin and the southern small and shallower one. In terms of age, the lake is the world's third oldest, with a history of some four million years. There are many rivers of various sizes flowing into the lake, however, only one outflow from the lake (the Seta River), apart from canals constructed during early modern times. The difference in the physical structure and nutrient status between the two basins have given rise to a valuable diversity of biological and chemical ecosystem in the lake. In the North basin, with the deep averaging 44 m, thermal stratification occurs from spring to autumn, typically monomictic with the turnover period between February and March, creating a specific ecosystem and biogeochemical processes. While the South Basin is warm polymictic due to the shallowness (Tezuka, 1992). In the North Basin, regarding the current trophic status, TN and TP assessed by Sakamoto (2011) the grade is mesotrophic in terms of TN but oligotrophic in terms of TP.

The catchment area of Lake Biwa reaches 3,174 km^2, the majority belonging to Shiga Prefecture, the remainder to Kyoto Prefecture. Land use in the catchment has been changing, driven by increasing population, ongoing urbanization, and changing industrial structures. Today, forests comprise about half the total land area of Shiga Prefecture; farmlands, mainly comprising paddy fields, comprise less than one-seventh of the total land area. Forests and farmlands help conserve the lake's environment, since they recharge groundwater, prevent sand/soil erosion, and retain/purify water. The area of forests and farmlands, however, is decreasing in Shiga Prefecture even more rapidly than the national average. In coming years, more forests and farmlands are predicted to be converted, though slowly, into roads and housing zones.

Currently, Lake Biwa has undergone progressive eutrophication in the past few decades. It is facing the issues of toxic algal blooms and may be affected by eutrophication and global warming. Because of rapid urbanization and industrialization in the Lake Biwa watershed, the lake water quality began deteriorating during the 1960s and 1970s, thus, eutrophication accelerated rapidly in this time (Hsieh et al. 2010; Tsugeki et al. 2010). Along with urbanization, Lake Biwa

has experienced increasingly nutrient loading since the 1960s and subsequently suffered from blooms of *Urolena Americana* since 1977 and cyanobacteria since 1983 (Kumagai, 2008). It was caused by external loading and then internal loading of nutrients from the catchment and aquatic ecosystem. Nutrients as phosphorus (P) and Silicon (Si), in particular, hold key roles in the water quality of lakes (Goto et al., 2007; Kowalczewska-Madura et al., 2018). It is a strong requirement for primary production through elucidating phytoplankton biomass - nutrients relationship in lakes (Filstrup and Downing 2017; Kuczyńska-Kippen N. 2010; Sondergaard M., 2001). Increasing nutrient loading to aquatic eco-system results in enhanced primary production leads to undesirable changes in aquatic resources such as degraded water quality, hypoxia, harmful algal bloom, losing biodiversity, and affected food web structure.

Nutrient concentration in rivers is particularly important to river ecology, and riverine transport of nutrients is also relevant to any receiving water body: lake, wetland, lagoon, and estuary. To measure nutrient inputs to a lake is necessary to relate the trophic status of the lake to its drainage basin. Previous projects have been carried out mainly to improve water quality or survey eutrophication status in Lake Biwa (Maeda 1992; Ishikawa et al. 2002; Kishimoto et al. 2013; Ichise et al. 2013). However, there are only a few studies on nutrient loading from rivers into Lake Biwa. (Kunimatsu and Kitamura, 1981) surveyed water quality of several rivers into Lake Biwa while Morii et al. (1993) discussed the relationship between the water quality of rivers flowing into the lake and the geological environment of the river heads. Based on water quality data at 75 points in the lake, Nagare et al. (2001) implemented 3 dimension surveys to estimated nutrient mass from 1995 to 2000. It was reported that nutrient discharges into Lake Biwa by rivers flowing into the eastern area of the lake were larger than those in the western area of the lake because of the high density of population in the urbanized area and many agricultural fields (Taniguchi and Tase, 1999). However, in most cases, water quality assessments are done based on short-term observations at limited environmental sampling points, which can't quantitatively assess the amount of the long-term external loads nor describe mechanisms of spatial-temporal water quality changes under comprehensive functions of hydrology, climate, and lake condition. Available data about nutrient levels from river discharge to the lake in the basin are sparse. Furthermore, the relationship and distribution of water quality in lake considered of external loads from its catchment basin have not been clarified enough so far and the effect of river loading on nutrient concentration in the water column are not identifed.

Eutrophication of most lakes is linked to the rate at which nutrients are added to the system. Nutrient loading is a generic term for which the definition varies depending on the context in which it is used. In a broad sense, loading is the rate of supply of a particular entity to receiving waters; it is expressed frequently as a rate (e.g., tons N y^{-1}). Ecosystem responses depend on several critical physical-chemical characteristics and processes. Estuary size (surface area), depth, volume, flushing rate, water residence time, tidal exchange, vertical mixing, and stratification are all factors that affect the transport, transformation, retention, and export of nutrients.

Although there are many methods for calculating loading, the simplest approach is to multiply the nutrient concentration (gN m^{-3}) by the river discharge rate (m^3s^{-1}), groundwater flow rate (m^3 s^{-1}), or rainfall amounts (cm m^{-2}). The accuracy of loading rate estimations is therefore related to the accuracy of measurements of two variables: flow rate and entity concentration. Nutrient loading rates, calculated on an annual basis, can be highly variable from year to year. The frequency of the measurements becomes especially important during episodic events that add large volumes of water to the system (rainstorms, hurricanes). During these events, nutrient and organic matter loading over just a few days can exceed the total loading for an entire year. Although concentrations of organic matter or nutrients may be low because of dilution by large volumes of water, the actual loading rates may be very high because of the total volume of water flowing into the estuary. Unfortunately, during extreme weather events, remote instrumentation (for measuring discharge rates) is frequently damaged and field collections of water samples for chemical analyses are postponed because of personnel safety concerns. Therefore, some of the largest loading events are frequently missed, or approximated with low accuracy, during such periods.

1.2 Tank model and loading curve

Mathematical modeling approaches could be used to describe the flow dynamics and solute transport. However, the hydrological model in most applications has been used in numerous projects. The tank model is an accounting model that tracks the flows of water into and out of the particular hydrologic system. Besides, a tank model has demonstrated satisfactory performance in depicting characteristics and vertical and horizontal water movement for the watershed, sub-watershed, and wet rice fields (Setiawan et al. 2003). With the practice of a tank model, vertical

and horizontal water distribution can be easily and simply demonstrated and could be modeled, hence it can exhibit flow distribution at a certain time for each layer of the watershed area (Arifjaya et al., 2012). In other words, several studies on the reliability of mass load estimates demonstrate that no individual estimation method is advantageous and superior while poor accuracy can be obtained using individual estimation method on a specific stream or river for a year or period (Kronvang and Bruhn, 1996). However, the tank model is an appreciation to use for long-term runoff and water table analysis. The advantage is the time series of streamflow behavior and solution can be determined by fitting the model parameter in applying this hydrological model. Other methods also have been often used for example GIS, the soil and water assessment tool (SWAT), but requires a huge amount of spatial information and is composed of complicated processes.

A simple L-Q curve is more popularly used for the estimation of nutrient transport (Alexander et al., 2002; Amano & Kazama, 2012; Clarke, 1990; Galat, 1990). Adaptability or accuracy of the loading curve is a remarkable topic (Phuong et al., 2018). The loading curve between nutrient load L and discharge Q simply provides a correlation as Q=LC although the loading curve sometimes has a bias (Ferguson, 1986). Numerous attempts have been made by researchers to demonstrate the relationship between L and Q through field observations in various basins. Amano and Kazama (2012) developed the loading curve to analyze the monthly data of discharge, ammonium, total phosphorus, and potassium in the lower Mekong River, Vietnam. Meanwhile, Hartmann et al. (2010) demonstrated the DSi-flux predicting model by using first-order controlling factors for the 516 Japanese catchments based on the chemical data collected. The data were also compiled by Harashima et al. (2006) to verify the silica deficiency hypothesis in a lake-river-bay system, and the upstream process in the lake was detected by collecting water samples to compare with the present situation of phosphate and silica concentrations flowing rivers into Lake Biwa, which would be discussed later in the present study. Lacustrine groundwater discharge (LGD) is one of the important pathways of nutrients from catchments to a lake. Onodera et al. (2018) described LGD and nutrient flux into Lake Biwa not only in beach sides with shallower depth but in deeper zones to indicate spatial and seasonal variations of LGD and to compare with the results of seepage observations.

1.3 Gyres and internal waves in Lake Biwa

Physical, chemical, and biological processes and water quality formation processes are closely affected by water currents. There are mainly currents caused by great gyres and periodic currents caused by internal waves in the lake. During the stratified period, Lake Biwa supports many basin-scale internal wave modes, as well as the Rossby wave modes which have very long periods, and effectively represent quasi-geostrophic flows such as strong and persistent gyres. It is well known that three Gyres namely First (counterclockwise), Second (clockwise), and Third (counterclockwise) occurred in the surface area of Lake Biwa during the stratification period from 1926. Endoh and Okumura (1993) propose a new gyre system in Lake Biwa during summer with the mean surface circulation was found to consist of two large gyres, one counterclockwise and the other clockwise. The gyre is continuously present from May to December each year. The gyres induce circular currents above thermocline with a typical velocity of 0.1 m s^{-1}. Its disappearance in winter implies that its existence depends on stratification (Toda, 2013). On the first gyre of the same basin, the anti-clockwise circular current appears between Funaki and Hikone, which is mostly noticed in the stratified seasons by the field, analytical, numerical, and laboratory studies (Okamoto & Morikawa 1961; Oonishi 1976; Okumura & Endoh 1985; Endoh 1986; Kumagai et al. 1998; Ookubo et al, 1984). Okamoto & Morikawa (1961) conducted to record temperature profiles along the survey lines to estimate geostrophic currents, showed that the first gyre in Lake Biwa is almost in geostrophic balance. Oonishi (1976) demonstrated that the gyre could be induced by surface heat flux within three months while the gyres can be induced by both winds. Later, Ookubo et al. (1984) conducted laboratory experiments of the gyres on a rotating turntable considering the similarity for both Rossby and vertical Ekman numbers. Okumura and Endoh (1985) compiled the existing current measurements at several stations to show the current roses. Endoh (1986) also revealed eddy viscous effects on the convective circulation by using measured temperature profiles on a computational grid. Kumagai et al. (1998) succeeded to show the current structure and gyre pattern by using an acoustic Doppler current profiler. Ishikawa et al. (2002) first described the ecological relationship with the flow field of the gyre. Akitomo et al. (2004) showed the annual process and mechanisms of the gyre under the annual heat flux.

After the inclination of the thermocline of the North Basin of Lake Biwa by strong winds, oscillations in the thermocline occurs as it attempts to return to its original horizontal position.

These oscillations are called internal waves. The rotating internal seiche is known as the internal Kelvin wave corresponding to the longitudinal, uni-nodal internal seiche in the non-rotating system. Gyres and seiches are two prominent features of lakes. Gyres largely transport sediments, nutrients, and algae in the horizontal direction. Seiches, on the other hand, can contribute to the vertical mixing in lakes. Shimizu et al. (2007) implied the importance of internal waves as energy sources for mixing and gyres for long-term horizontal transport. However, the role of Gyre and internal seiches to phytoplankton activities and nutrient dynamics is still unknown and become an interesting topic for recent studies. The distributions of dissolved or suspended materials in water, as well as sedimentation processes, was studied, for example, a high concentration of Chlorophyll a was observed near the center of the First Gyre (Saijo and Kamoto, 1970) and found very fine bottom sediment in this area (Kamitani, 1988) and the horizontal convergence of surface water associated with the gyre (Endoh, 1986). Gyre should play an important role in the transportation and selection of suspended materials. The current speed of the gyres is critical for problems arising from the transportation of materials related to water pollution.

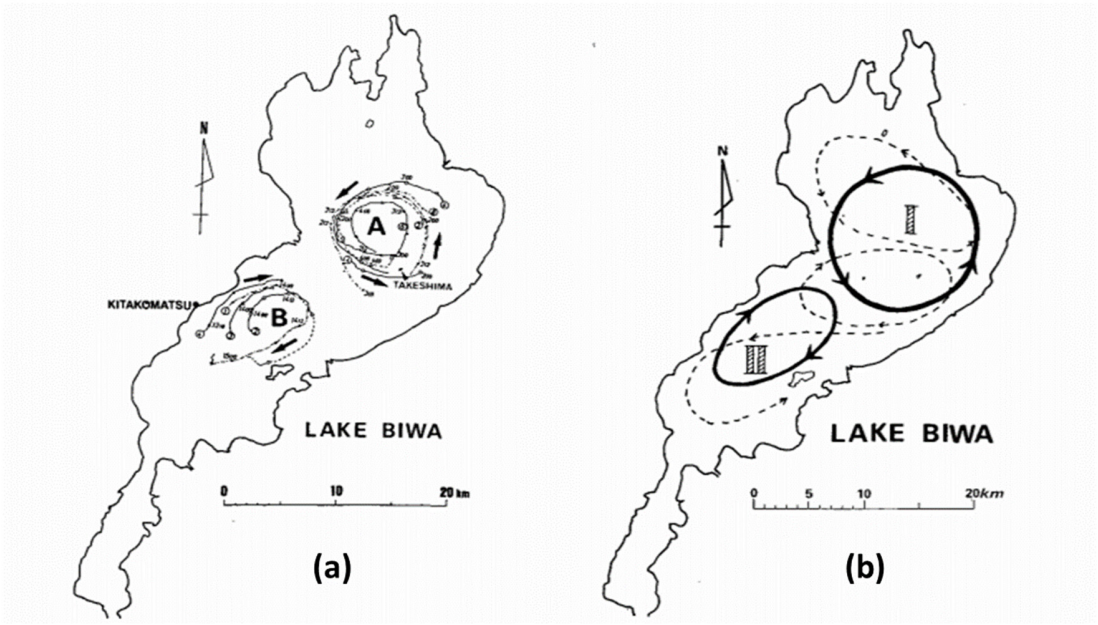

Figure 1.1 Gyre system in Lake Biwa was exhibited (a) radar tracking by Endoh and Okumura (1993) and (b) broken line by Suda et al. (1926), solid line by Endoh and Okumura (1993)

1.4 Aims of the thesis

The overarching objective of this thesis was to improve understanding of the seasonal and vertical dynamic of nutrient cycle and phytoplankton change under the effect of biological and physical processes in Lake Biwa. With that overarching goal, the study was conducted to estimate the external nutrient loading from the river and groundwater system surrounding the Lake (i), analyze the nutrient flux to assess the seasonal time lag fluctuation, calculate the vertical and seasonal mass in the water column (ii), calculate the water currents and horizontal, vertical transport to evaluate the distribution of phytoplankton and nutrient by Gyres and internal wave (iii). To archive those objectives, the following steps were conducted:

The first study combined the L-Q equation and tank model to estimate external nutrient loading into Lake Biwa. It would be focused to discuss the applicability of the loading curve through the relationship between river discharge and nutrient loads, calculate long-term discharge and change of nutrient fluxes from river and groundwater system into the lake. (Chapter 2).

The second study concentrated on seasonal and annual changes of nutrients and chlorophyll-a in Lake Biwa over 35 years period, to compile and analyze historical water quality data collected by the prefecture. On the other hand, it will focus on monthly vertical flux profiles based on the time change in nitrogen, phosphorus, and chlorophyll-a, clarify the supply and removing dynamics in the lake with the production rate of through nitrification and gross metabolic rate of through assimilation and denitrification (nitrogen) or uptake, recycle and sedimentation (phosphorus) (Chapter 3)

The last study was aimed to obtain records of successive temperature profiles at stations of opposite phases for the internal Kelvin wave, and relationship to thermally- or wind-induced gyres and difference from the topographic Rossby wave. The internal seiching in autumn was of finite amplitude and both the evidence from Gyres and the internal seiches were obtained in the summer. Seasonal surface water quality data including temperature, nutrient, and Chl-a concentration were compared to show the result of horizontal transport from inshore to offshore stations under the effect of Gyres and internal waves (Chapter 4)

Chapter 5 was discussed the relationship of previous chapters. It analyzes lasting eutrophication by nutrient through the relationship between external nutrient concentration and in-

lake nutrient concentration (chapters 2 and 3). Discussing the effects of current (Gyres) and the mixing process to vertical and horizontal Chl-a change (chapters 3 and 4). It also showed general conclusions and suggestions for further studies. We also would like to suggest a new concept to explain fully the seasonal and vertical nutrient and phytoplankton dynamics in the water body.

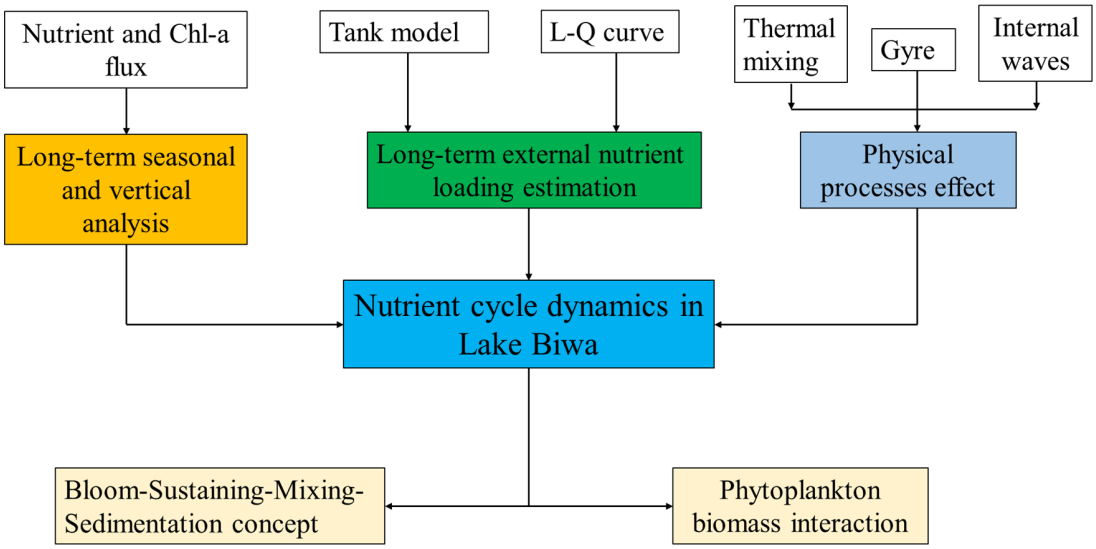

Figure 1.2 The schematic - overview of the dissertation composition

CHAPTER 2. EVALUATION OF THE EXTERNAL NUTRIENT LOADING FROM WATERSHEDS INTO LAKE BIWA BY THE COMBINATION OF RAINFALL-RUNOFF MODEL AND LOADING CURVE APPROACH

2.1 Introduction

Lake Biwa is the largest lake in Japan, providing water resources to more than 14 million people in Western Japan (Kumagai, 2008). It is a body of water known worldwide for its massive sink of silica (Goto et al., 2007) and has been classified as one of the phosphorus-limited lakes (Tezuka, 1986). Also, the level of silica (Si) sink is related to a load of phosphorus (P) from the watershed of Lake Biwa (Goto et al., 2007). External supply rate is one of the biogeochemical processes effect on nutrient limitation of primary production (Howarth, 1988), and this may lead to an expansion in the silica sink and phosphorus retention causing a subsequent alteration of the aquatic ecosystem. Therefore, an evaluation of the external nutrient loading to the lake is important to understand the eutrophication condition in the lake and the impact on algal biomass and phytoplankton community composition (Ding et al., 2019; Longley et al., 2019). Previous work has reviewed the role of external loading to water quality or eutrophication status in Lake Biwa (Hsieh et al., 2011), as well as analyzed the water quality of several rivers that exit into Lake Biwa (Kunimatsu and Kitamura, 1981; Taniguchi and Tase, 1999); and discussed the relationship between the inflow river water quality and geological environment of the river heads (Morii et al., 1993). However, the available data of nutrient levels, including phosphorus and silica from river discharge and groundwater discharge into Lake Biwa are sparse and still lack a quantitative assessment that reveals the long-term external loads. Furthermore, estimating nutrient loading from all rivers surrounding Lake Biwa requires a huge amount of spatial information and complicated processes. Nevertheless, the simultaneous application of these approaches has rarely been mentioned in previous hydrological studies. Therefore, this paper focuses on and A loading curve simply provides the correlation between nutrient load (L) and discharge (Q), which has been popularly used for the estimation of nutrient transport (Galat, 1990; Alexander et al., 2002; Salvia-Castellví et al., 2005; Amano and Kazama, 2012). Tank model commonly used for long-term runoff analysis and can exhibit flow distribution at a certain time for each layer of the watershed

area (Arifjaya et al., 2012). discusses the applicability of a combination method, which includes the rainfall-runoff model and the L-Q curve to evaluate long-term external nutrient fluxes from the surface and groundwater discharge into the lake.

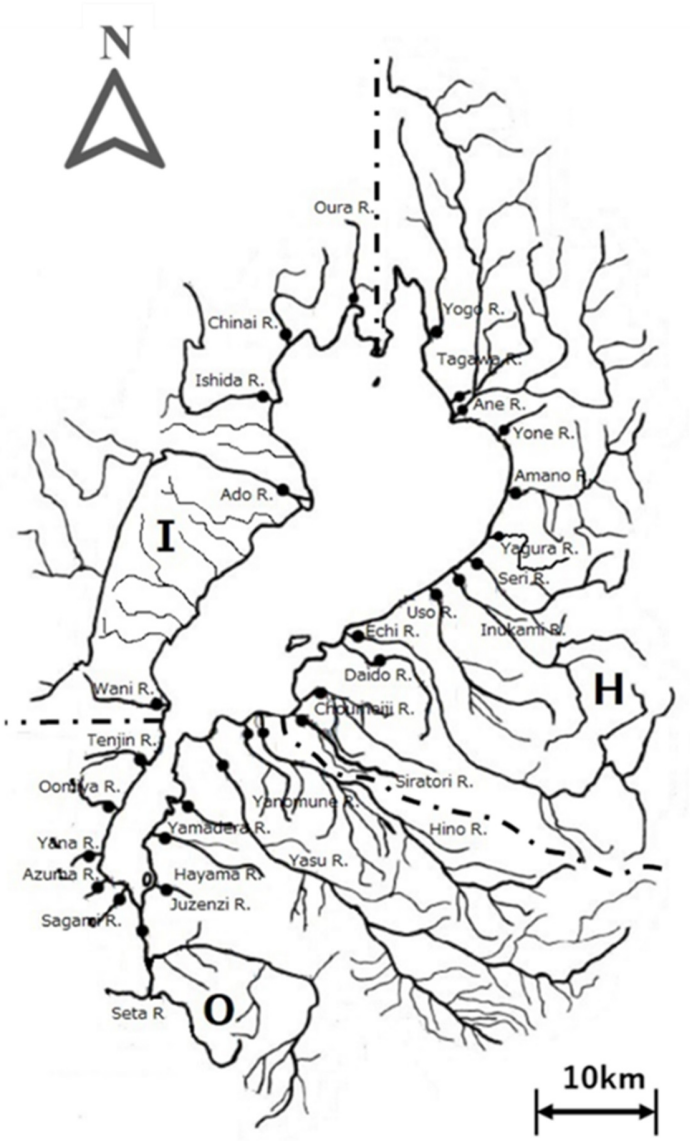

Figure 2.1 The river systems of three catchments in Lake Biwa. (Sampling rivers were divided into three catchments, Imazu (I), Hikone (H) in North Basin, Otsu (O) in South Basin)

2.2 Methods

Lake Biwa consists of a monomictic North Basin (616 km^2, 45.5 m), and a warm polymictic South Basin (58 km^2, 3.5 m) (Tezuka, 1992) that are surrounded by about 115 rivers of various sizes that flow into the lake (see Figure 2.1) but only the Seta River and the Kyoto Canal are outflows from the lake. The collective basin was divided into three parts, namely Otsu, Hikone, and Imazu sub-basin (table 2.1). Discharges increase during snowmelt (March - April), Eastern Asian summer monsoon (June - July), and typhoon season (September, October), respectively.

Table 2.1 Dimensions of the divided sub-basins

Basin	Otsu	Imazu	Hikone	Total
Total Area (km^2)	613	673	1,915	3,201
Sampling area	384	421	1,197	2,002
Sampling/Area	62.6	62.6	62.5	62.5
Rivers (sampling site)	37 (15)	38 (19)	40 (20)	115 (54)

2.2.1 Tank model

Hydrological tank models (Sugawara, 1979) were used to trace the local water cycle in and around Lake Biwa. The model includes four serial storage tanks, which is a simple and efficient method to convert rain into discharge and flux paths for nutrients. Each basin has been given different rainfall and evapotranspiration rates using meteorological data on precipitation and air temperature that were provided by the Ministry of Land, Infrastructure, Transport and Tourism (MLIT, 2020) at Otsu, Imazu, and Hikone, respectively. Because rainfall was considered uniform in each sub-basin, the local rain was given according to the areal fraction to the partial sum of sampling rivers in each sub-basin.

The discharge for the output of each tank is defined as the surface (top tank: $q_{11}+q_{12}$), intermediate (upper-middle tank: q_2), sub-base (lower middle tank: q_3), and base (bottom tank: q_4), as in Figure 2.2. Parameters of the models are presented in Table 2.2, 2.3. The fourth tank was diverted to connect to a certain depth of the lake floor in this study. Evapotranspiration is

incorporated via subtraction from the top tank. The runoff from side outlets of a storage tank (q) is proportional to the water head over the outlet, and infiltration (p) is proportional to the water depth. Water balance and its component can be described as:

$$\triangle \mathrm{Q} = Q_{in} - Q_{out} = dV/dt = S\,dH/dt \quad (1)$$

$$dh_1/dt = \mathrm{P} - \mathrm{E} - q_{11} - q_{12} - p_1 \quad (2)$$

$$q_{11} = \alpha_{11}(h_{11} - z_{11}) \quad (3)$$

$$q_{12} = \alpha_{12}(h_{12} - z_{12});\ p_1 = \beta_1 h_1 \quad (4)$$

$$dh_2/dt = p_1 - q_2 - p_2 \quad (5)$$

$$q_2 = \alpha_2(h_2 - z_2);\ p_2 = \beta_2 h_2 \quad (6)$$

$$dh_3/dt = p_2 - q_3 - p_3 \quad (7)$$

$$q_3 = \alpha_3(h_3 - z_3);\ p_3 = \beta_3 h_3 \quad (8)$$

$$dh_4/dt = p_3 - q_4 \quad (9)$$

$$q_4 = \alpha_4 h_4 \quad (10)$$

$$Q = Q_r + Q_g \quad (11)$$

$$Q_r = \sum_1^3 q_i\, A/\Delta\mathrm{t},\ Q_g = q_4 A/\Delta\mathrm{t} \quad (12)$$

where Q is discharge; Q_r is river discharge; Q_g is ground water discharge [m^3s^{-1}]. V: lake volume [m^3]; A and S: drainage and lake surface areas [km^2]; H: water level of the lake [m]; ΔT: time interval [s/h/d]; p and q: infiltration and discharge ($mm/\Delta T$); P and E: precipitation and evaporation ($mm/\Delta T$); h_i : water depth of the i-th tank; z is the height of outlet above the base of a tank; $\alpha_i\ and\ \beta_i$ are the runoff and infiltration coefficient.

Following Dalton's model (Korzukhin et al., 2011), the evaporation rate has been established as:

$$E = \rho C_E U(e_s - e_a)/p \quad (13)$$

where E is evapotranspiration rate (mmday^{-1}); ρ: air density (kgm^{-3}); C_E : bulk coefficient; U: average wind speed (ms^{-1}); e_s, e_a: saturated and actual water vapor pressure (hPa), p is air pressure (hPa), respectively.

Basic parameters are defined as:

$$r_E = \Sigma E/\Sigma P;\ r_G = \Sigma Q_g/\Sigma Q_r;\ R_L = V_{Lake}/\Sigma Q/86400/365 \quad (14)$$

to check budgets in the fraction of river water, groundwater (r_E, r_G) and residence time of water (R_L) in year.

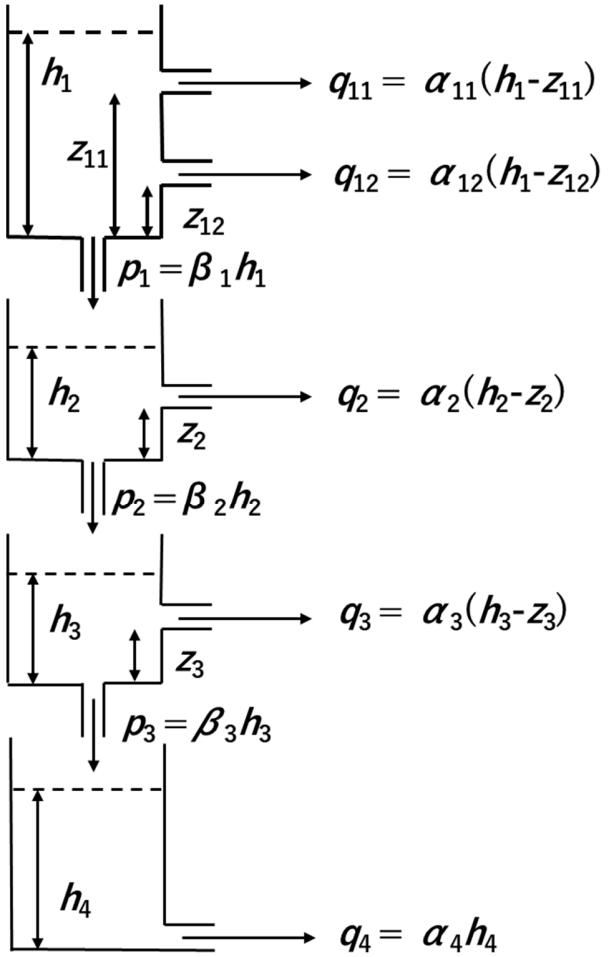

Figure 2.2 Structure of the tank model. The surface discharge (q_{11}+q_{12}), intermediate discharge (q_2), sub-base discharge (q_3), and base discharge (q_4). p is infiltration to the lower reservoir. α and β are the coefficients. h is the water level. z is the out height

Table 2.2 Parameters of the tank model (hourly scale)

Runoff coefficients	**unit**	**Otsu**	**Imazu**	**Hikone**
α_{11}	1/day	0.02	0.02	0.02
α_{12}	-	0.02	0.01	0.02
α_2	-	0.002	0.002	0.001
α_3	-	0.002	0.002	0.0005
α_4	-	0.0002	0.0005	0.0005
Infiltration				
β_1	1/day	0.02	0.02	0.02
β_2	-	0.01	0.001	0.003
β_3	-	0.001	0.001	0.001
out heights				
z_{11}	mm	15	15	15
z_{12}	-	5	1	1
z_2	-	0.005	0.005	0.005
z_3	-	0.005	0.005	0.005
z_4	-	0	0	0

Table 2.3 Parameters of the tank model (daily scale)

Runoff coefficients	**unit**	**Otsu**	**Imazu**	**Hikone**
α_{11}	1/day	0.025	0.029	0.025
α_{12}	-	0.095	0.094	0.093
α_2	-	0.006	0.006	0.006
α_3	-	0.004	0.004	0.004
α_4	-	0.0002	0.0005	0.0003

Infiltration				
β_1	1/day	0.01	0.01	0.01
β_2	-	0.01	0.01	0.01
β_3	-	0.001	0.001	0.001
out heights				
z_{11}	mm	2	2	2
z_{12}	-	1	1	1
z_2	-	1	1	1
z_3	-	1	1	1
z_4	-	0	0	0

2.2.2 L-Q curve

In this study, we built the L-Q curve based on hourly consistent data of nutrients and discharge. The relationship among instantaneous nutrient load L (gs^{-1}), weight concentration C (gm^{-3}), and instantaneous discharge Q (m^3s^{-1}) following the suggestion of Amano et al. (2012) as:

$$C = k\hat{Q}^m \tag{15}$$

Multiplying discharge with the above, the nutrient load is

$$L_n = k\hat{Q}^{m+1} = \mathrm{k}\hat{Q}^p \tag{16}$$

where k, m, and p are the parameters for normalized discharge

$$\hat{Q} = (Q_r + \gamma Q_g)/Q_1, \tag{17}$$

Equation (17) represents the dimensional intercept of the regime curve at Q=Q_1, the unit discharge where Q_1 is taken 1 m^3s^{-1} so dimensionless discharge keeps value as dimensional one. In equation (16), the exponent p is close to unity and it is possible to separate the loading by groundwater discharge as:

$$L_g = k\gamma Q_g \tag{18}$$

The actual path of the lacustrine groundwater discharge might be different. The gamma (γ) is used to express extra loads due to the groundwater discharge at the floor in the lake. There are particular cases:

$\gamma = 0$: No extra loading other than rivers

$\gamma = 1$: No difference in concentration with river water

$\gamma > 1$: The higher concentration in groundwater

Tsurumaki and Kobayashi (1989) reported that PO_4-P in groundwater at the three sites in Lake Biwa was more than 0.1 mgL^{-1}. In this study, we assumed that $\gamma = 3$ for the PO_4-P estimation and $\gamma = 1$ for the SiO_2 estimation.

Only 54 among the 115 rivers were selected as sampling sites during the 2002-2003 field trips (Table 2.1). A partial drainage area of sampled rivers in sub-basins was summed up to 2,002 km^2, which were around 63% of the total drainage area of 3,601 km^2. PO_4 and SiO_2 were determined using a colorimeter for the three sub-basins bimonthly: July (preliminary), September, and November of 2002; January, March, May, and July of 2003 during the project of the Ministry of Environment (Harashima et al., 2006). Discharge corresponding with sampling time in the rivers was calculated as $Q_i = (A_i/A_N)Q_N$ using an hourly scale tank model where Q_i, A_i, A_N and Q_N are calculated discharge, sampling area, sub-basin area, and initial discharge, respectively. Instead of 155 basin-wise models given individual river discharges, we considered a virtual river of the sub-basin that was calculated for the partial discharge of the individual sampling river where the nutrient concentration sample was taken.

The tank model (daily) was set up to evaluate long-term inflow discharge (1980-2017) and time change in water level. The difference between outflow or runoff in Equation (1) from the North Basin to the South Basin and runoff of Otsu sub-basin can be compared to the measured water level of the lake to determine water balance and the reliable capability of the model. Measured water level data were collected from 1991 to 2015 at Mihogasaki station (South part). Observed outflow discharge at Toriigawa was only obtained from 1991 to 1995.

2.2.3 Evaluation criteria

Statistical parameters were applied to measure the model performance: Nash–Sutcliffe efficiency coefficient (NSE), the percentage of bias (PBIAS), and the root mean square error or observations standard deviation ratio (RSR), according to (Gupta et al., 2009; Moriasi et al., 2007). The equations were set as follows:

$$NSE = 1 - \frac{\sum(Q_{obs} - Q_{cal})^2}{\sum(Q_{obs} - \bar{Q}_{obs})^2} \quad (19)$$

$$RSR = \frac{\sqrt{\sum_1^n (Q_{obs} - Q_{cal})^2}}{\sqrt{\sum_1^n (Q_{obs} - \bar{Q}_{obs})^2}} \quad (20)$$

$$PBIAS = \frac{\sum_1^n (Q_{obs} - Q_{cal})}{\sum_1^n Q_{obs}} \text{ x } 100 \quad (21)$$

where Q_{obs} is the observed daily discharge, Q_{cal} is the calculated daily discharge, $\bar{Q}_{obs}$ is the mean observed daily discharge and n is the total number of observation.

2.3 Results and Discussion

The hourly model calculation was established using hourly streamflow data across 2 years, 2002 and 2003, and is presented in Figure 2.3. The calibration period is from July 11st of 2002 until December 31st of 2002 and the validation period is from January 1st until July 31st of 2003. Due to the limited availability of discharge data in the catchment surrounding Lake Biwa, the observation data obtained from MLIT are from the Yasu river for the Otsu sub-basin, Kita river of the Ado river for the Imazu sub-basin, and Takatoki river of the Ane river for the Hikone sub-basin. The precipitations at Otsu, Imazu, and Hikone were used in the model by the standard precipitation R and is expected as the average of the local precipitation r_i and $\Sigma(r_i/r_{mi}) = R/R_m$. Statistical analysis revealed the acceptability performance of the tank model during the calibration period at the Otsu station (NSE = 0.7, RSR = 0.29, PBIAS = 9.7%), Imazu station (NSE = 0.98, RSR = 0.01, PBIAS = 14.9%) and Hikone station (NSE = 0.9, RSR = 0.09, PBIAS = 13%). The NSE, RSR, and PBIAS values during the validation period for the North basin at Imazu station were 0.98, 0.01, and 9.4%, respectively. The corresponding values for Hikone were 0.91, 0.08, and -5.0%, respectively. Meanwhile, the validation values at Otsu were 0.78, 0.22, and -3.6%, respectively. Normally, early peaks of floods were seen only in the calculated hydrograph.

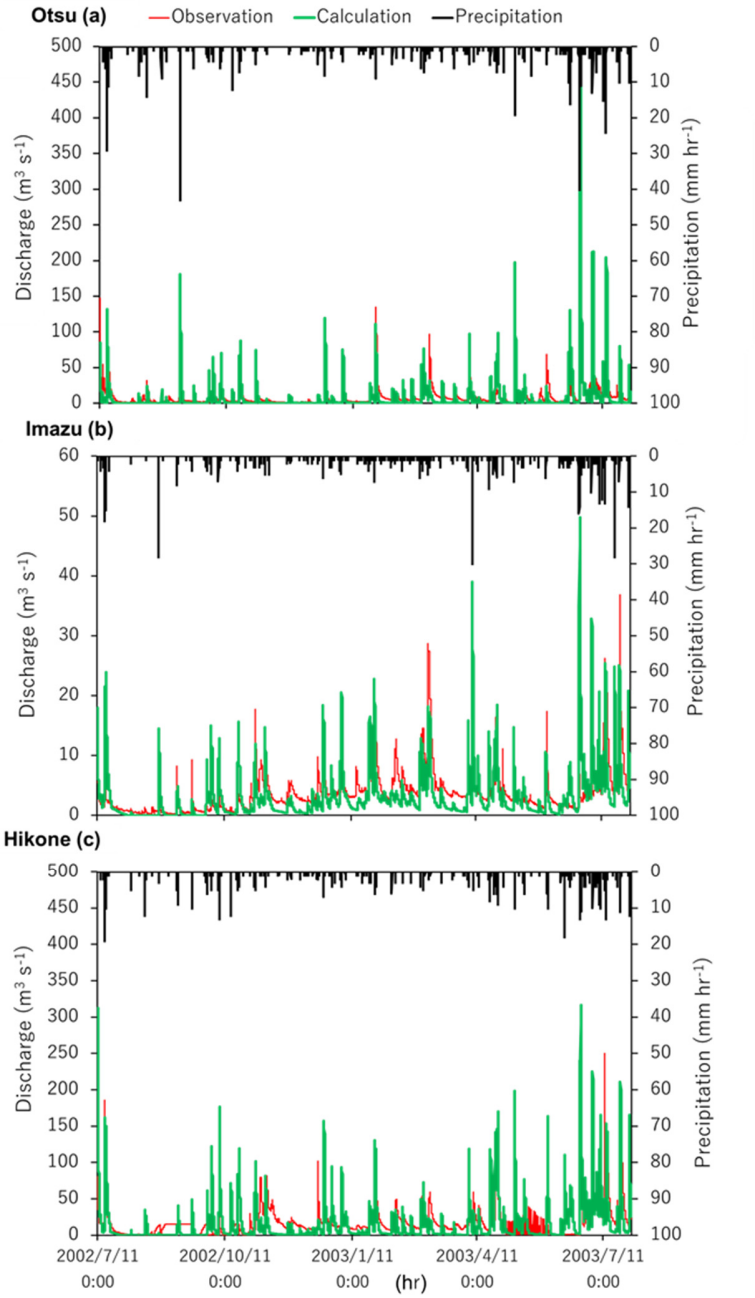

Figure 2.3 The hourly tank model application as a hydrograph for each catchment:(a) Otsu, (b) Imazu, (c) Hikone from July of 2002 until July of 2003

The second approach was applied in estimating the discharge from 2002 to 2003 using an hourly model to investigate the L-Q curve. The concentration of P and Si were plotted against instantaneous discharge. The external loading to Lake Biwa was assessed using the L-Q curve equation in Figure 3.4, which exemplifies a basic component of phosphorus and silica that was

identified in the three rivers' systems around Lake Biwa. The relationship between the hourly river discharge and nutrient loading is shown. From this regression, the mean L was calculated from the mean Q. Furthermore, the result showed that the incline of the SiO_2 line is greater than that of PO_4. These results reveal the equation for calculating the loading base on discharge as:

Otsu sub-basin:

$$L_1 = 0.08Q_1^{0.9893} \quad R^2 = 0.95 \tag{22}$$

$$L_2 = 11.7Q_1^{0.9602} \quad R^2 = 0.98 \tag{23}$$

Imazu sub-basin:

$$L_1 = 0.05Q_2^{0.9766} \quad R^2 = 0.97 \tag{24}$$

$$L_2 = 10.7Q_2^{0.9693} \quad R^2 = 0.99 \tag{25}$$

Hikone sub-basin:

$$L_1 = 0.07Q_3^{0.9854} \quad R^2 = 0.98 \tag{26}$$

$$L_2 = 10.4Q_3^{0.9818} \quad R^2 = 0.99 \tag{27}$$

Total three sub-basins:

$$L_1 = 0.07Q^{0.9825} \quad R^2 = 0.97 \tag{28}$$

$$L_2 = 10.7Q^{0.9701} \quad R^2 = 0.99 \tag{29}$$

Where L_1 is PO_4 load, L_2 is SiO_2 load, and Q, Q_1, Q_2, Q_3 are the total discharge, partial discharges at Otsu, Imazu, and Hikone, respectively. SiO_2 and PO_4 loads increased with an increasing river flow as a power function of SiO_2 loads in the North Basin.

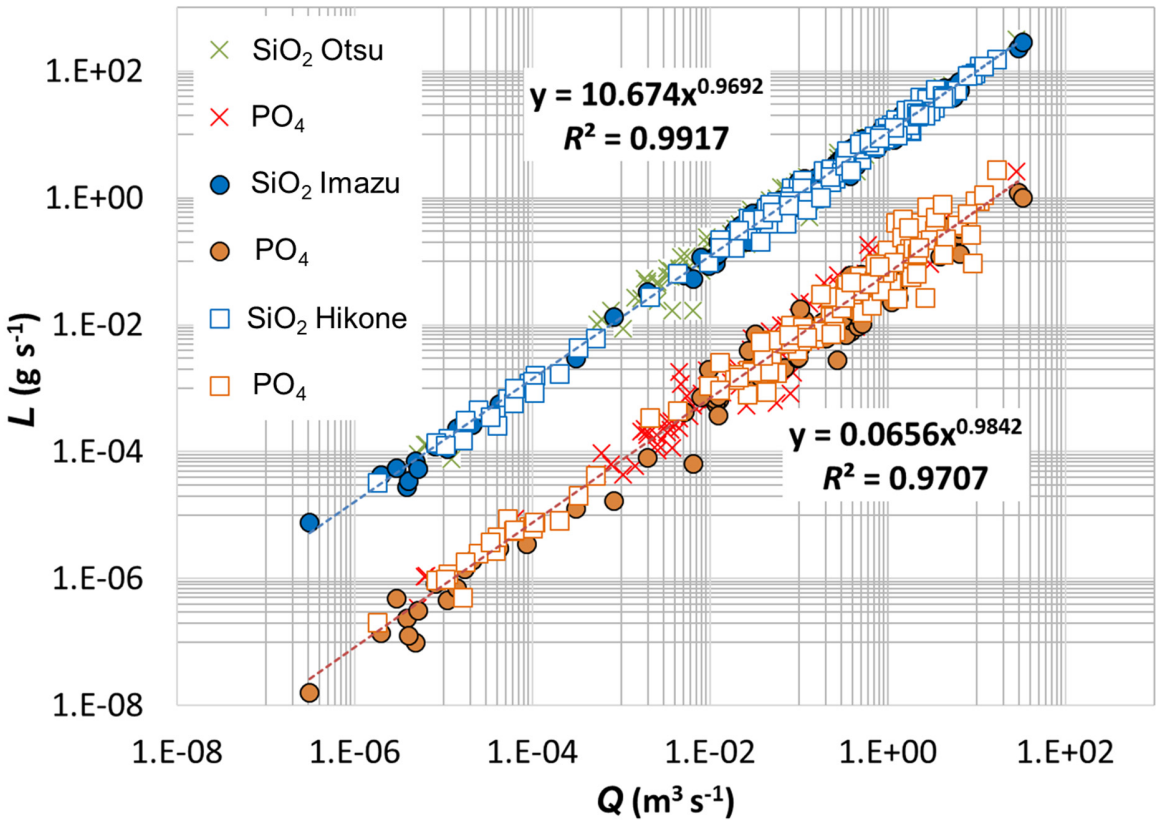

Figure 2.4 The loading curve for PO_4 and SiO_2 which regarded as unified for the nutrients. The coefficient correlation between nutrient loads and river discharge was performed as $R^2 = 0.99$ (SiO_2) and $R^2 = 0.97$ (PO_4)

After establishing the loading L-Q curve as equations (28) and (29) for a total of 3 sub-basins, the riverine nutrients loading was estimated. The nutrient discharge from Imazu and Hikone sub-basins were used to integrate the result of external nutrient from inflows into the North basin of Lake Biwa. Meanwhile, the nutrient loads into the South basin were based on the calculation from the Otsu station. Ferguson (1986) mentioned that the loading method that used a log-log loading curve can underestimate rivers' loads from a statistical point of view. However, the log-log equation was found to minimize the deviation from the logarithmic data set, although there exists a negligible scattering about the regression equation in the low region for PO_4 and SiO_2, which is illustrated in Figure 2.4. Each straight line, which indicates a regression equation, fits the distribution of the point well. The load-flow relationship for SiO_2 is higher than PO_4 indicating the sensitive effect of water discharge on PO_4.

Table 2.4 Daily calibration and validation results of water level

Indices	Lake Biwa- Mihogasaki station			
	n	NSE	RSR	PBIAS %
Calibration (1991-2003)	4,747	0.98	0.15	-0.01
Validation (2004-2015)	4,383	0.94	0.25	0.25
Total period (1991-2015)	9,130	0.97	0.19	0.1

The runoff rate (mm day^{-1}) into the North and South basins was estimated and compared with the water level in Lake Biwa. The performance of the daily scale model concerning the simulated water level was further examined using statistical criteria applied to the calibration and validation periods. Model calibration and validation statistics, which compared observed and simulated water levels for the daily time intervals are displayed in Table 3.4. Daily water level data across 13 years (1991 to 2003) were used to calibrate the remaining data from 2004 to 2015 and were used to validate the model performance (Figure 2.5).

The results during the calibration and validation periods indicated that the simulated water level matches well with observations. A statistical comparison revealed NSE, RSR and PBIAS indices for the calibration (0.98, 0.15, and -0.01%) and validation (0.94, 0.25, and 0.25%) periods. The performance is a good category for both of the cases according to the suggestion of Moriasi et al. (2007). The coefficient of determination (R^2) between the simulation and observed data was 0.98 and 0.93, respectively. Outflow through the Seta River was first estimated as the total inflow minus the volumetric change rate of the water level at Mihogasaki. The observed water level, especially in the South Basin, would be affected by the surface seiche. The outflow at Toriigawa midstream has been regulated by Nango Araizeki (old weir) in Seta River since 1905, and the new weir was constructed in 1992. Therefore, the discharge at Toriigawa was under the operation of the weir and less variable than the discharge calculated by the local rate of change in the water

level. The formers have two and the latter has three sluices to adjust the crest height. For total discharge and water level, various cases depend on opening gates (Figure 2.6).

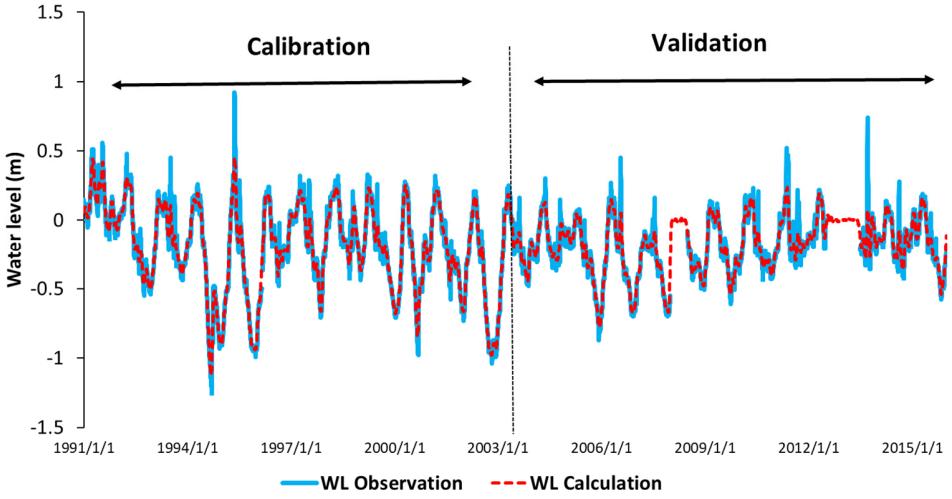

Figure 2.5 Daily water level from 1991 to 2015 with the calibration period (1991-2003) and the validation period (2004-2015)

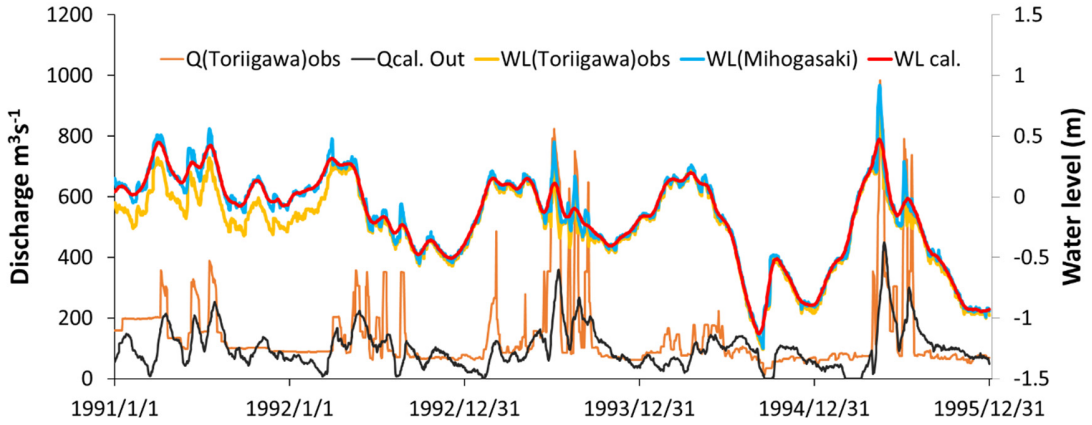

Figure 2.6 Comparison of water level and water discharge in Lake and Toriigawa outflow from 1991 to 1995

Figure 2.7 shows the annual variation of PO_4-P increased from 1980, drop dramatically in 1994 due to the drought, and then fluctuated after 2000. Meanwhile, Silicate loading fluctuated from 1980, decreased in 1994 and 1998 and then increasing onwards. A high concentration of PO4-P in groundwater discharge contributed to the increasing trend of total loading into Lake Biwa. Hsieh et al.(2010) reported that the PO_4 and SiO_2 concentrations in the North basin of Lake

Biwa increased during the 1980-2005 period. The change of nutrient loading from the river and groundwater system surrounding the lake has an apparent relationship to the trophic status of the lake. Besides, it also exhibited the seasonal change in nutrient loading from rivers and groundwater. The flux increasing from spring to summer and reach a maximum in July, then decreasing in winter. The application of agricultural fertilizers might be one of the reasons for increasing nutrient loads in rivers and groundwater during the spring and summer seasons. Rainy periods from the end of May and until July also contributed to the increased nutrient loading into Lake Biwa.

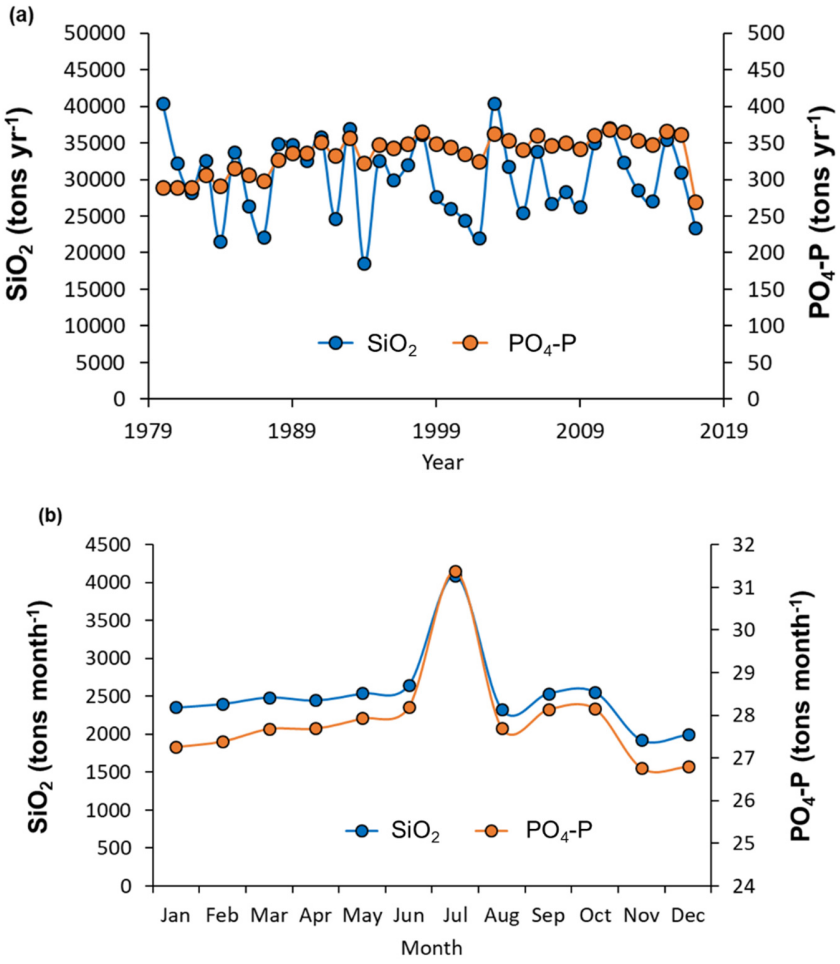

Figure 2.7 Long-term annual variation (a) and seasonal variation (b) of nutrient loading into Lake Biwa

By using the results of the L-Q curve and the daily tank model, external nutrients from rivers into Lake Biwa were estimated and the water budget was established. Table 2.5 shows the annual river budget was 3.1 km^3year^{-1} while the annual groundwater budget was 0.8 km^3year^{-1}.

Fujino (1980) and Tsurumaki and Kobayashi (1989) reported the river water and groundwater inflows were 3.02 $km^3 year^{-1}$ and from 1 to 1.5 $km^3 year^{-1}$, respectively. On the other hand, PO_4-P (converted from PO_4) loading into the North basin of Lake Biwa ranged from 217 to 296 tons $year^{-1}$ while loading in the south part averaged around 63 tons $year^{-1}$, ranging from 45 to 76 tons $year^{-1}$. PO_4-P loading in the North basin is also considered as a source of nutrients for the South basin. Another report revealed that the P budget removed from outflow is 26% in the pelagic site in the North basin of Lake Biwa, and the inflow rate of P from the watershed corresponds to 56% of the algal P uptake rate (Yoshimizu et al., 2002). However, according to Nagare et al. (2001), P mass measured from 1995 to 2000 was around 190 to 340 tons, and the output of P occupied 15% of the total budget (North and South Basin). In this study, the total PO_4-P loading from the river in the North basin occupied 81% of the total PO_4-P loading.

Besides, Goto et al. (2007) reported that the inflow discharge of Si was calculated to be 25,000 tons $year^{-1}$, while the output was approximately 5,000 tons $year^{-1}$. These findings are quite similar to our estimation of 30,244 tons $year^{-1}$ average SiO_2 inflow (Table 2.5) in which Si loading of the North part was found to be 82% of the annual Si input to the watershed, ranging from 16,000 to 33,000 tons $year^{-1}$. SiO_2 loading from the South ranged from 2,500 to 8,000 tons $year^{-1}$. The estimation for the Si sink represented by Goto et al. (2013) showed that 20,000 ton Si $year^{-1}$ was retained in Lake Biwa, which accounts for 80% of the annual inflow discharge. The remaining fraction of Si sedimentation was removed from the water by the outflow of biogenic silica from Lake Biwa to the Seta river and/or physicochemical processes (Goto et al., 2007). Lake Biwa becomes a trap, retaining most Si input and reducing the Si-flux to the Seto Inland Sea by 38,000 tons SiO_2, and also the total Japanese output by about 0.46% according to Hartmann *et al.* (2010).

Table 2.5 PO_4-P and SiO_2 loading from rivers and groundwater and water budget in Lake Biwa

	Unit	Otsu	Imazu	Hikone	Lake Biwa
Drainage area	km^2	613	673	1915	674
Precipitation	$mmyr^{-1}$	1,604	1,907	1,628	1,640
Evaporation	$mmyr^{-1}$	563	610	501	771
PO_4-P loading	$tonsyr^{-1}$	63	61	211	
SiO_2 loading	$tonsyr^{-1}$	5,490	7,290	17,464	
River water	km^3yr^{-1}	0.5	0.8	1.8	
Ground water	km^3yr^{-1}	0.1	0.2	0.5	
Annual yields	km^3yr^{-1}	0.6	1	2.3	
$\boldsymbol{r_E = \Sigma E/\Sigma P}$		0.4	0.32	0.31	
$\boldsymbol{r_G = \Sigma Q_g/\Sigma Q_r}$		0.2	0.25	0.28	
$\boldsymbol{R_L}$	year				5.8

2.4 Conclusions

The external loading process into Lake Biwa was described using a hydrological tank model in three steps. The hourly tank model has been calibrated on a discharge basis by replacing the central rain data with the local rain. The loading curves were obtained by using local discharges of individual rivers, however, these were used for the total discharge of each sub-basin. The exponents of loading curves were close to unity, which suggests the load is proportional to the discharge (Step 1). The daily tank model was calibrated on a water-level basis and the stage-discharge rating curve for the outflow (1991-1995) showed that it was highly controlled and less variated. The second model was validated by using water level data (1991-2015) under the natural outflow condition. Evaporation and lacustrine groundwater discharge were also considered (Step 2). The daily-basis tank model was extended (1980-2017) and established to determine the long-

term external nutrient loadings into the lake and was also used to analyze the water budget among the catchments. The results from these studies indicate the seasonal change of nutrient loads increasing in spring and summer, fluctuated in autumn but decreasing in winter. The average PO_4-P loading was 336 tons $year^{-1}$, while the average SiO_2 loading was 30,244 tons $year^{-1}$, respectively. These values compare favorably to other recent studies.

CHAPTER 3. SEASONAL AND VERTICAL DYNAMICS OF NUTRIENT AND CHLOROPHYLL-*A* IN THE NORTH BASIN OF LAKE BIWA

3.1 Introduction

Nutrient concentration in rivers is particularly important to river ecology, and riverine transport of nutrients is also relevant to lake water. Increasing nutrient loading to the aquatic ecosystem results in an enhanced primary production that leads to undesirable changes in aquatic resources such as degraded water quality, hypoxia, harmful algal bloom, losing biodiversity, and affected food web structure. Lake Biwa is the largest lake in Japan and provides great ecological and economic value (Kumagai, 2008) but over the past few decades, as with many lakes worldwide, Lake Biwa has undergone progressive eutrophication which is an example of the impact of anthropogenic factors such as agriculture activity, tourism, wastewater, and global warming on the lake ecosystem (Hsieh et al., 2010; Tsugeki et al., 2010). Lake Biwa's phytoplankton biomass has decreased and the dominant phytoplankton species has changed from net phytoplankton to nano-phytoplankton (Kishimoto et al., 2013). However, the primary productivity, otherwise, has increased because picoplankton has increased in Lake Biwa which showed small biomass, but higher productivity. Changes to the phytoplankton biomass (composition and size) and the fluctuation of nutrients have been recorded annually for decades. According to Nagata (1990), 50-90% of the primary production was occupied by picoplankton and Kishimoto et al. (2015) reported that the primary production in the North Basin of Lake Biwa increased from 1980 to 2008 while Chl-a concentration exhibited an inverse trend. Cyanobacteria produce the majority of the lake's organic matter and largely determine the chemical oxygen demand (Ichise et al., 2013). The blooming cyanobacteria were observed such as Synechococcus spp. in the north basin of Lake Biwa during early summer in 1989 and 1990 (Maeda et al., 1992). Until now, nutritional status was found to track eutrophication and phytoplankton abundance closely. Nutrient levels, including total phosphorus (TP), total nitrogen (TN) have been used extensively to assess the degree of eutrophication and to predict the productivity of virtually all of the biological components of lakes and ponds (Peters, 1986). Previous reports have attempted to diagnose the nutritional status mainly in the upper 20 m of Lake Biwa and used this metric to represent changes to the lake's trophic status annually (Hsieh et al. 2010, 2011; Kishimoto et al. 2013). Only a few studies mentioned the

seasonal supply rate or metabolic rate. Tsunogai et al. (2011) estimated both the average nitrification rate and average assimilation rate of nitrate in the lake successfully, assuming that the metabolic rate of nitrate through denitrification was much less than in the highly oxic lake. Yoshimizu et al. (2002) determined the budgets for P nutrients in Lake Biwa and estimated that input via inflows occupied 56% of the total P metabolized in the lake's water column; thus, remineralized P occupied only 44%. Besides, Tsunogai et al (2018) found most NO_3 that was metabolized in spring and summer was supplied through in situ nitrification within the epilimnion and upper thermocline. However, the methods to quantify nutrient dynamics are complicated and often can be inaccurate. The nutrient mass gradient fluctuated by time change was an interesting way to calculate the nutrient gradient by time change in the lake which could be given the information of the nutrient cycle process (supply and use). Furthermore, the change of seasonal nutrient gradient could be linked with the succession of phytoplankton biomass and species in the seasonal and annual assessment through the flux profile of Chl-a.

Therefore, this study focuses to investigate the long-term and seasonal changes in the chemical and physical water quality data in Lake Biwa over 35 years. To compile and analyze the seasonal fluctuation of N, P, and phytoplankton (using Chl-a) gradient, the vertical nutrients flux profiles were evaluated.

3.2 Site description

Lake Biwa is located in the center of the Honshu Islands in the Shiga Prefecture, northeast of Kyoto, Japan with an area of 674 km^2 and a maximum depth is 104 m. It contains two basins, a large north basin (616 km^2, mean depth 45.5 m) and a small south basin (58 km^2, mean depth 3.5 m) (Figure 3.1). The north basin is a warm monomictic lake with a circulation period from January to March, while the south basin is polymictic due to its shallowness (Tezuka, 1992). The trophic status of the north basin was determined by Kishimoto et al. (2013) as mesotrophic in terms of TN and oligotrophic in terms of TP.

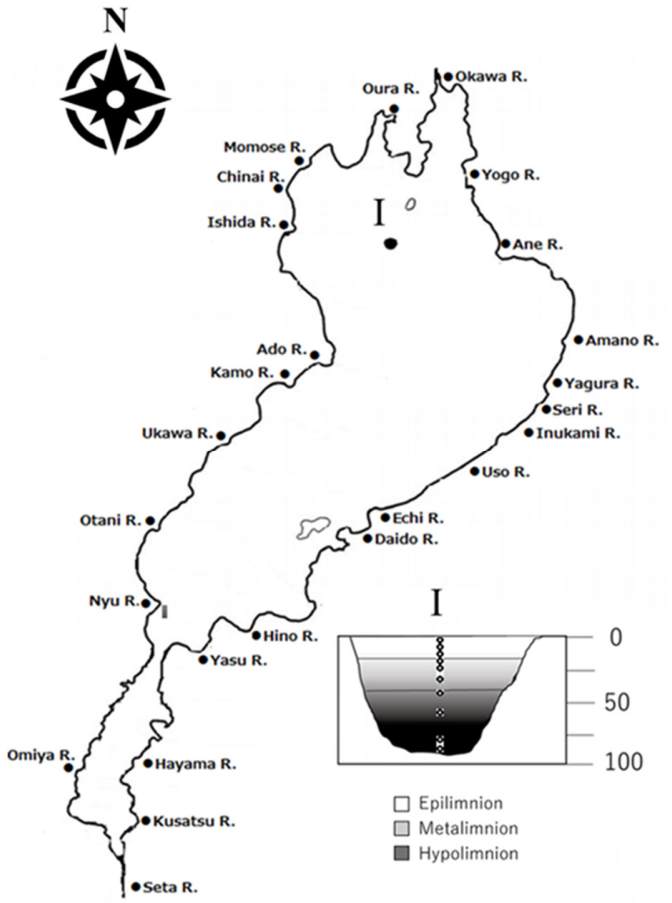

Figure 3.1 Map showing the sampling location at Imazuokichuo (I point) with layers of measurement in Lake Biwa. Filled circles along the coastline are river mouths

3.3 Materials and Methods

The environmental data from 1980 to 2015 used in this study, including the concentration of TN, TP, Chl-a, silicate (SiO_2), pH, Dissolved Oxygen (DO), and temperature measures, were collected by Lake Biwa Environmental Research Institute (LBERI) at the station named Imazuokichuo (35º23'41" N, 136º07'57" E). The samples were taken every other week during the day at depths of 0.5, 5, 10, 15, 20, 30, 40, 60, 80, and the bottom (88 m) in the north basin in Fig.1. The monthly average values of the layers were calculated. Furthermore, the 35 years of serial data were divided into five periods of seven years each (Period I-V). Because the resident time of Biwa Lake is around 5.5 years, this way, the data can be ordered in a reasonable description, and the

change in seasonal of all factors could be described clearly and with more accuracy. To visualize water quality, we created contour plots for each of the three aforementioned factors. This method also enabled the following eutrophication trends in the north basin of Lake Biwa. In addition to nutrient concentration, TN, TP, and Chl-a fluxes were estimated to demonstrate the nutrient fluctuation according to vertical and seasonal changes. Although the changing rate of Chl-a is determined by both vertical transportation and production by phytoplankton on-site, the downcore distribution of Chl-a could calculate with a random diffusive model (Boon & Duineveld, 1998). The flux profiles $q_x(z)$ for x = TP, TN, and Chl-a were determined by

$$q_x(z) = \int_0^z \frac{\partial x}{\partial t} d\zeta \quad (1)$$

where x is the monthly concentration of TP, TN, or Chl-a; t is time; ζ (m) is depth interval. The flux $q_x(0)$ at the surface was assumed to be zero for both nutrients and Chl-a. To visualize the Chl-a response concerning TN and TP, ordinary regression was used to model Chl-a as a function of TN and TP where linear, squared predictor was included; these relationships were also considered in the vertical and seasonal valuations. Seasons were defined as spring (March-May), summer (June – August), autumn (September – November), and winter (December – February). TP, TN, and Chl-a flux are represented by average monthly values and the change between the monthly integrals is represented by the value at the end of the former month or the first of the latter month. With local smoothing to grid data, this smoothing scheme begins by setting X_1 to x_1, where Xi stands for smoothed observation and x stand s for original observation. The subscripts refer to the period, the smoothed series started with the smoothed version of the second observation. For time interval d between the closest measurements, the smoothed value is found by calculating:

$$X_i = \frac{x_{i-1} d_{i+1} + x_i (d_i + d_{i+1}) + x_{i+1} d_i}{2(d_i + d_{i+1})} \quad (2)$$

with i ≥2.

Mass of nutrient and Chl-a in each water column was estimated from flux profile

Mass = Flux ($mgm^{-2}day^{-1}$) * Area of North Basin (m^2) * 365 (day/year)

3.4 Results and Discussion

3.4.1 Seasonal environmental status

All the panels show total mixing in the water column due to monomictic turnover that happened from February to March. The events were followed by thermocline and in the lower hypolimnion, with higher concentrations of TP, TN, and SiO_2, or with lower values of Chl-a, pH, WT and DO until the turnover in the next spring. From the second period, this import was reduced, and TP concentration decreased, high value only observed from June to August. TP was lowest in the thermocline and accumulated in the bottom, especially in winter during the given periods. The average values are 0.0074, 0.0059, 0.0098 mgL^{-1} for epilimnion, thermocline, and hypolimnion, respectively. In recent years (period V), interestingly, the resuspension of TP from lower to upper water layers was observed again in spring although the concentration is not higher than before. However, the accumulated nutrient in the bottom still is higher than in another period, from autumn to winter. Other studies reported the TP trend was thought to be oligotrophic (Hsieh et al., 2010; Kishimoto et al., 2013). The time series of TN in Lake Biwa revealed that TN increased rapidly from period II onward, the highest TN concentration was observed in period IV, however, the concentration decreased after period V. In the upper layer, TN increased from January to June but dropped from July, lowest value in October. In contrast, TN accumulated in hypolimnion from the first period to the last one, particularly in autumn and winter. Period IV revealed that TN concentration was up to 0.45 mgL^{-1} from last August to December before decreasing the same level with other previous years in period V. In period IV, it reached the highest concentration of TN compare to other periods. Kishimoto et al. (2013); Shrivastava (2014) found that TN trended toward eutrophication before 2000 but seemed to reverse after 2003. Due to a successful governmental water treatment regulation enforced in 1982, nutrient loading progressively declined and then stabilized since 1985 (Kumagai, 2008). Those reports are similar to the trend seen in our data. In period II, the nutrients were depleted in the epilimnion; this can be explained by the little rainfall and well-developed thermocline (Sohrin et al., 1996). Chl-a data show that the concentration varied greatly in the period I compared to periods IV and V; however, periods II and III looked stable trend. Overall, the Chl-a concentration decreased during time observation, from 3.63 μgL^{-1} in the first period to 1.44 μgL^{-1} in recent investigating. In vertical analysis, Chl-a is

high in water surface and decreased in lower layers, average 3.95 μgL^{-1} for epilimnion and 0.97 μgL^{-1} for hypolimnion. Moreover, Figure 3.2 reveals the transition of Chl-a concentration which represents phytoplankton biomass during the 35 years. It is increased gradually from spring and then reached a peak in October before decreasing in winter (period I and II). From period III onwards, the shift changed as follows: increasing from spring, the highest value in summer and then decreased in autumn and winter. The trend of silicate concentration is totally increased and looks different during the time. It is high value in spring and decreased in another season from period III while increasing gradually from spring in the period I, II. On the other hand, silicate from Figure 3.2 shows that the accumulated budget is increasing from the beginning time and reached the highest value in the last period (4-4.5 mgL^{-1}) from September to December.

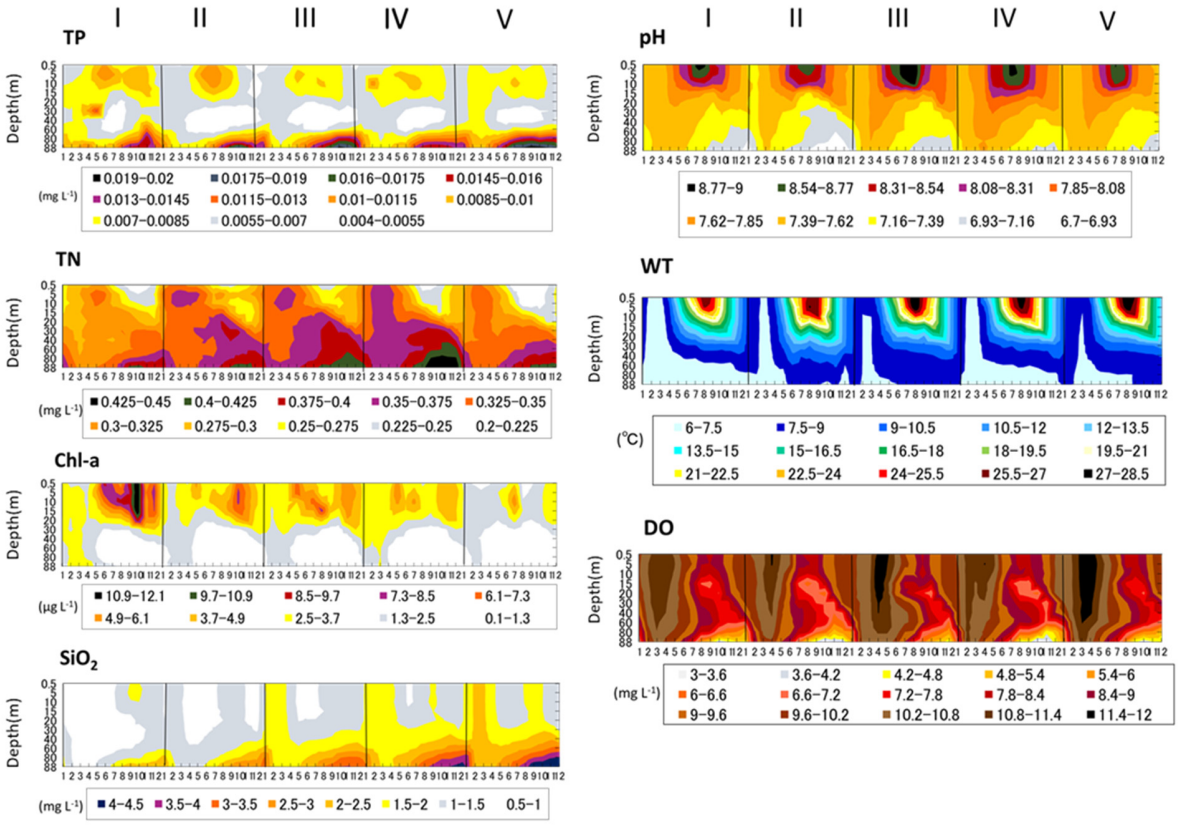

Figure 3.2 Monthly-vertical patterns of variable contours of TP, TN, Chl-a, SiO_2, WT, pH, and DO. Average were done in periods of 7 successive years for successive five periods, which are Period I (1980-1986), II (1987-1993), III (1994- 2000), IV (2001-2007), and V (2008- 2015)

(Le Tien Huu and Okubo, unpublish data)

Figure 3.2 continuously shows the water quality data exhibited significant seasonal variability in the north basin of Lake Biwa for every seven years (Period I–V). pH was very stable across the five periods and fluctuated according to the season: high in the summer, reach the peak in July-August, and low in the winter and spring. Vertical value also indicated the difference among water layers, high in the epilimnion, and low in the hypolimnion, average 7.3. The figure revealed that pH was increased in period III compared to other periods. The DO increased in the spring and summer (highest value in March and April), fluctuated around 8.54 mgL^{-1} to 9 mgL^{-1}, and then decreased gradually in autumn and winter (November and December), with high values at the surface and low values at the bottom, with little fluctuation from year to year. However, DO concentration increased in Period III and Period V but decreased in period I and IV. The water temperature ranged between 6.31°C and 28.4°C, highest in August. The average photic zone temperature was 14.3°C in Period I and 15.3°C in Period V. According to Kishimoto et al. (2013), the annual mean water temperature increased steadily at a rate of 0.045°C per year during two decades from 1980 to 2010. The mean increase in water temperature in the stratification period is higher than in the circulation period (0.058°C and 0.037°C per year, respectively).

3.4.2 Seasonal variation of phytoplankton biomass

Population densities of phytoplankton species were recorded by using the method of Ichise et al, (1999), the total bio-volume density was transformed into wet weigh biomass by multiplying the biovolume and water density. The total biomass in annual was analyzed from 1979 to 2009, named *S-nano* for small nano phytoplankton (<100 $\mu m^3 cell^{-1}$), *L-nano* for large nano phytoplankton (100-4000 $\mu m^3 cell^{-1}$), *Net* for net phytoplankton (≥4000 $\mu m^3 cell^{-1}$), followed by Kishimoto et al., (2013). Figure 3.3 shows the variation in wet weight biomass of phytoplankton and reveals an apparent decrease in phytoplankton occurrence during the study period. The biomass decreased rapidly in the 1980s before increasing gradually during the 1990s and finally displayed a decreasing trend from 2000.

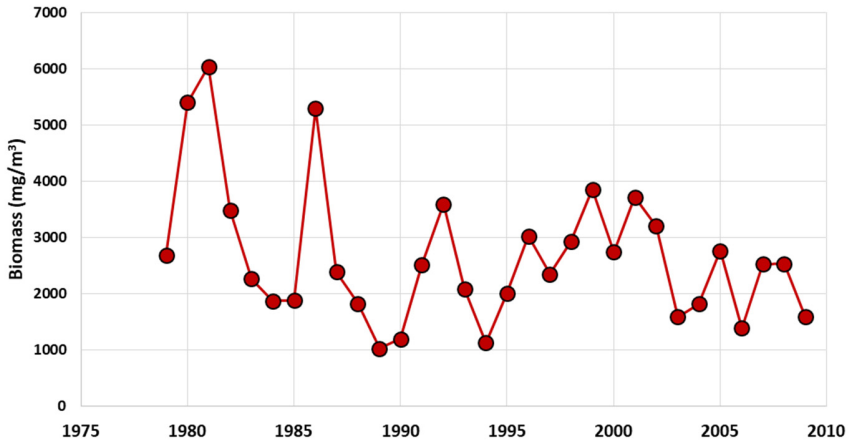

Figure 3.3 Long-term annual phytoplankton biomass in the North Basin of Lake Biwa

The inter-annual variation in seasonal biomass during the study period is indicated in Figure 3.4. The result summarized that the trend in seasonal biomass fluctuated differently due to each season. During the study period, the biomass tended to slightly increase while the biomass in summer remained almost constant but decreased in autumn. In general, biomass in summer and autumn was higher than in spring and winter. Especially, it can be seen that the biomass in seasonal fluctuation side was seemed similar observation in the recent year compared to the past excluding blooming time in summer.

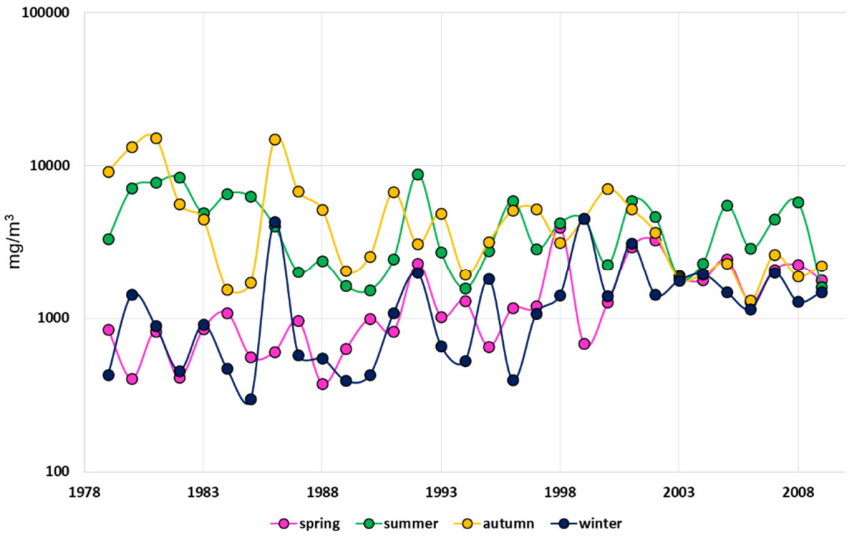

Figure 3.4 Seasonal variation in phytoplankton biomass

Figure 3.5 demonstrated the transition in the seasonal variation of the biomass of each size phytoplankton species. The biomass of small phytoplankton very low in the first period but it tended to increase gradually and change the percentage of the population from autumn to summer from 1997 onward. Nevertheless, the large phytoplankton fluctuated its population during the study period and slightly decreased in the recent year. It can be seen the clear transition of blooming season from summer to autumn and spring started from 1998. In contrast, the net phytoplankton biomass was highest in the first decade but revealed a rapidly decreasing trend during the remaining period. Furthermore, it is apparent to see that the blooming season of this species changed from autumn to summer in the decade of 1990s and 2000s. In general, the biomass of a 3 sizes fraction of species was high in summer and autumn and low in winter and spring.

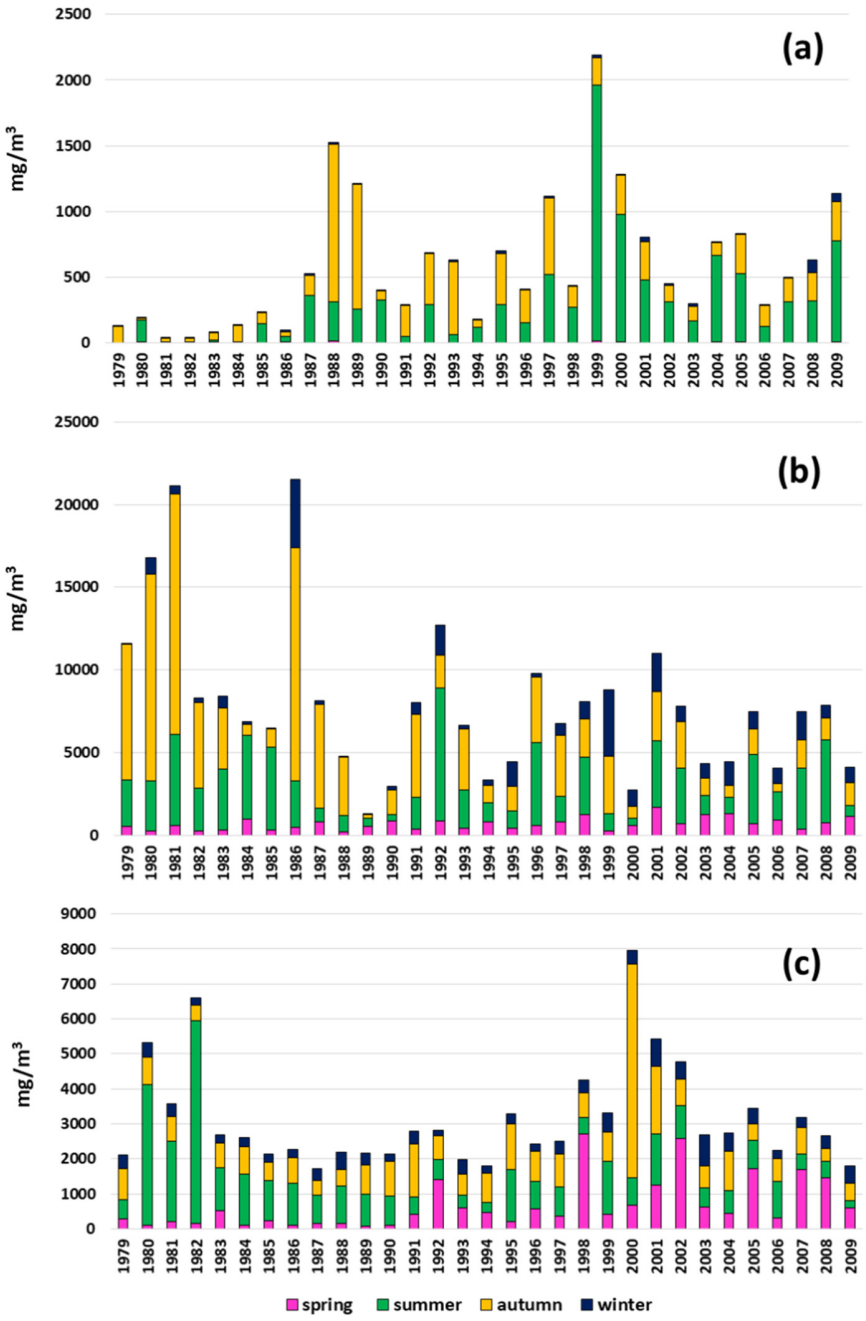

Figure 3.5 Seasonal variation in the different sizes of biomass for each species. **(a)** S－nano: small nano phytoplankton（＜100 μm^{3}cell^{-1}, **(b)** L－nano: large nano phytoplankton（100－4,000 μm^{3}cell^{-1}, **(c)** Net: net phytoplankton（≥4,000 μm^{3}cell^{-1}）

3.4.3 Vertical and seasonal variation in Chl-a and nutrients fluxes

The monthly flux profiles are shown as a seasonal change of Chl-a, TN, and TP in Lake Biwa. The Chl-a flux is positive in the photic zone (0 - 20 m) from March to May as spring blooms with the thermal stratification development (Figure 3.6). The flux is weakly negative from June to August, which is possible due to a divergence of the convective circulation of the thermally induced gyre in the epilimnion and depletion of nutrients. The bloom of cyanobacteria is transported offshore and stays at the surface of the down-welling center of the gyre (Ishikawa et al., 2002). The flux is also positive from September to October and steepened gradually from the surface to the bottom. Organic matter sinks from upper to lower layers nearly constantly when a settling period initiates after this internal wave activity. The negative flux is observed when Chl-a decreased gradually by the decomposition process during winter from December to February. In figure 3.6, A shows the blooming time that occurs leads to increasing biomass. B shows the strong activity of Gyre in epilimnion and thermocline which prevent the sinking of biomass and separated the density of phytoplankton. C shows the sinking process occurs from thermocline to the hypolimnion by a part of the effect of internal waves. D shows the decomposition process in a 30 m depth of water column.

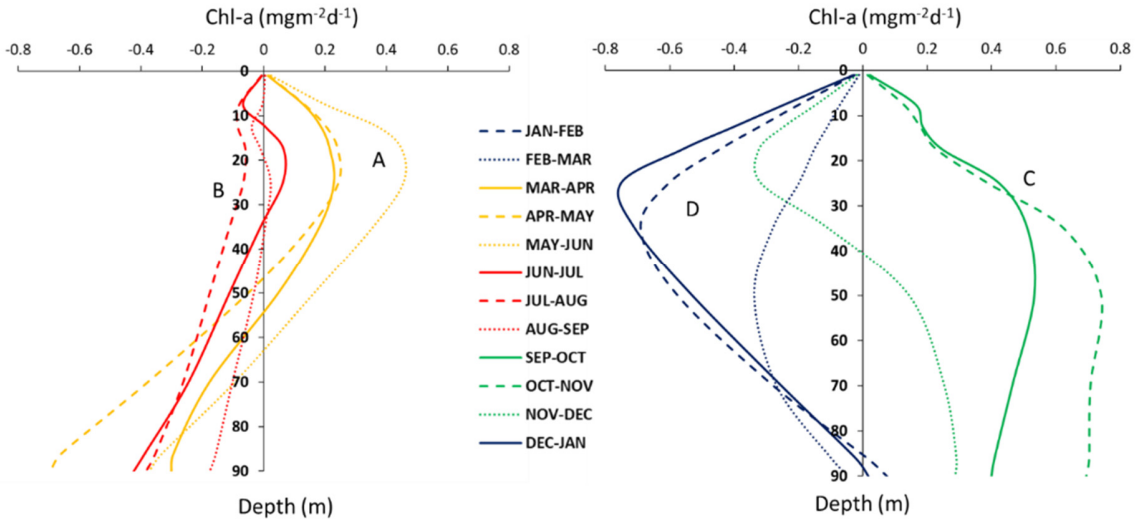

Figure 3.6 Average vertical profile of Chl-a flux, the positive period from spring to early autumn, and a negative period from late autumn to winter during the 5 periods

Interestingly, the positive TN flux in winter showing an inverse trend compared with Chl-a flux, it is positive in the upper layers from October to February and soon decreased from March to become negative during spring and summer. TN is consumed strongly from June to July from 10 m to 20 m in depth (Figure 3.7). During the bloom, the TN is used by algae but then increased. The removal of N from lakes is usually dominated by denitrification concomitantly with the oxidation of organic matter, but in highly productive surface waters, high pH would favor N release to the atmosphere as NH_3. The decrease from May to October could result from denitrification. Meanwhile, the TP flux exhibits a depth variation that decreases abruptly in the last 10 m during the winter, a minor increase at deeper layers (40 - 70 m), followed by a major decrease in the hypolimnion. The positive flux is observed in the upper layer (0 - 30 m) in spring and hypolimnion in summer and autumn (Figure 3.8). From June to November, especially September to November, TP is lost (negative) in the photic layer and gained (positive) in the anaerobic environment.

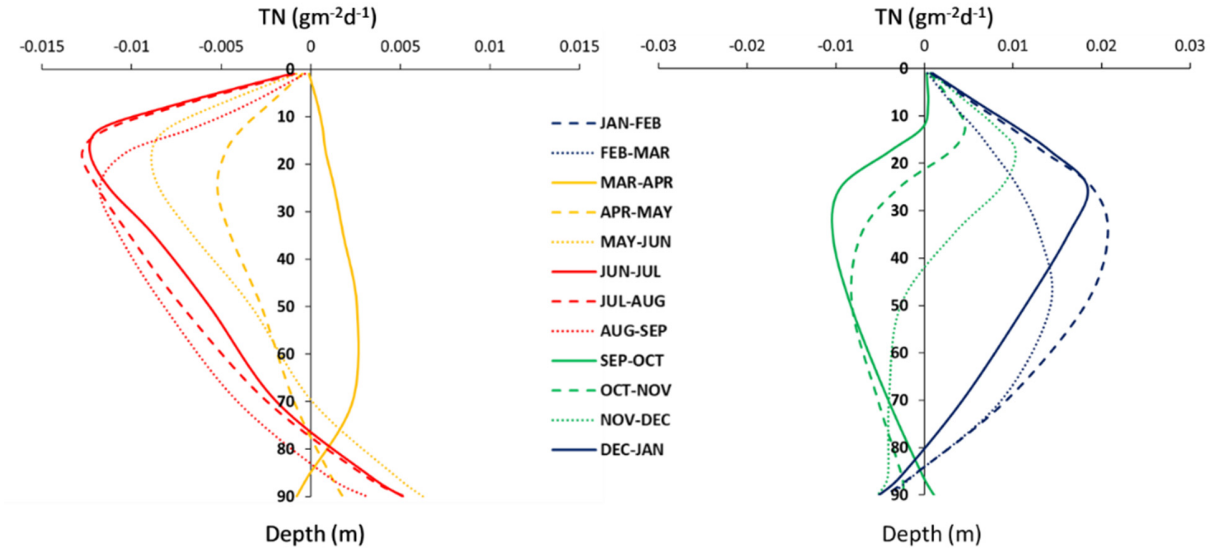

Figure 3.7 Average vertical profile of TN flux, the positive period from mid-autumn to winter, and the negative period from spring to early autumn at 0 to 90 m during the 5 periods

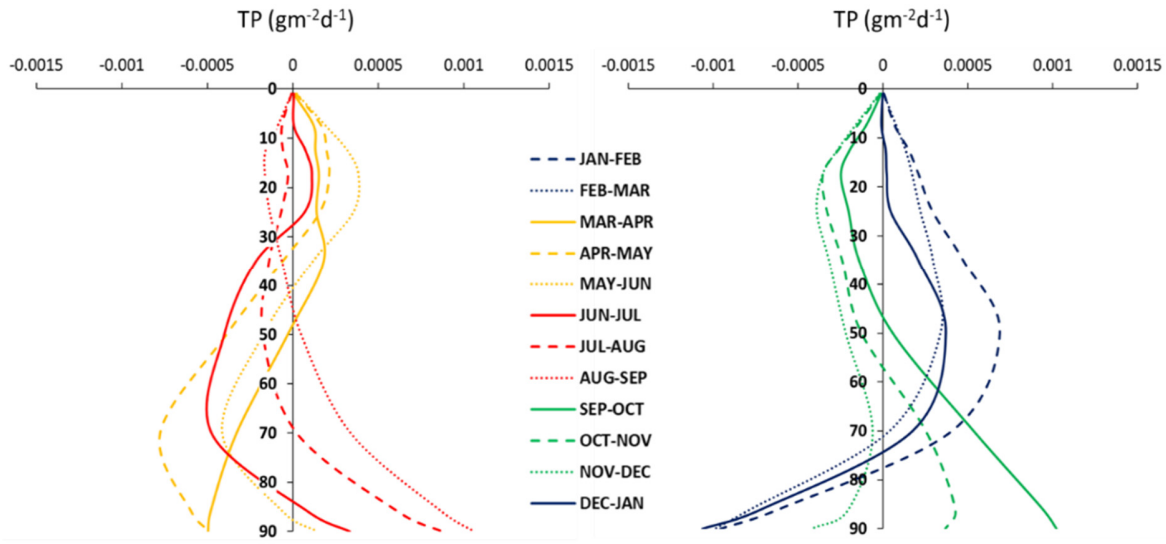

Figure 3.8 Average vertical of TP fluxes divided into 2 parts, the positive period from winter to early summer and the negative period from late summer to autumn during the 5 periods

The relationship between the fluxes of TP and Chl-a was evidenced in the epilimnion and hypolimnion (Figure 3.9). $\triangle$Chl-a > 0 and $\triangle$P > 0 in the surface layers are due to photosynthesis, which is elevated between March and May before reducing gradually in the thermocline. Positive values for both Chl-a and TP suggested active photosynthesis (production) and nutrient addition. Specifically, Chl-a and TP were both negative in the summer from the surface to the thermocline, which correlates to the activity of the thermally induced gyre in the epilimnion. From September to November, $\triangle$Chl-a > 0 and $\triangle$P < 0 at the surface and both were positive in the hypolimnion, suggesting that production occurred due to physical processes. The pattern was negative in the winter on the surface yet still produced in the bottom before undergoing the opposite fluctuation from top to the bottom during January and February. That both nutrients and Chl-a were negative in the bottom suggests that no major production or decomposition was occurring. Nutrients were stored or adsorbed in the water, but earlier in the top and later in the bottom.

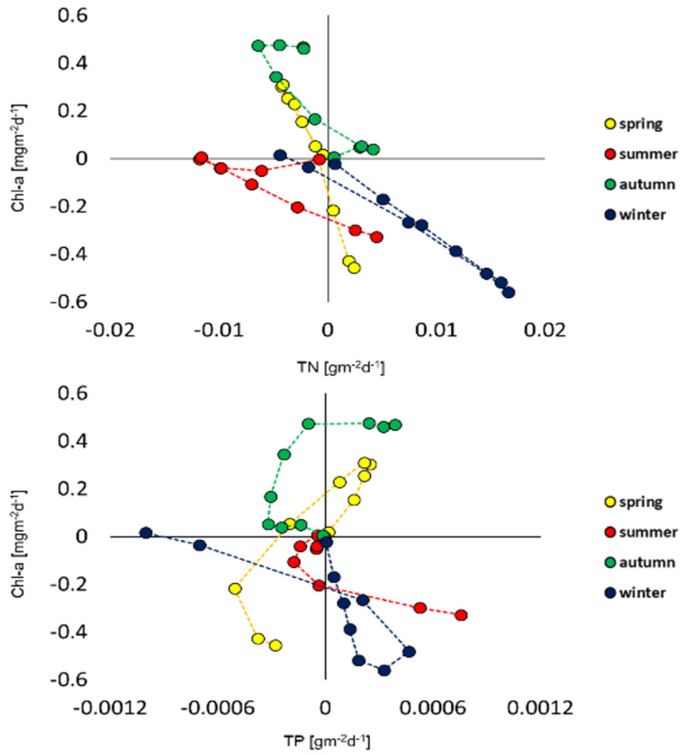

Figure 3.9 The relationship between the fluxes of Chl-a, TN, and TP in water columns. Each point represents the water depth from 0 to 88m

The results presented in Figure 3.9 also describe the season-dependent relationship between TN and Chl-a, similar to TP and Chl-a. In the summer, the Chl-a flux was negative when TN and TP were being lost and the concentration of nutrients grew in the hypolimnion. Biomass is dropped in the summer and causes a decrease in the total nutrients with the activity of strong physical process as gyres. The opposite trend was observed in the data during the winter when the nutrient flux was positive, but the Chl-a flux was negative. During the autumn and spring, the Chl-a flux was almost positive, while the TN flux was negative in the spring and positive in the autumn. The TP flux, in contrast, positive in the spring but negative in the autumn. When TP concentration decreased (negative flux) in the summer and autumn, the relationship between TN and Chl-a ($R^2_{summer} = 0.69$, $R^2_{autumn} = 0.75$; $p<0.05$) was significant weaker than cooling period ($R^2_{winter} = 0.98$, $p < 0.05$) (Table 3.1). The effect of TP and TN on Chl-a was considered relevant, which indicated that TN was strongly related to Chl-a when TP was high and less so at lower TP concentrations. The effect of TN on the TP-Chl-a relationship was not

so much clear. During the summer and autumn, the concentration of TN decreased and then increased in the winter; the correlation among these three patterns of TP-Chl-a was similar ($R^2_{winter} = 0.62$, $R^2_{summer} = 0.69$, $R^2_{autumn} = 0.46$, $p < 0.05$) (Table 3.1). Taken together, these data indicate that while the effects of the TN and TP as nutrient resources on phytoplankton biomass are both considerable and relevant, but TP plays a larger role, suggests that TP rather than TN, limits Chl-a. (Filstrup et al. 2017) discussed that Chl-a and TN relationship differed depending on TP concentration and covaried with both TN and TP. Chl-a showed a stronger and novel relationship with TN for hypereutrophic condition (TP > 100 μgL^{-1}) but little with increasing TN for mesotrophic or eutrophic condition (TP ≤ 100 μgL^{-1}). The finding supports an argument that the effect of TN on Chl-a is little at low TP but stronger in TP-rich lakes (Canfield et al. 1985; McCauley et al. 1989).

Table 3.1 Spearman's correlation at P<0.05 result between Chl-a and TN, TP during the study period

Variables	**Chl-a**			
	Spring	Summer	Autumn	Winter
TN	0.97	0.69	0.75	0.98
TP	0.78	0.69	0.46	0.62

3.4.4 Chl-a and nutrient mass remaining in the water column

After calculating the flux profile of Chl-a and nutrient, the difference of seasonal mass (ton/month) of them would be estimated to clarify the supply rate through nitrification process and removal rate through assimilation and denitrification processes. Fig 3.10 shows that the inventory of Chl-a, TN, TP remaining in the lake in the interval of each month was varied.

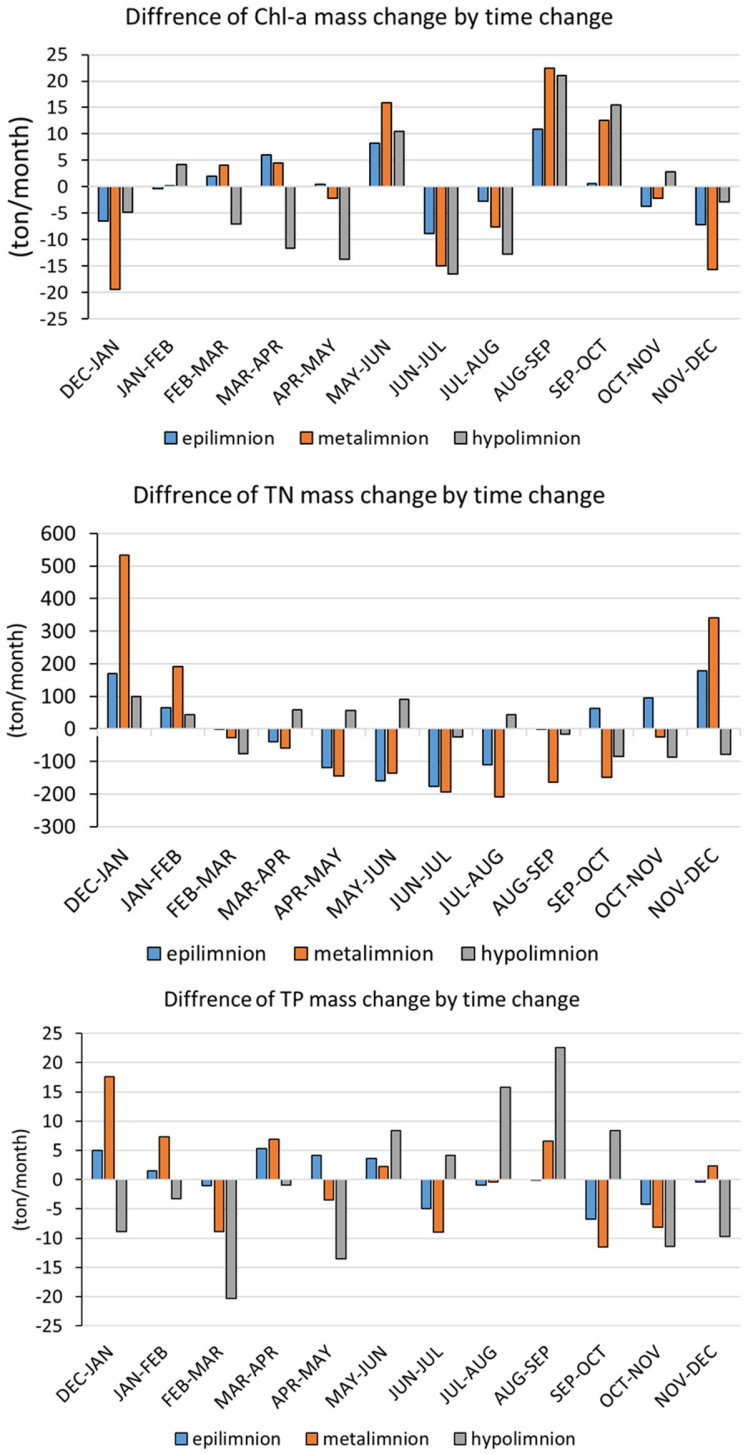

Figure 3.10 The monthly deposition and vertical distribution of the remaining mass of nutrient and Chl-a

The vertical profile shows the interval difference of supply and removing TN mass was ranged from -0.18 to 177 ton month^{-1} in the epilimnion, from - 208 to 533 ton month^{-1} in the metalimnion, and -87 to 100 ton month^{-1} in the hypolimnion. It means the mass change was very different in the upper and middle layer while small in the lowest layer for TN. In the same manner, the vertical profile of supply and removing Chl-a mass fluctuated from -8.7 ton to 10.8 ton month^{-1} in the epilimnion, -19.4 to 22.5 ton month^{-1} in metalimnion and -16.4 to 21 ton month^{-1} in the hypolimnion. The highest mass exchange occurred in the thermocline. For TP mass, we estimated that -0.08 to 5.27 ton month^{-1} in the epilimnion, 0.4 to 17.5ton month^{-1} in metalimnion, and -0.89 to 22.5 ton month^{-1} in hypolimnion was remaining.

Regard the seasonal aspect, the TN mass was recovered during wintertime by nitrification before losing in early March for metabolism in the epilimnion during summer and early autumn. Meanwhile, the deposit of TP was high in winter and early spring but the shortage was seen in summer and late autumn.

Tsunogai et al. (2018) mentioned 75% of the N metabolism was via assimilation (primary production) and assume that nitrification in the surface 15 m (epilimnion and upper thermocline) supplied the N needed for the assimilation. This point expresses the gain and loss of mass in those layers are very strong. On the other hand, his study found the supplied/removed ratio was 0.6 in spring, increased to 0.9 in summer, and 1.5 in autumn before decreasing 0.6 in winter. The areal assimilation rate increased from spring to summer and decreased in autumn and winter. It is reasonable with our result when the used mass rate was higher than the supplied mass rate from spring.

Yoshimizu et al. (2002) shown that only 44% P uptake by algae was recycled within a lake, the high mass observed in the bottom shows most of the P settled to the bottom and was fixed in the sediments of the lake. The P release from the bottom of the lake could be responded to the recovery of P.

3.4.5 Seasonal-vertical N:P ratio in Lake Biwa

Lake Biwa has been classified as one of the phosphorus-limited lakes (Tezuka, 1992). To predict algal biomass and composition, the N:P ratio in lentic systems has been often used as a key indicator (Tilman, 1982). Nutrients are well known as the main nutrients for phytoplankton and usually the limiting factors in algal growth, thus, the ratio of N:P is used to compare the

availability of these nutrients. Moreover, this ratio can become a useful method which is one of the meaning components for the calculation of the trophic state index of lakes (Grzetic Ivan et al., 2009). However, the N:P ratio has been a problematic and messy variable for limnology. It is a ratio variable and, therefore, is not a good state variable to study lake processes. It usually varies inversely with lake trophic state and biological standing stocks (Downing and McCauley, 1992; Quiros, 1990b). However, the N:P ratio may be a good variable to study state change in lakes because the N:P ratio and the trophic status are closely and inversely related for lakes. The atomic ratio, 16N:1P, which is known as the Redfield ratio, has been used for generally marine and freshwater phytoplankton studies to describe the average elemental composition. It has been suggested that a mass N:P ratio above 17 indicates P limitation, a ratio below 10 indicates N limitation, and values between 10 and 17 indicate that either of the nutrients may be limiting (Ulén, B.,1978; Hellström T., 1996). The corresponding molecular ratios are > 38, < 22 and 22–38, respectively.

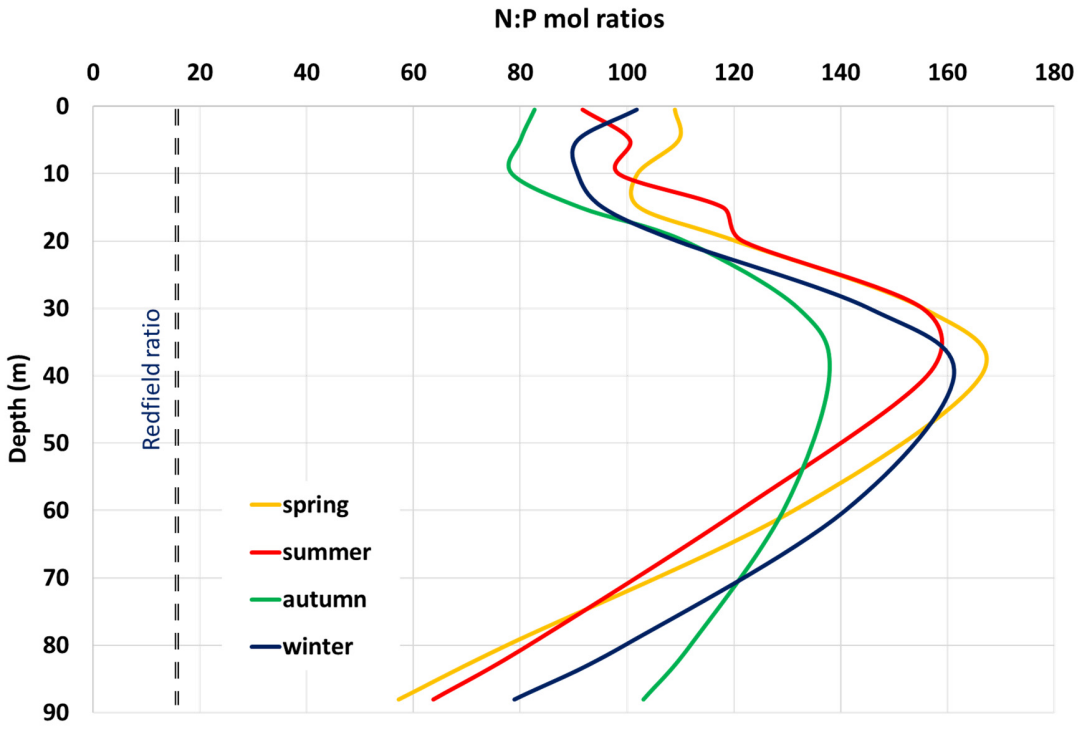

Figure 3.11 Seasonal-vertical N:P ratios in North basin, Lake Biwa

A large number of theories have been proposed to reveal the N:P ratio may be explained the status of the lake. For instant, an N to P ratio ≤ of 10:1 appears to favor algal blooms, especially blue-green algae. On the other hand, one of the most recognized theories, the low N:P hypothesis (Bulgakov and Levich, 1999) predicts that cyanobacteria will dominate lakes.

Figure 3.11 shows N:P ratios in Lake Biwa as an indicator of phosphorus deficiency are normally higher than the Redfield ratio (16). Almost all values of the N:P ratio in the whole layer were higher than 50. The value of the N:P ratio increased at 40 m depth as P decreases then N:P ratios decrease to the normal value as P increase near the floor. Moreover, the N:P ratio was variated in each season, the value was highest in spring and lowest in autumn in the epilimnion but was converted in the hypolimnion. According to Ichise et al (2001), the mean of N:P ratios in the North basin increased from 67 to 104 from 1979 to 1999 with the decrease of the population of phytoplankton. Nakanishi et al. (2001) reported that those values were found to be 77 and 134 during 1980-1992 and 1993-2000, respectively. Recently, Shrivastava et al. (2014) concluded that TN: TP in the Northern Basin is 76 from 1963 to 2008.

The ratio assumes that algal increase rapidly in the photic zone then the increasing trend of the N:P ratio in the metalimnion indicates that the input of nitrogen increase slightly or that phosphorus disappears from the water and could be the limiting factor for algal growth at this layer. Subsequently, this ratio decrease may be related to the rate of P liberation from sediments and increased rates of N loss (i.e. denitrification). Denitrification was the most important mechanism for reducing N:P ratios in the water column, whereas both nitrogen fixation and sediment resuspension raised N:P ratios. The ratio of the nutrient can markedly influence the community structure of the phytoplankton (Tilman, 1982). From the standpoint of the N:P ratio, it can be probably suggested that almost all phosphorus entering the lake is transported to the bottom sediment and fixed there without being recycled, the assimilation of P in the upper layers in spring and accumulation in lower layers in autumn. A level of phosphorus annually into and retained in lake Biwa falls as particulate phosphorus to the lake bottom.

The impact of the increase of N:P ratios on the lake ecosystem is unknown. However, this ratio was higher compared to the other lakes seemed to be one of the significant limnological characteristics of Lake Biwa (Nakanishi et al, 2001). Future studies should examine the response and adaptation of lacustrine organisms to the N:P increase. Previous ecological studies of the other

lake suggest that N:P ratios can affect the species composition and phytoplankton and zooplankton (Elser and Hass,1994; Jeppssen et al., 2000).

3.5 Conclusions

Seasonal series data of water quality of the North basin of Lake Biwa which was analyzed from 1980 to 2015, divided 5 periods, have been described, indicated that the trophic status in the Lake has been changed. As a result, it is found that TP and TN concentration were still decreased and the accumulation in the bottom area of nutrients is higher than before while the resuspension process occurred during springtime in term of TP, recently. Phytoplankton biomass indicated by Chl-a data revealed the collapse and response of phytoplankton species due to the fluctuation of nutrient changes and physical factors during the analyzing period. The season-specific Chl-a profile generated in this study concluded that the vertical flux profiles of TP, TN were compared, and a definite difference was found especially in the inversion of TN and Chl-a in wintertime. Seasonal events in the flux profiles are described. Although the mechanism of the relationship requires further study, Chl-a and TN, TP fluxes suggest that Chl-a flux negative or positive depending on the fluctuation of TN, TP fluxes. The effects of the TN and TP nutrient resources on Chl-a are both considerable and relevant, however, TP plays a more important role than TN to Chl-a. Finally, from the flux profile, we also can know how much amount of nutrients and Chl-a has remained in each layer and each season. The mass change was very different in the upper and middle layer while small in the lowest layer for TN, wide range in the metalimnion for Chl-a, and varied in the hypolimnion for TP. N:P ratios in Lake Biwa were high in the metalimnion, ranged from 83 to 108, highest in spring, lowest in autumn - in surface area, but decreasing from 57 to 103, highest in autumn, and lowest in spring - in bottom layers.

CHAPTER 4. INTERNAL WAVES, GYRES ASSESSMENT AND THE IMPACT ON DISTRIBUTION OF CHLOROPHYLL-A IN LAKE BIWA

4.1 Introduction

Lake Biwa consists of the shallow South basin that is 4 m deep and the north basin 50 m deep. Those basins are divided by the Grand Bridge at the narrowest Katata section, and the basin-scale internal seiches are possible only in the North basin. Internal seiches, basin-scale internal waves of the longest period in the North basin of Lake Biwa, have been investigated mainly in numerical studies (Kanari 1975; Oonishi & Imasato 1975; Shimizu et al. 2007); only a few field studies have recorded the internal seiche process *in situ.* The earliest record was shown in the pioneering work of Kanari (1975), where the simultaneous measurements at Kido and Sugaura points in North Basin with nearly opposite phases of the seiche, lasted for a week in early October of 1971. Endoh (1978) measured in Lake Biwa to get bathy-thermographs covering the whole basin for successive four days in August 1973, which revealed two cycles of the internal seiche with a rotating nodal line and it was the first appearance of the internal Kelvin wave in Lake Biwa. Hayami et al. (1996) demonstrated the records in September 1993 from multiple current meters and thermistor chains in the southmost part of the North Basin including internal surges which were part of the internal Kelvin wave.

In contrast, in the first gyre in the northern part of North Basin, the counter-clockwise rotating circular current appears between Funaki and Hikone in the stratified seasons, which has attracted to several field-based studies in which measurements were done to record vertical profiles of water temperature along the survey lines to estimate geostrophic currents forming the gyre. Akitomo et al. (2009a) considered the cyclonic first gyre from May to December assuming that it was wind-driven, especially due to wind-curl, and described the annual process as monthly averaged current patterns. Toda (2013) reviewed these studies to show the prospects of energetics and the formative mechanisms.

The current was thought to be wind-driven however Oonishi (1976) demonstrated that the gyre could be induced by surface heat fluxes within three months of summer, which was confirmed by Ookubo et al. (1984) in laboratory experiments of the gyres on rotating turntables considering

similarities of both Rossby and the vertical Ekman numbers. Akitomo et al. (2009b) discussed formative mechanisms of the gyre under the annual variation of surface heat fluxes. Endoh (1986) revealed the effects of eddy viscosity on the meridional convective circulation and the gyre by using measured temperature profiles to get numerical velocity field on the computational grid apart from the inviscid theories. Endoh et al. (1993) also compiled existing current data at several stations to show the gyre structure because of the current direction. Kumagai et al. (1998) succeeded in finding the current structure and gyre patterns by using the acoustic Doppler current profiler, then Ishikawa et al. (2002) discussed the gyre hypothesis suggesting a combination of physical and biotic processes whereby buoyant particles such as bloom-forming cyanobacteria are conveyed offshore and accumulate in surface waters at the down-welling center of the gyre and that the gyre ecosystem model could be possible as a good natural indicator to understand the offshore-inshore and physio-biological coupling processes.

The uni-nodal internal seiche with an approximate two-day period, which is longer than the inertial time scale, and the Coriolis effect has an essential role for the fluid motion. It is the internal Kelvin wave of the basin scale, and the period is not affected by the Coriolis parameter. Kanari (1975) showed simultaneous measurement at two stations (Sugaura in the north and Kido in the south), and they were of antiphase in the internal seiches and with a period that ranges from 46 hours to 53 hours and measured as 66 hours.

The uni-nodal internal seiche is known as the uni-nodal internal Kelvin wave (UIKW) in Lake Biwa. The topography is important in the north basin of Lake Biwa, and it is deeper in the west and shallower in the east. Oonishi and Imasato (1975) described a topographic Rossby wave in which potential vorticity changes according to the local topography instead of the latitude.

However, previous studies did not analyze the current and internal waves during a long period and the relationship between them. According to the concept that the gyre is thermally induced and a quasi-steady current, is the wind that sets up the internal seiches. Once a large-scale internal wave occurs, the gyre disappears and then recovers afterward. During temperature transects in field surveys of the gyre, evidence on the internal Kelvin wave was found and reported. We would like to examine this hypothesis. Therefore, this study aims to obtain records of successive temperature profiles at stations of opposite phases for the internal Kelvin wave, and relationship to the internal Poincaré wave or lateral internal seiches as well as coexistence with

thermally- or wind-induced gyres and difference from the topographic Rossby wave. The Interval time of internal waves and velocity of gyre would be calculated. The internal seiche in autumn could of finite amplitude and both the evidence from the gyre and the internal seiches would be obtained in the summer at two stations.

4.2 Methods

Two thermistor chains were anchored as close as possible to Sta.12B (Central off Minami-Hira: 8 layers in 60 m) and Sta.17B (Central off Imazu: 10 layers in 90 m), as shown in Figure 4.1. This was done by the Research Vessel BIWAKAZE from Lake Biwa Environmental Research Institute (LBERI). Two arrays of temperature loggers were deployed twice from 14 October 2016 and from 14 June 2017 for around three months each, where it was additionally expected to be used to interpolate the half-monthly measured data of the routine by the prefecture. Each location of the temperature stations was not far from Sugaura or Kido station used by Kanari (1975). The northern Sta.17B is close to the first gyre at its northern rim, and the southern Sta.12B is on the western rim of the third gyre.

Arrays of temperature loggers (HOBO Water Temp Pro v2 ONSET) were set at the depths as the sampling in the monthly survey routine (0.5 m, 5 m, 10 m, 15 m, 20 m, 30 m, 40 m, and 50 m at Station 12B with 60 m and 80 m at Station 17B). By doing this, it would become possible to understand the effects of stratification and internal seiching on properties of water quality such as dissolved oxygen or chlorophyll-*a* as passive tracers. This is the additional merit to interpret the results of half-monthly intermittent measurements as a temporally continuous record by using an hour interval, as in Table 4.1

Table 4.1 Temperature profile records measured in the present study

Station	Layers	Depth	Autumn 2016	Summer 2017
17B	10 layers	86 m	Oct 14, 2016	Jun 14, 2017
12B	8 layers	59 m	to Jan 6, 2017	to Sep 13, 2017

On the first and the last day, the CTD profiler (AAQ-RINKO: JFE Advantech Co., Ltd.) was cast to detect limnological conditions on the days of install and uninstall of instruments. Simultaneous profiles of water qualities were also taken on the first and the last day of the first mooring for the record: 14 October 2016 and 6 January 2017 and of the second series: 14 June and 13 September 2017.

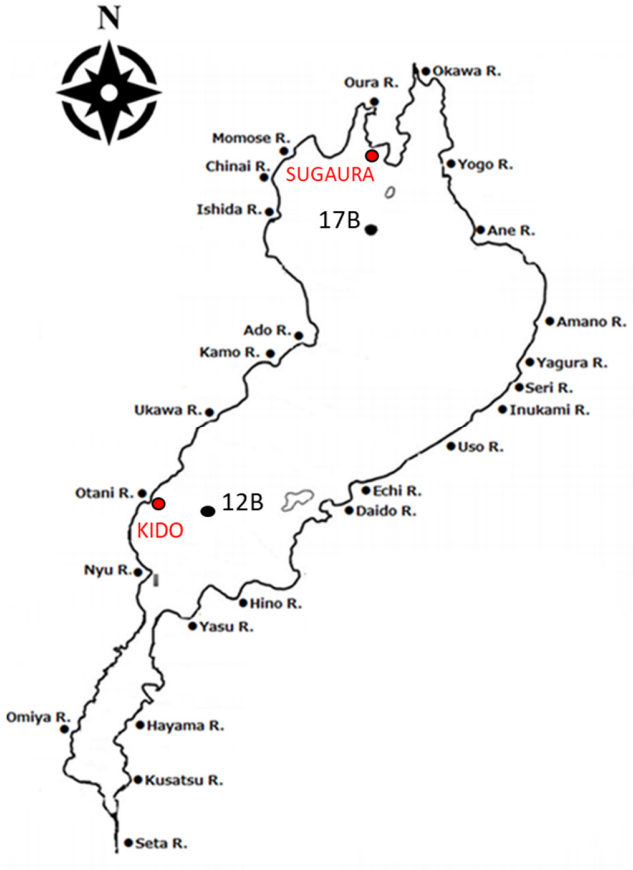

Figure 4.1 Location of limnological stations with Sugaura and Kido points (partially modified from Okubo et al. 2021)

Shimizu et al. (2007) compared several modes of the internal waves in the north basin of Lake Biwa, among which vertical mode 1, horizontal mode 1 (hear after V1H1) Kelvin (43 h), and V1H1 Poincare (11 h) according to their notation will be considered here. The former covers the total basin and is identified as the internal Kelvin wave on which Kanari is considered, and the latter is similar to V1H3 (or V1H4) Kelvin. The topographic effect in Lake Biwa is perhaps not easy to identify, and no data can be compared to the numerical results.

Kanari (1975) reproduced the internal Kelvin wave in a two-layered numerical model of the square lake (50 km in altitude, 14 km in longitude, and a uniform depth of 50 m), which is the sum of the upper layer of h_1=17.5 m and the lower layer of h_2=32.5 m, leading to an internal celerity of C_2=0.53 ms^{-1} by using the typical value of the relative density difference between the layers, $\varepsilon = \Delta\rho/\rho$. This resulted in a calculation of the period of the uni-nodal seiche: T_2＝52.4 hours. According to his records at Sugaura and Kido, the period of the internal seiche was 45.5 hours in the mid of August, 53.0 hours in late September, while in the model it was 66.1 hours conducted under an autumnal condition in excellent accordance with the measurement.

4.3 Results and discussion

4.3.1 Vertical profiles in water temperature and dissolved oxygen

On the days above, profiles of water temperature and dissolved oxygen at Imazu (solid lines) and Minami-Hira (dashed lines) are shown in Figure 4.2. Vertical profiles of water temperature and dissolved oxygen are shown on the first and the last day of the first series of the record: 14 October 2016 and 6 January 2017 and of the second series: 14 June and 13 September 2017. Temperature profiles October 14 show a sharp thermocline, which is a 3 m shallower at Imazu, and a similar difference between the DO profiles. In the epilimnion, Chl-*a* was uniform 2 gL^{-1} beneath which DO profiles took the local minimum, and a gradual decomposition in late summer of phytoplankton was likely occurring. All of the profiles are uniform in the upper 50 m on January 6, 2017.

The thermocline was shallower at Imazu on June 14 but deeper on September 13, which seems certainly due to the internal seiche and it is considered to be the main reason for the variation in the profiles obtained in the monthly survey routine. The difference in the thermocline

displacements looks typical. The DO profiles showed the local minimum in September; however, the local maximum occurred during the blooming in June. The situation in the second term was a stratification and followed seasonally by the first term, monomictic destratification.

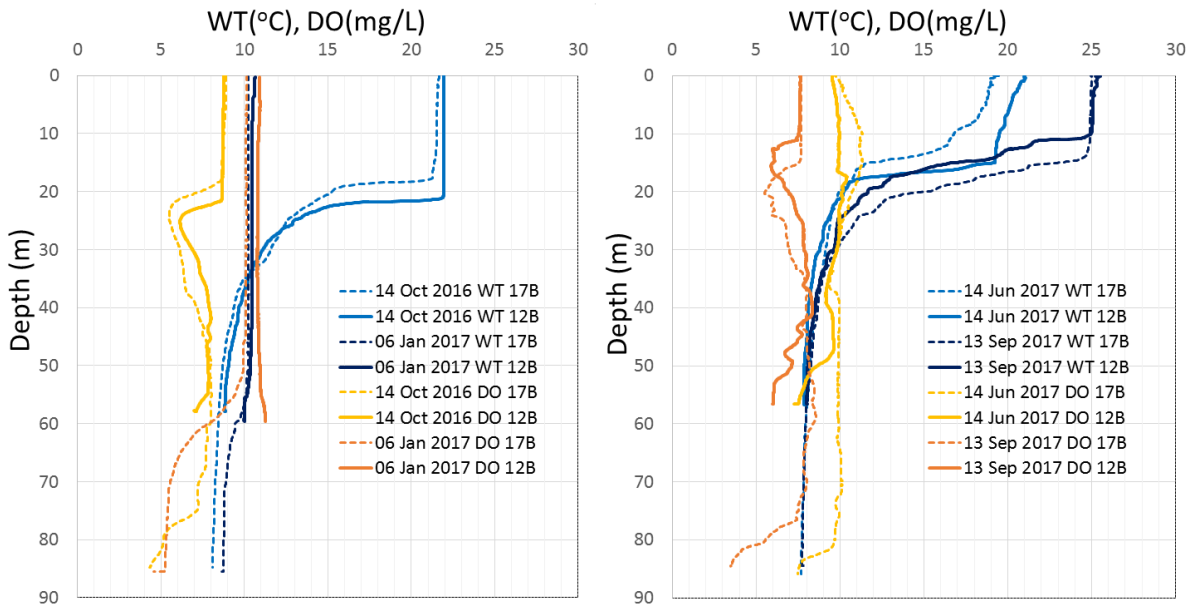

Figure 4.2 Vertical profiles in water temperature and dissolved oxygen on the first and the last day of the measurements: 1) 14 October 2016 and 6 January 2017; 2) 14 June and 13 September 2017 (partially modified from Okubo et al. 2021)

4.3.2 Seasonal temperature record

Temperature records from the two stations are shown for the autumn of 2016 in Figure 4.3 and the summer of 2017 in Figure 4.4. The former shows the temperature records at the stations and wind speed squared in the autumn of 2016. Temperatures at 20 m and 30 m depths off Imazu (Sta. 17B) and 20, 30, 40 m off Minami-Hira (Sta. 12B) exceeded a variation of 5 degrees at those depths. Three dashed square frames showed “M” or “W” characters like temporal temperature variation patterns in 1.5 times the seiching period, and the squares become wider as the temperature difference reduces and the internal celerity falls. The seasonal destratification shows a total mixing event with deepening thermocline as a modulation in the wave period. In contrast, Figure 4.4 shows

the temperature records at the stations of the forming stratification and established thermocline with maximum stability and wind speed squared (summer of 2017). Temperatures fluctuate over 5 degrees at 15 m depth off Imazu and at 10 m, 15 m, 20 m and 30 m off Minami-Hira except for the typhoon event around August 8, before which the temperature fluctuations were calm for a month at Imazu, corresponding to the established gyre current. The squared wind often exceeded 100 m^2s^{-2} in the autumn but rare in the other summer.

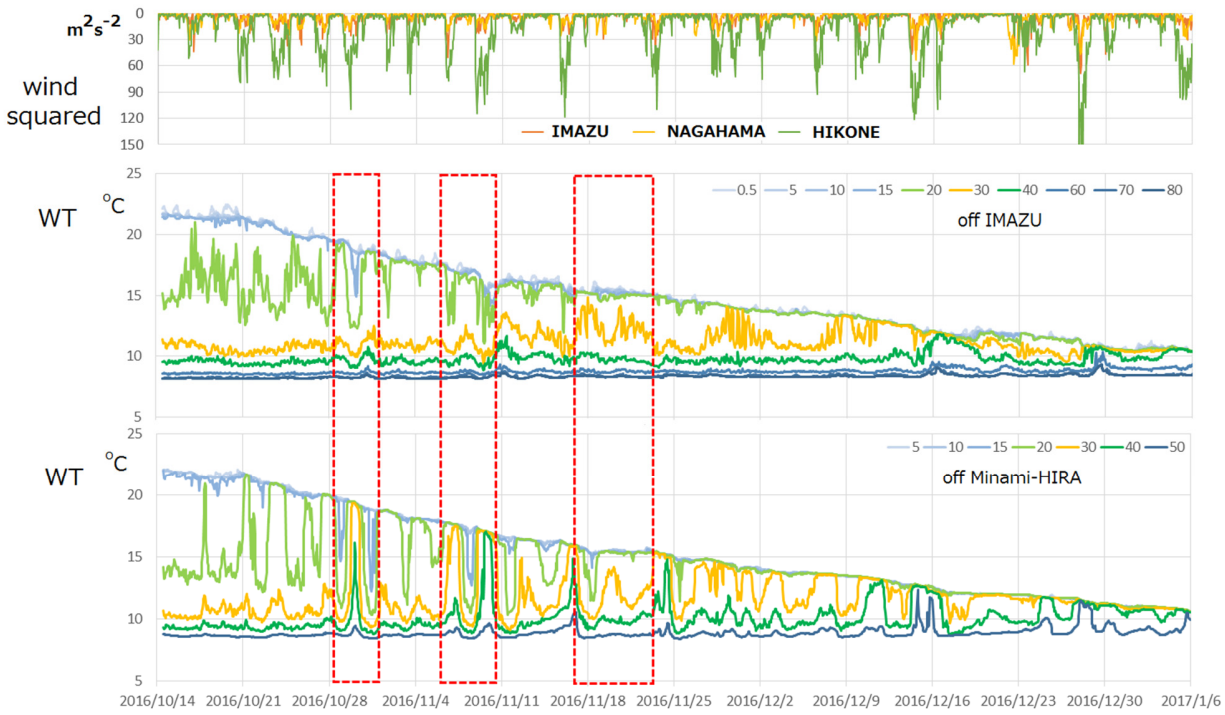

Figure 4.3 Temperature records at the stations and wind speed squared (2016 autumn) (Temperatures at 20 m and 30 m at 17B (Imazu) and 20, 30, 40 m at 12B (Minami-Hira) exceed variations of 5 degrees. Three dashed squares show “M” or “W” patterns for 1.5 times the period, and the squares get wider as the temperature difference reduces) (partially modified from Okubo et al. 2021)

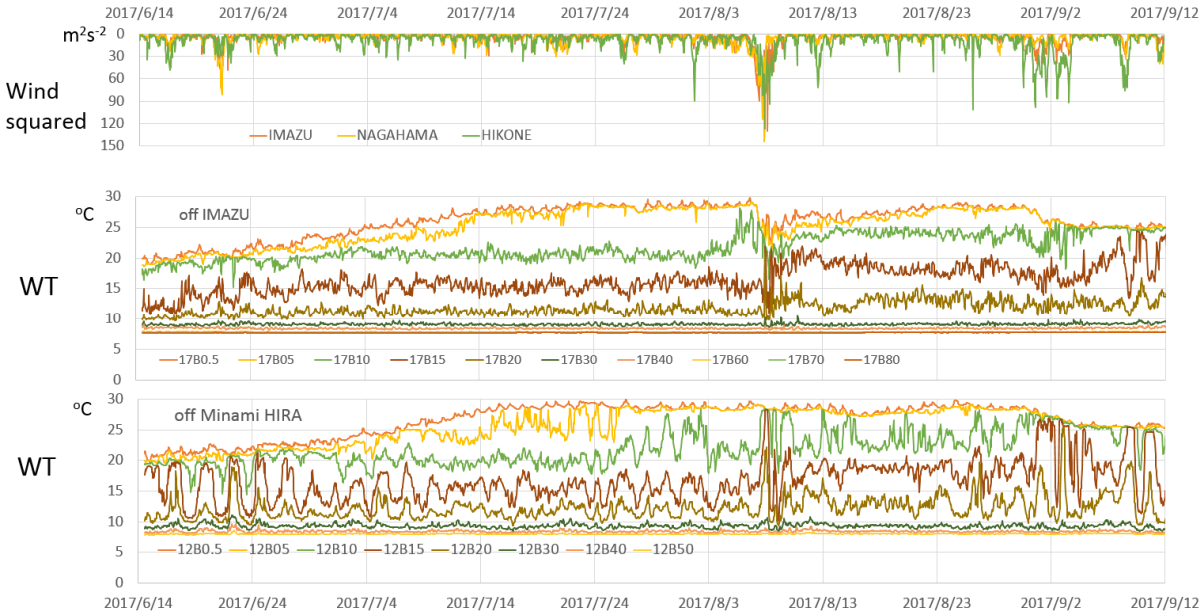

Figure 4.4 Temperature records at the stations and wind speed squared (2017 summer) (Temperatures fluctuate over 5 degrees at 15 m at 17B (Imazu) and 10, 15, 20 m at 12B (Minami-Hira) except for the typhoon event around August 8, before which temperature fluctuation was calm off Imazu, corresponding to the established gyre current) (partially modified from Okubo et al. 2021)

4.3.3 Buoyancy flux calculation

In Figure 4.3 and Figure 4.4, amplitudes of isotherm displacements are larger off Minami-Hira Sta. 12B than off Imazu Sta. 17B. However, vertically integrated spectra are similar in magnitude at these stations of different depths 60 m and 90 m. On the other hand, the buoyancy flux could be shown as the vertical profile, and the surface value $B(0)$ is converted to the thermal energy flux, H $[Js^{-1}m^{-2}]$. The unit of the depth-integrated spectra for temperature variation is [mK^{2}d], which is proportional to the part of buoyancy flux as $B = [\alpha g\{\Delta Th/\Delta t\}]^2/[m^2s^{-3}]$.

Buoyancy flux is the local time change in the fluid density multiplied by the gravity acceleration and divided by the reference density integrated over the depth. It would be discussed on the relationships with the gyre where it is necessary to calculate the vertical component of the

buoyancy flux. When B is buoyancy flux (m^2s^{-3}), g is gravity, ρ is the density of water. h is the thickness of the water column. By using instantaneous maximum density, and the positive flux stabilizes the water column. In case that the bottom temperature (density) is almost constant (e.g., at the deepest area in the north basin of Lake Biwa), the zero thermal flux is thought to be at the bottom. In other cases, especially in winter, the maximum density is disturbed by the dense bottom current on the sloping bottom.

$$\mathrm{A} = \frac{g}{\rho_0}\int_{-h}^{z}\frac{\partial(\rho_0-\rho_{max})}{\partial t}d\zeta$$

where $\rho_0 > \rho_{max}$ is selected, then

$$B_0(\mathrm{z}) = \frac{g}{\rho_0}\int_{-h}^{z}\frac{\partial(\rho_0-\rho)}{\partial t}d\zeta = B(z) + A$$

The bottom temperatures in Fig. 4.3 and Fig. 4.4 are normally the lowest at around 8ºC but varied somehow in late autumn, especially off Minami-Hira. Only minor effects are seen in the buoyancy flux when the internal seiching becomes dominant.

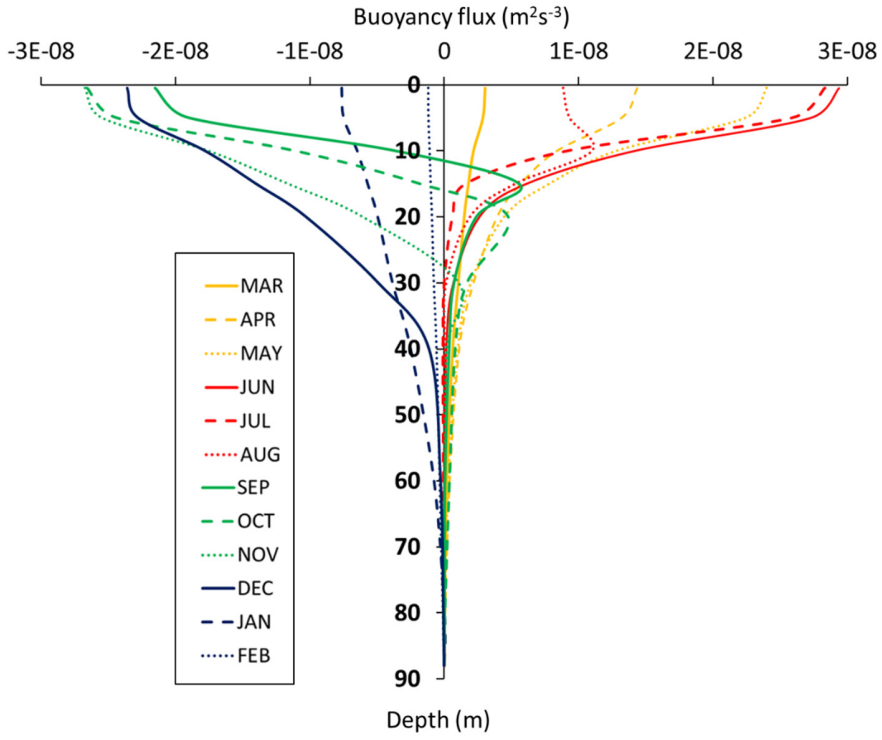

Figure 4.5 The 35 years averaged monthly buoyancy flux profiles indicate total mixing processes among layers in Lake Biwa at 17B

On the other hand, by analyzing long-term seasonal buoyancy flux, the profile shows the result that the high temperature that happens in the surface layer was in May, June, and July before decreasing after August (Figure 4.5). The cooling period starts in September and prolongs until January. The temperature profile became almost uniform in February, reached minimum total heat budget, before slightly increasing from March, and the lake was again stratified. The buoyancy flux of temperature indicated that it is only considered in the epilimnion but into the upper thermocline by the turbid intrusion in early autumn. The surface process in the heating period because of biotic photosynthesis. Akitomo et al. (2004) revealed that cyclonic circulation was created by the combined effect of bottom topography and vertical diffusion with the heat accumulation effect. At the end of the stagnant period (September), the difference in the temperature between the epilimnion and the hypolimnion becomes small and the amplitude of the internal wave consequently increased. Sakai et al. (2002) reported that it is not only the availability of the released phosphorus compounds for biota but also internal wave-induced resuspension of the bottom sediment that could be a source of phosphorus other than the external sources such as stream water. Internal waves consequently occur in seasonally different water depths, range from 5 m to 40 m during the stagnant period. Okubo et al. (1984) declared that an internal wave is likely to induce resuspension of a wide area of bottom sediment. Bottom sediments also include much higher amounts of nutrients and reduced substances, such as phosphorus and ammonium, than the water column, and resuspension of the sediment due to internal waves could influence chemical characteristics of lake water (Pierson and Weyhenmeyer, 1994). Okubo et al. (1984) mentioned that the larger-scale currents in lakes such as the gyres in Lake Biwa are formed by heat accumulation due to solar radiation. The strongest gyre activity occurs at the peak time of the buoyancy flux in June to July and the established gyre decays and ceases from September to October. The first gyre in the north basin could be thermally induced, and its velocity is relevant to the buoyancy flux at the lake surface in July. The gyre should be in the balance of geostrophic or gradient currents where the configuration of the epilimnion is established in equilibrium and maintained algae ecosystem calm by the meridional circulations, which is convergent in the top epilimnion and divergent in the upper metalimnion. The gyre becomes strongest at the maximum buoyancy flux from June to July. Then the gyre decays and instead the internal seiches increase amplitude at the depth range of 10 m to 40 m in autumn from October to November. Detect the

local maximums showing “turbid intrusion” from August to November, which are the entrance to the eco-system for the nutrients due to flooding. From the result of buoyancy flux, the gyre formation and internal seiches effect on nutrient distribution during the stratified season were discussing together with analyzing nutrient and Chl-a fluxes.

The fluxes are normally higher than in seasonal heating or cooling reported in Figure 4.5, typically

$$|B| \leq 3.0 \times 10^{-8} [m^2 s^{-3}]$$

Through the conversion, $B = \alpha g H / c\rho [m^2 s^{-3}]$, the thermal energy flux, H could be

$$|H| \leq 45 \, [W m^{-2}]$$

for the value of thermal expansion, $\alpha = 0.00028 \, [K^{-1}]$.

The surface buoyancy fluxes off Imazu and off Minami-Hira at the top surface (the air-sea interface) are shown in Figure 4.6 and Figure 4.7 for the autumn of 2016 and the summer of 2017, respectively. In the figures, surface buoyancy fluxes at the stations during the measurement could variate between positive and negative values and the amplitude is described as follows: Except for the typhoon attack, it is usually higher in the stratified and mixing seasons,

$$|B| \leq 3.0 \times 10^{-6} [m^2 s^{-3}]$$

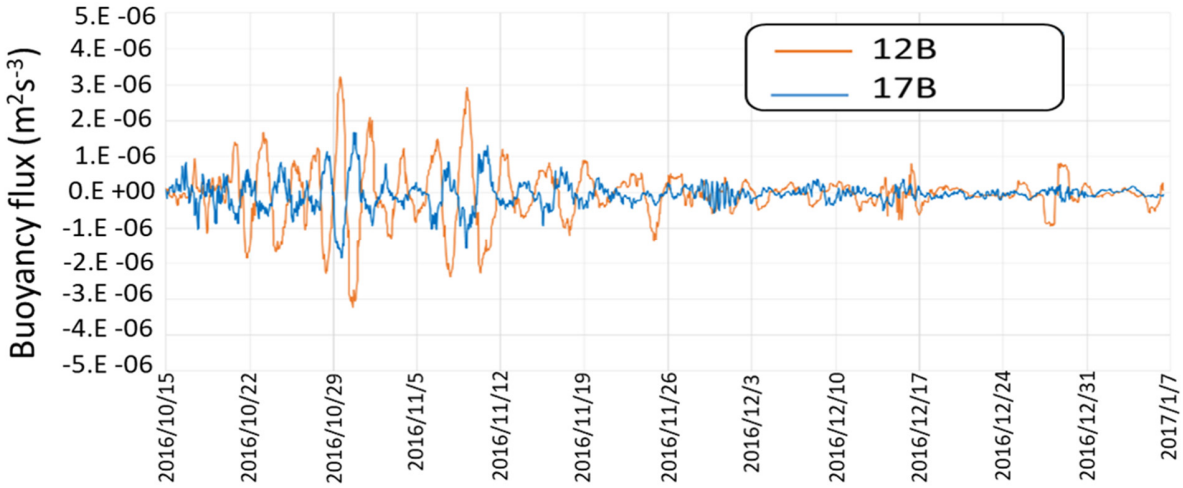

Figure 4.6 Surface buoyancy flux at the stations during the measurement in the autumn of 2016 (partially modified from Okubo et al. 2021)

Figure 4.7 Surface buoyancy flux at the stations during the measurement in the summer of 2017 (partially modified from Okubo et al. 2021)

When the epilimnion increases its depth at a station, the heat content or the stored buoyancy at the water column reaches a local maximum and vice versa at the other station. Comparing with the other panel of each figure, positive buoyancy flux arose when the thermocline went down at the station as a result of advective buoyancy flux due to the internal Kelvin wave. Figure 4.8 schematically shows the functions with the time lag of $\pi/2$ between thermocline depth and the surface buoyancy flux at a station, while the lags are π between the stations for the quantities. Isotherm depths and surface buoyancy fluxes at the stations were both of opposite phases between the north and the south stations. When the surface buoyancy flux takes a local maximum at one station, it takes a local minimum at the other station, the isothermal depth was around average toward the deepest at the former station and toward the shallowest at the other station. The surface buoyancy flux is thus a depth-integrated indicator of the phase of the internal seiches, which enables the analysis of transition in the periodicity.

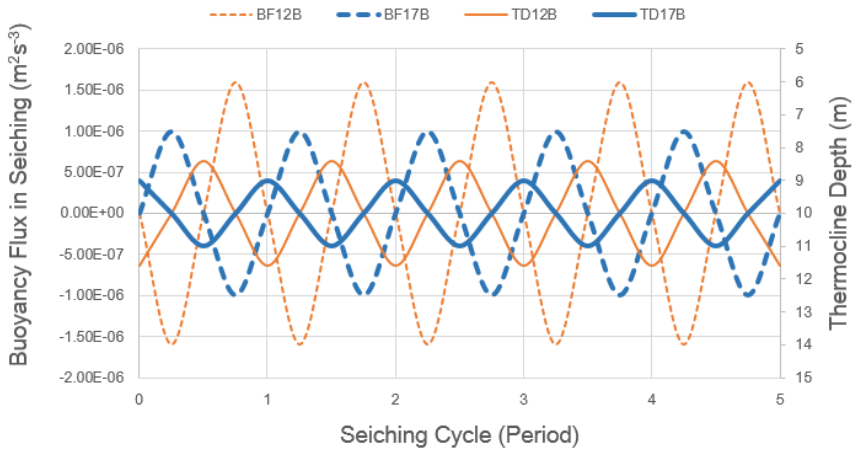

Figure 4.8 Schematic of the buoyancy flux (BF) and the corresponding thermocline depth (TD) with opposite phases between the stations (partially modified from Okubo et al. 2021)

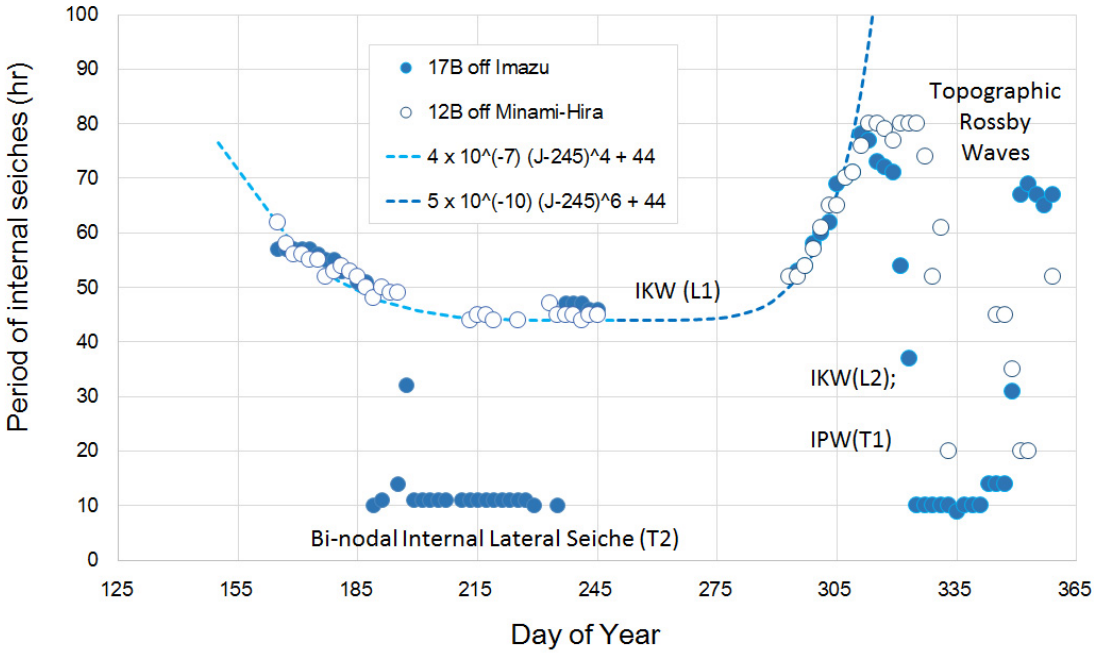

Figure 4.9 Seasonal variation in the period of the UIKW, the rotating uni-nodal internal seiche in Lake Biwa (partially modified from Okubo et al. 2021)

4.3.4 Internal Kelvin waves and Gyre velocity calculation

The results show that the IKW period before and after September 2 (J=245) are respectively as shown in Figure 4.9. The fluxes at the stations are of almost opposite phases, and there is a seasonal variation in the period depending on the day of the year. Data from the measurements in the autumn of 2016 and the summer of 2017 were used, where the periods were measured as the first positive peak of autocorrelation function in the surface buoyancy flux instead of temperatures of layers. Antenucci and Imberger (2003) described the seasonal change in the period of the internal seiches in a lake, cyclonic, and anti-cyclonic in Lake Kinneret. This may relate to the second gyre observed between the first and the third gyres in the case of Lake Biwa. Long lakes of a geophysical size such as Lake Geneva have multiple internal Kelvin waves of alternative rotations.

$$P[hr] = 4 \times 10^{-7}(J - 245)^4 + 44 \qquad \text{J<245}$$

$$P[hr] = 5.0 \times 10^{-10}(J - 245)^6 + 44 \qquad \text{J> 245}$$

It is positive correlations of the full period, and negative correlations of half the period were also seen between 22 h to 33 h, where *J* denotes the Julian date. The latter is considered the diurnal internal Poincare wave, relating to the lateral scale shown in Figure 4.1 such as between Anegawa and Wani (35 km), Imazu - Hikone (22 km), Adogawa - Hikone (14 km), Omizo - Echigawa (11 km). It is possible to determine the internal celerity by using the longitudinal scale of UIKW as 44 km with the period. The celerity is calculated from the stratification as

$$C_i = \sqrt{\varepsilon g h_1 h_2/(h_1 + h_2)} \qquad \text{or } P_i = 2l_i/3600C_i$$

for the northern part including Station 17B and the southern part including Station 12B of the north basin. The relative density difference ε was found in the average monthly profile data from LBERI. Thermal expansion and temperature difference scale T were selected by using the monthly averaged profiles over years. Thus, assuming the wavelength, the measured period was compared with the calculated celerity from monthly temperature profiles, and some parameters are seen in Table 4.2.

Table 4.2 Monthly conditions for the internal waves in Lake Biwa. S/NB, N/NB: Southern and Northern part of North Basin, Lake Biwa; KW/PW: Internal Kelvin and Poincaré Wave; B: Buoyancy flux at the air-water interface; V: Gyre velocity; Ro: Rossby number; F: densimetric Froude number; R_{io}: Overall Richardson number. (partially modified from Okubo et al. 2021)

Month	h_1 (m)	h_2 (m)		10^3 ε	Celerity (ms^{-1})		c_i	Period (h)		10^8 B m^2s^{-3}	V ms^{-1}	Ro	F	R_{io}
		12 B	17 B		12 B	17 B	Ave	KW	PW					
May	20	20	30	1.3	0.36	0.39	0.37	65.4	32.7	2.4	0.15	0.12	0.30	11
Jun	15	25	35	1.9	0.42	0.44	0.43	56.8	28.4	3.0	0.17	0.13	0.31	10
Jul	12	28	38	3.4	0.53	0.55	0.54	45.3	22.6	3.0	0.17	0.13	0.26	15
Aug	12	28	38	3.5	0.54	0.56	0.55	44.6	22.3	1.0	0.11	0.09	0.18	31
Sep	15	25	35	1.9	0.42	0.44	0.43	56.8	28.4	-2.2	-0.15	0.11	0.28	13
Oct	22	18	28	1.3	0.36	0.40	0.38	65.1	32.5	-2.7	-0.16	0.13	0.30	11
Nov	25	15	25	0.9	0.29	0.33	0.31	78.9	39.5	-2.7	-0.16	0.13	0.34	8.7
Dec	40	-	10	0.5	-	0.20	-	-	-	-2.4	-0.15	0.12	0.35	8.3

A considerable reason for the difference in amplitudes between the stations is in the Rossby number, which is higher due to the reduced width off Minami-Hira. For the same gyre velocity, the Rossby number is double in the south showing internal seiching but the gyre is more stable in the north as well as higher buoyancy frequency is seen in the forming process of the gyre current, and it was established in mid-July, especially at 17B off Imazu. The flux amplitude is more significant at 12B off Minami-Hira station due to the differences in area, width, shallower depth, or in a minor gyre.

The Rossby number of the gyre is defined as by using gyre diameter *D*

$$Ro = V/fD$$

The velocity of the gyre is dimensional

$$V = \chi(BD)^{1/3}$$

where V is the gyre velocity, f the Coriolis parameter; D the diameter of the gyre or the width of the lake; χ: a coefficient close to unity; B is the buoyancy flux; and h_1 is the epilimnion depth.

The buoyancy flux scales B_i [m^2s^{-3}] were shown in two temporal scales (in a day), hourly ($B_{1/24}$), and bi-weekly (B_{14}). The flux amplitudes and corresponding velocity scales for D=15,000 m and $\chi = 1$ are, respectively

Hourly basis $B_{1/24} = 3 \times 10^{-6}$ $V_{1/24} = 0.36$

Bi-weekly basis $B_{14} = 3 \times 10^{-8}$ $V_{14} = 0.077$

As the geometric mean,

On daily basis $B_{0.76} = 3 \times 10^{-7}$: $V_{0.76} = 0.17$

where the suffix denotes the corresponding days of the variable, and

$$B_{0.76} = \sqrt{B_{1/24}B_{14}}$$

The condition was found due to finite-amplitude variations in the thickness of epilimnion within half the period of the internal seiche. For $\Delta h_1 = 2\ m, and\ P/2 = 23\ h,$

$$B = \varepsilon g \Delta h_1 / 0.5P = 0.001 \times 9.8 \times 2/23/3600 = 2.4 \times 10^{-7},$$

while condition B_{14} was estimated from the maximum among bi-weekly averaged buoyancy fluxes, and it is about half the observed gyre velocity of 0.15 ms^{-1}. It is also possible to use the factor 10 to convert the monthly flux into the daily buoyancy flux or into the gyre velocity, which is to use the factor $\chi = 10^{1/3} = 2.2$ in the above. The $V_{0.76}$ gives a realistic gyre velocity and some deduced quantities are shown in Table 4.2. The negative gyre velocity corresponds to the negative buoyancy flux as surface cooling with the order of O(10^{-8}) m^2s^{-3} or seiche advection of O(10^{-6}) m^2s^{-3}, however, the velocity conversion is not expected as the vertical profile of velocity under the unstable cooling situation, are the same as the neutrally stratified, homogeneous case.

The overall Richardson number, as the inverse Froude number squared, is about 16, and the usual definition, $R_{i*} = g'h_1/u_*^2$ could be more than 10^3, which is sufficiently stable. By definition, half the squared Froude number shows kinetic to potential energy ratio, which is

$F^2/2 = 0.2^2/2 - 0.8^2/2 = 0.02 - 0.32 = 1: 50 – 1: 3$

in 8 months from May to December.

It is possible to consider the envelope of the gyres is along the closed perimeter of the internal Kelvin wave rotating counterclockwise around the amphiprotic point. According to the deepening of the thermocline, the aspect ratio between the major and minor axis varies, and there would be two amphiprotic points when the internal seiche gets close to the bi-nodal internal seiche.

The internal seiches and the gyres are temporally exclusive but share the space and the rotation. The hourly buoyancy flux is 3×10^{-6} [m^2s^{-3}], which is more than 100 times the annual maximum among monthly averaged flux of 3×10^{-8} [m^2s^{-3}]. The ratio is simply explained by the presence of the horizontal heat flux due to internal seiche. According to the vertical thermal buoyancy flux, thermal energy flux, and mass fluxes arise in a similar way across the thermocline, which is not simply vertical mixing but causes basin-scale horizontal transport of algae from south to north. From that viewpoint, we thought that physical processes may be related to the distribution of nutrients and Chl-a in the lake. The role of internal wave and gyre will be discussed in chapter 5.

4.4 Conclusions

Two thermistor chains were anchored as close as possible to Sta.12B (Central off Minami-Hira: 8 layers in 59 m) and Sta.17B (Central off Imazu: 10 layers in 86 m). Two arrays of temperature loggers were deployed twice from 14 October 2016 and from 14 June 2017 for around three months each, where it was additionally expected to be used to interpolate the record about half-monthly measured data of the routine survey conducted by the prefecture. Each location of the limnological stations was not far from the stations used by Kanari (1975). The northern Station 17B is close to the first gyre at its northern near Sugaura point, and the southern Station 12B is on the western rim of the third gyre near Kido point. Arrays of temperature loggers were set at the depths as for sampling in the monthly survey routine. By doing the measurements this time, it would become possible to understand the effects of stratification and internal seiche on properties of water quality such as dissolved oxygen or chlorophyll-*a* as passive tracers. This is the additional

merit to interpret the results of half-monthly intermittent measurements as a temporally continuous record by using an hour interval.

Auto-correlation analyses of the surface buoyancy flux allowed a calendar showing the seasonal change in periods of internal seiches. Along with the thermal stratification, the gyre is formed, established, then weakened every year. The basin-scale internal waves become amplified in autumn, when destratification goes on, and followed by topographic Rossby waves and topographic gyres. Dominant geophysical processes containing anti-cyclonic were listed up with Rossby, Burger, and Froude numbers.

The first gyre was seen during the term when the thermocline was most stable from mid-July to early October. The internal Kelvin waves decrease the period in early summer, keep constant during the mid-summer, and getting longer in process of destratification and are followed by fully mixed conditions in winter showing an inertial sub-range at the higher frequency of homogeneous side of the surface or barotropic modes. The uni-nodal internal seiche, internal Kelvin wave is the main process and the mechanism of the seasonal monomictic destratification.

The buoyancy flux changes two orders of magnitude according to the time interval between the temperature profiles. The surface buoyancy fluxes variate to the Kelvin wave and estimate the gyre velocity by specifying the time interval of the fluxes. In winter, it becomes negative showing anticyclonic or cooling gyre. The advective fluxes of internal Kelvin waves also convey particles with a weak settling velocity. The kinetic energy fraction suggested by the densimetric Froude number of the gyre is from 2% in mid-summer to 32% in autumn. This should be the ecological role of the gyre (current) and the seiching (wave) of Lake Biwa. It is a central dome of cold water of the hypolimnion, dual points on the isotherm of the average temperature of the thermocline, which is the similar shape of the bi-nodal internal lateral seiche of the period of 10 hours. The variation of 10 hours period was also seen off Minami-Hira in the fall so it is rather true of the local internal Poincaré wave of the southern part of the North Basin. It has been reported before the first gyre in autumn is clockwise, which is supported by the thermally driven gyre however the internal Kelvin wave of counterclockwise rotation persists in late November.

CHAPTER 5. GENERAL DISCUSSION

5.1 The relationship between external nutrient loading and water quality in the lake

Kunimatsu (1979) surveyed the water quality of several rivers into Lake Biwa while Morii et al. (1993) discussed the relationship between the water quality of rivers flowing into the lake and the geological environment of the river heads. The relationship of external loading to lake water quality also was limited mention. Base on the calculated nutrient loads (in seasonal) from the river and groundwater into the lake (in chapter 2) and nutrient analysis (in Chapter 3), Figure 5.1 revealed the relationship of nutrient loading and water quality in the lake which were analyzed in chapter 3. TP concentration and PO_4-P loads have the same tendency in epilimnion during the summer when the activity of gyre occurs, this might be the effective phosphorus reuse in a microbial ecosystem resulting from the severe condition on phosphorus. Because phosphorus is supplied from watershed unsteady, phytoplankton enhanced the phosphorus recycling capability such as phosphorus mineralization with phosphatase under the starving condition (Nagare et al. 2001). The high correlation coefficient between PO_4-P loads and TP concentration is 0.8 and 0.6 in epilimnion and metalimnion but low in hypolimnion could be suggested that PO_4-P loads are more relative to TP in upper layers but the impact on lower layer due to phosphorus releasing from sediment. The result of increasing TP in the surface could represent increased external loading but also reflects mobilization of phosphorus from deeper sediment. The correlation between SiO_2 loads and in-lake concentration is higher in metalimnion than other layers for SiO_2 where the diatom assimilated dissolved silica and accumulated rapidly in the bottom sediment as Si concentration in the water column decreased. The phosphorus loads effect sharply to TP concentration in the surface area suggest P is mainly taken into the ecosystem by phytoplankton while the effect of SiO_2 loads on internal nutrient is more visible in lower layers suggesting high efficiency of the silicate sink process. The size of the silica sink increasing during the circulation period through interaction between physical, chemical, and biological processes (Goto et al., 2007). In general, the contribution of phosphorus in the water column was large in epilimnion (38.3%), meanwhile, the distribution of silica was highest at 42.2% for hypolimnion. These findings have coincided with previous studies from Nagare et al. (2001); 39% phosphorus contributed to large epilimnion in a year. Goto et al. (2013) reported that the ratio of winter biogenic silica (BSi) flux to annual BSi flux was 52 to 53% in epilimnion but reached 62% in the hypolimnion.

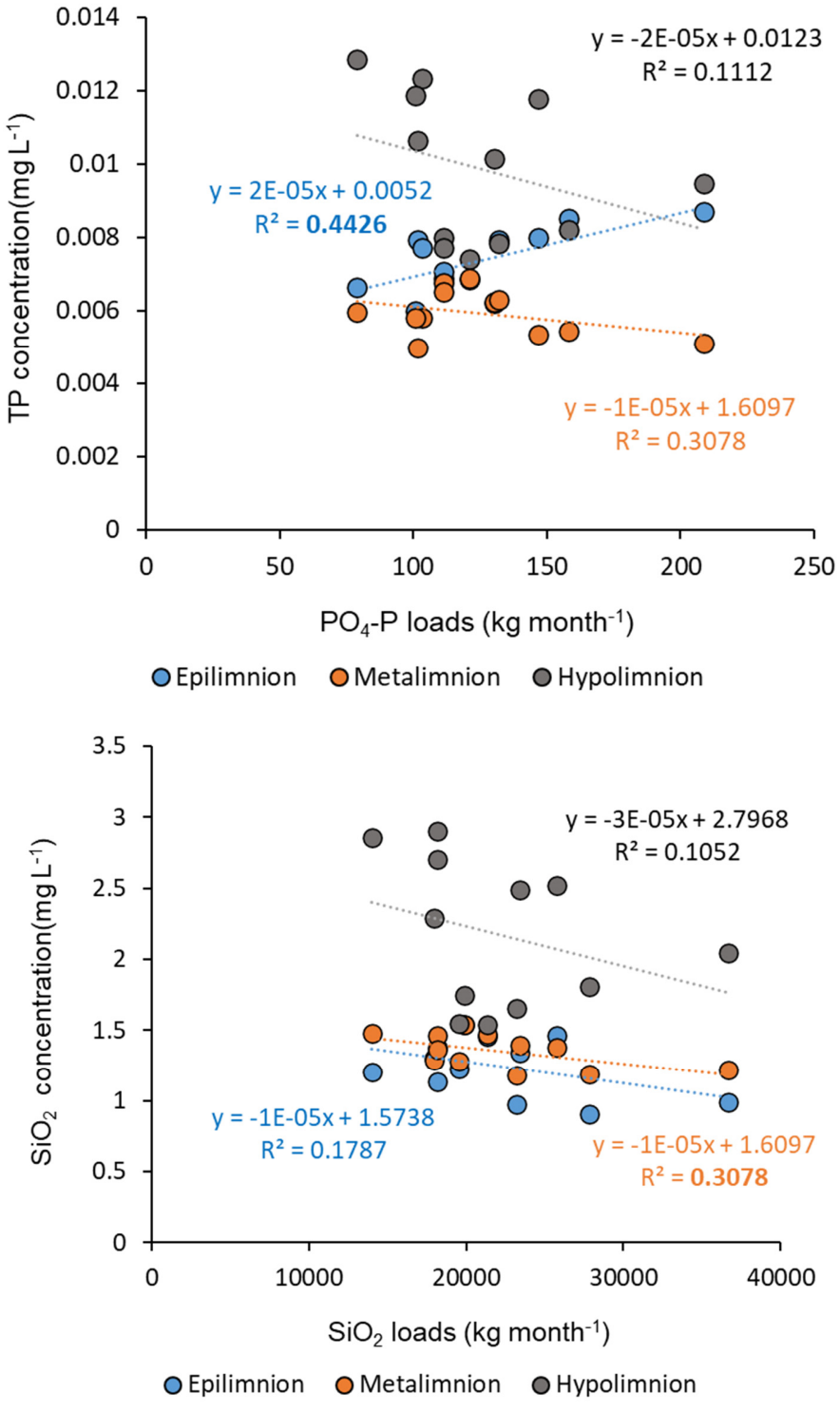

Figure 5.1 The relative concentrations in limnological layers to the monthly-averaged river concentrations of TP and SiO_2

Harashima (2006) reported that measured Si concentrations are weighted by discharge and averaged into 178 μM, while it is only 33 μM in the out-flowing Seta river. The 80% of the gain is kept in the stems of reed and rice, the cell wall of diatoms, and their cists and detritus in the muddy bottom. The recent observation of 30-year phytoplankton census data revealed that the biovolume of phytoplankton including diatoms tended to decrease with changes in their composition (Kishimoto et al. 2013) while most macrophyte species are invasive and their quantity seems to increase drastically over the years (Rabemanolontsoa and Saka, 2012). Mitamura and Tachibana (1999) investigated biogeochemical characteristics in reed zones and high concentrations of Si were observed in the Nishinoko reed zone in the North basin which was influenced by the river water from its watershed. They reported that the silicate concentration seems to be sufficient as a silica source for epiphytic algae and phytoplankton. Recently, it was shown that wetland vegetation has a considerable impact on silica biogeochemistry. Schoelynck et al. (2010) demonstrated that macrophytes contain significant amounts of BSi in the same order of magnitude as wetland species (especially grasses). They conclude that macrophytes have an overlooked but potentially vast storage capacity for Si. Furthermore, Si storage capacity is temporary owing to the annual decomposition of macrophytes in autumn and winter. The effect could be a seasonal cycle similar to that observed for spring and summer Si uptake by diatoms (Schoelynck et al. 2010). Figure 5.1 compares concentrations among the waters in rivers and lakes. The river and hypolimnion concentration revealed that external loading was just diluted by direct rainfall taking a peak in summer; while nutrients are sinking as liquid and solid including the season of internal Kelvin waves. It is commonly seen both in silica and phosphorus. In other words, epilimnion and metalimnion layers are mutual complementary for TP but strongly periodic and related to the macrophyte cycle described as, reed and macrophyte begins to sprout from the end of April, grows rapidly until about June, and the grass length continues to grow until the beginning time in late July. The upper leaves grow much from May to August, but the leaves below begin to wither around the beginning of July, and in October, the number of dead leaves increases, and all the ground parts die around November. The fluctuation of Si is related to the growth and decline of macrophytes in Lake Biwa. The total biomass on a dried weight basis of macrophytes in the southern basin of the Lake Biwa was estimated to be 10,735 ± 3,030 tons (Rabemanolontsoa and Saka, 2012) while our average total Si loading from the river is 33,290 ton. Assuming 10% weight

of the plant for Si amount, we can estimate that only 2.3% to 3.9% Si is used for reed or macrophyte growth. The remaining Si is could take part in the sedimentation process in the lake.

5.2 Comparing the N:P ratios variation at pelagic sites in Lake Biwa

In chapter 3, the N:P ratios at 17B points have been analyzed in seasonal and vertical aspects. To compare the 17B data and other stations, we collected the surface concentration of TN, TP from stations 18 to 10 from Shiga Prefecture. The map point was shown in Figure 5.2.

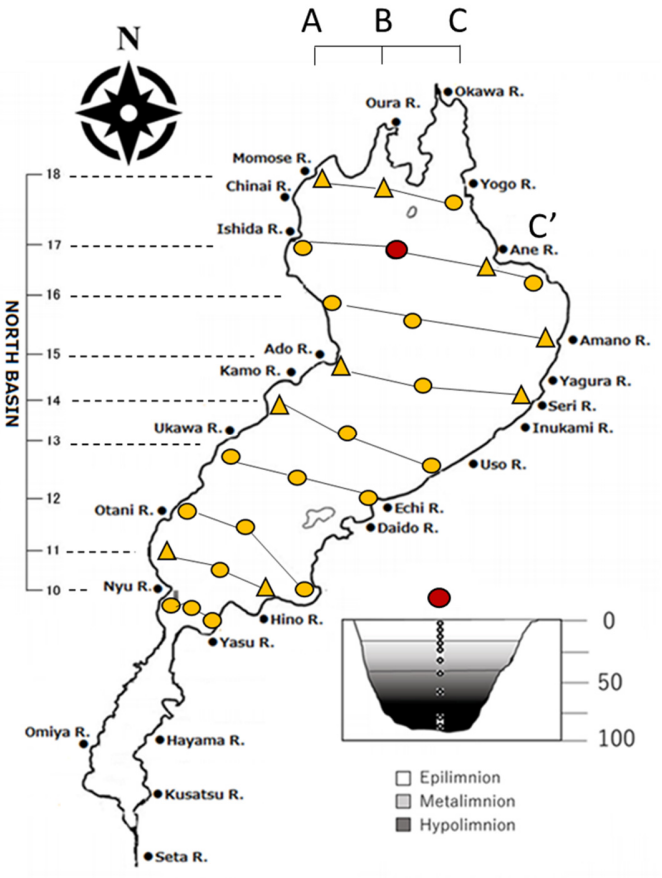

Figure 5.2 The sampling point of the surface concentration of Chl-a in the North basin of Lake Biwa (redpoint is the deepest point was studied in chapter 3) (partially modified from Shiga Prefecture, 2020)

It can be seen that the N:P ratios on the surface were high in winter and spring with the highest values about 126 but low in summer and autumn (around 60) but different in each site (Figure 5.5). In the north part, N:P ratios were highest at 15B and lowest at 12B. At station 12B, the TP concentration increased from February, reached a peak in May, and decreased after that. However, from station 15B to 18B, the tendency of TP was increased until July and kept stable after that. The TP concentration at 12B was higher than other stations (Figure 5.3) while the TN concentration was similar to other stations (Figure 5.4).

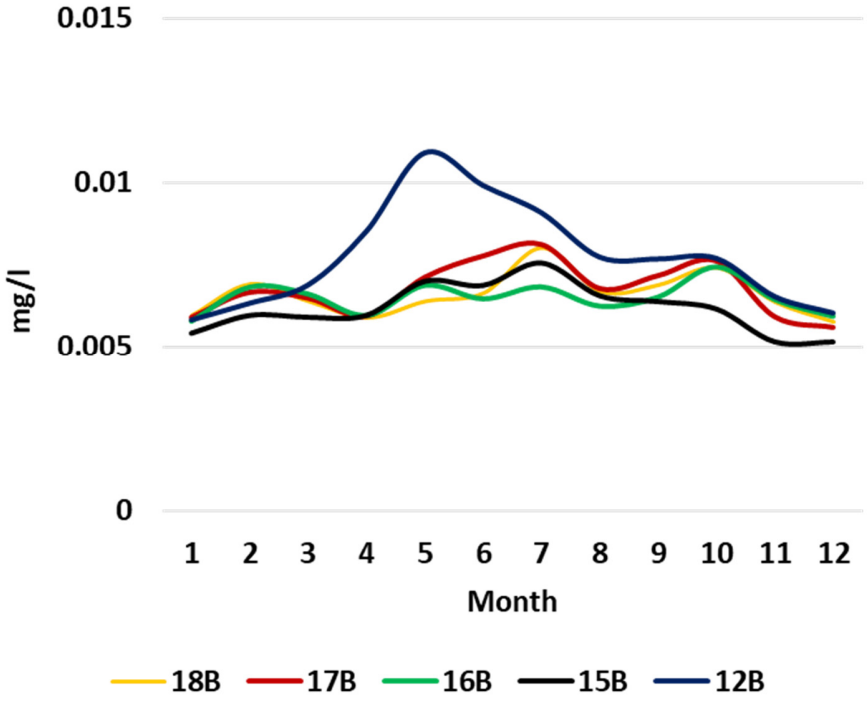

Figure 5.3 Monthly TP concentration at the pelagic stations in Lake Biwa

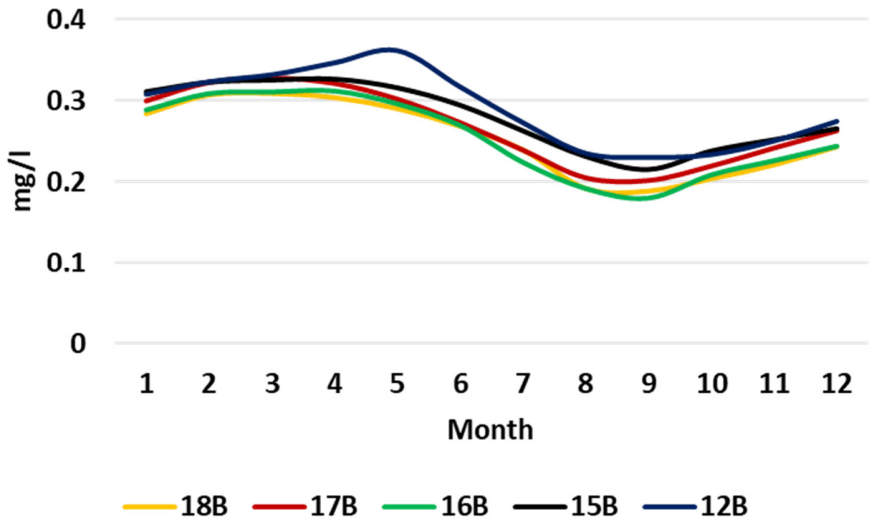

Figure 5.4 Monthly TN concentration at the pelagic stations in Lake Biwa

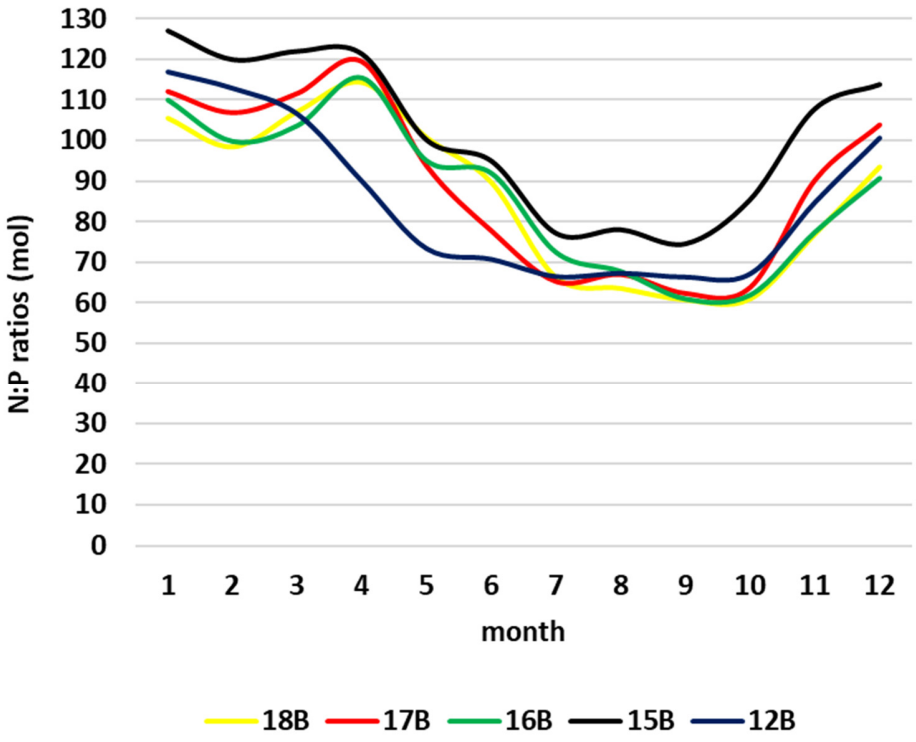

Figure 5.5 Monthly N:P variation at the pelagic stations in Lake Biwa

5.3 Physical processes impact the distribution of Chl-a

Chl-a is commonly considered as a bio-indicator of phytoplankton biomass to assess the eutrophication status in lakes. It is a pigment that can be found in phytoplankton and directly involved in the photosynthesis process. However, Chl-a fluctuations are affected not only by biological processes such as the shift of phytoplankton succession, nutrient supply but also the interaction of physical factors, especially with water bodies with complex physical processes. Recently, the physical processes as the activities of gyres existed in the epilimnion of the lake during thermal stratification (Oonishi 1976, Endoh et al.1981, Okubo 1984; Akitomo et al. 2004) and the basin-scale internal waves and internal seiche (Kanari 1975, Oonishi and Imasato 1975, Shimizu et al. 2007) were attracted several field-based studies. A few studies recorded that the great influence of advection and turbulent mixing processes on phytoplankton distribution (Okubo, 1978; Serra et al., 2003). Ishikawa et al. (1999) suggested that the wind-driven transport of phytoplankton by measuring the horizontal distribution of Chl-a concentration and cell density counting was different due to the varying physiology or morphology of these species. The distribution of dissolved or suspended material, as well as the sedimentation process, was associated with the gyres (Endoh and Okumura, 1993). Microcystis biomass increased at the center but was lower at the edge of the gyre (Ishikawa et al., 2002).

In chapter 4, we found that the first gyre was seen during the term when the thermocline was most stable from mid-July to early October. The internal Kelvin waves, on the other hand, decrease the period in early summer, keep constant during the mid-summer, and getting longer in process of destratification. In chapter 3, the vertical and seasonal flux profile provides us the difference gradient of Chl-a by month. The little fluctuation in summer increasing in autumn of this difference gradient may be related to gyres and internal wave activity. To compare the 17B data and other stations. We collected the surface concentration of Chl-a from stations 18 to 10 from LBERI. The map point was shown in Figure 5.2.

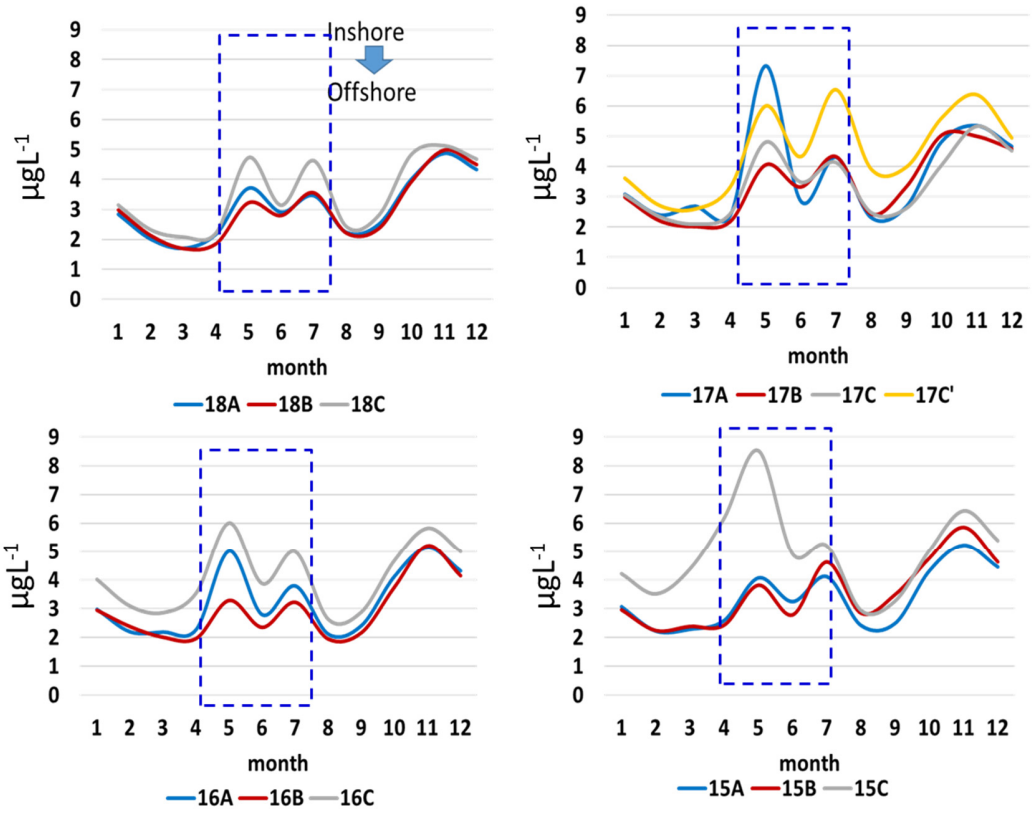

Figure 5.6 Chl-a distribution from inshore to offshore zone in Gyre-affected region

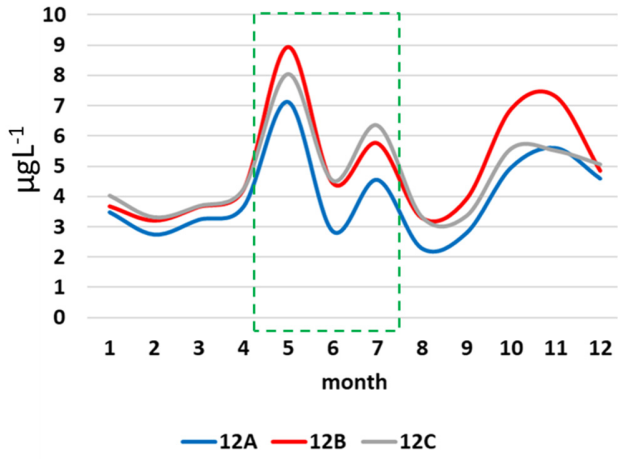

Figure 5.7 Chl-a distribution from inshore to offshore zone in Gyre-less affected region

Due to the effect of current in summer, the horizontal advection occurred and the concentration of Chl-a was lower in offshore areas than in inshore areas. The concentration of Chl-a in C and A stations were higher than station B in the area of strong Gyres activity in summer

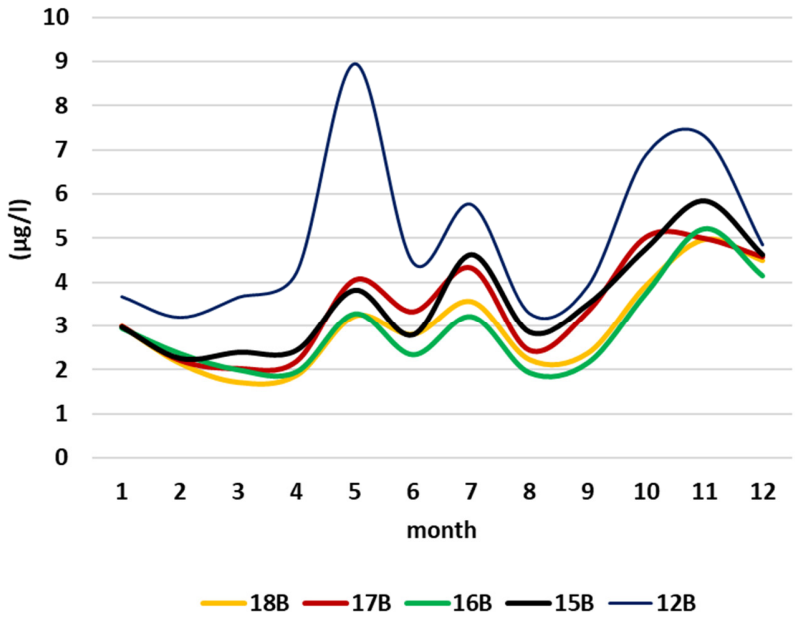

Figure 5.8 Monthly Chl-a distribution in the surface layer at the pelagic stations in North basin, Lake Biwa

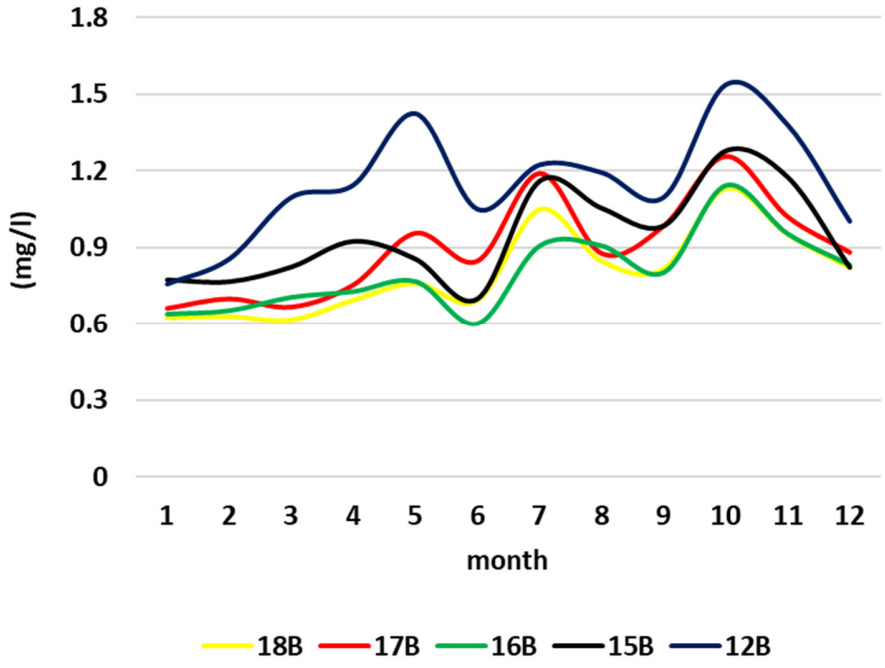

Figure 5.9 Monthly SS distribution in the surface layer at the pelagic stations in North basin, Lake Biwa

(Figure 5.6) while the difference was not clear in other seasons. However, the concentration of Chl-a in C and A stations were lower than station B in Gyre- less affected region in summer (Figure 5.7). Figure 5.8 shows a monthly variation in the surface Chl-*a*, the concentration of Chl-a at 12B station was higher than 17B, the blooming was transferred to stations 12B and 17B due to the advective flux of the internal Kelvin wave. Meanwhile, the suspended solids (SS) concentration at 12B also higher than at 17B (Figure 5.9). The peak of SS and Chl-a concentration reached in May and early November at 12B while it occurred at 17B in July and October. The horizontal fluxes are 100 times stronger than the seasonal vertical fluxes of heating or cooling was found in chapter 4. It is not only advective but rotating from the south to the north.

From 3 studies that have been conducted, we found that not only physical processes such as thermal mixing, gyres, internal waves but also external processes such as nutrient loads correspond to the in-lake nutrient and Chl-a cycle. We implied that physical processes such as Gyres activity and internal wave and nutrient external loading have an important role in the fluctuation of lake seasonal nutrient cycle and biomass shifting. The effect can be observed during the seasons and water layers. Finally, it can be exhibited by a schematic diagram as below.

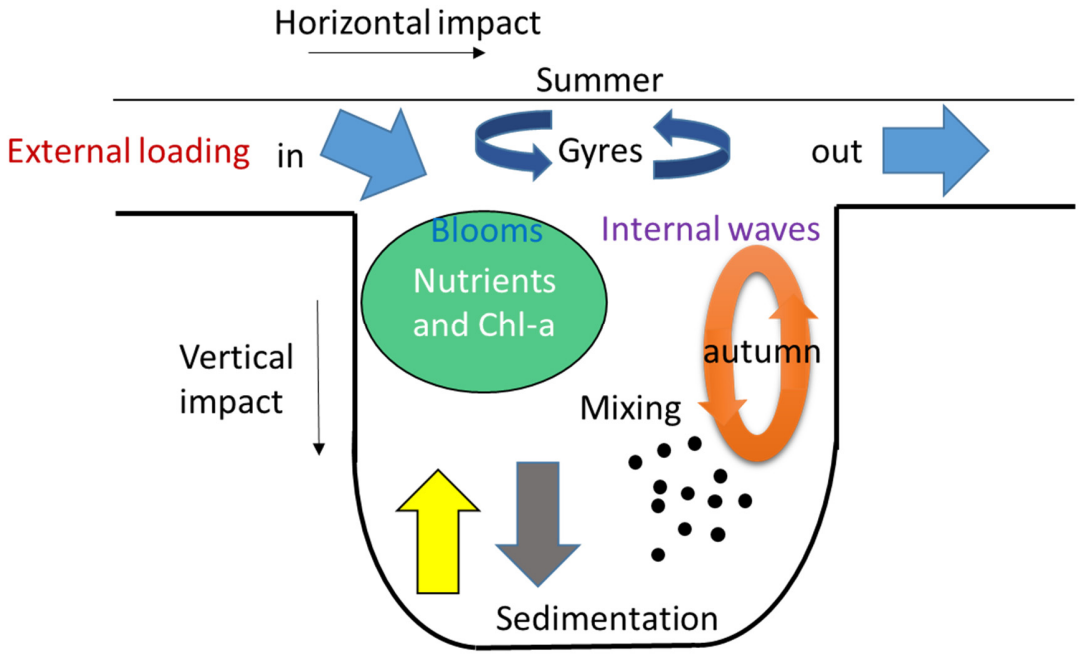

Figure 5.10 Schematic diagram showing the impact of external and internal factors on nutrient and Chl-a cycle in Lake Biwa

CHAPTER 6. CONCLUSIONS

This thesis has examined the topic of external nutrient loading to lake ecosystems, and, explored how such variations affect lake water quality, with a specific focus on the related topics of phytoplankton dynamic and physical processes. In general, the study contributes the simply combined methods by tank model and L-Q curves to calculate directly external nutrients loading from river and groundwater discharges surrounding Lake Biwa catchment. The vertical and seasonal flux of nutrients and Chl-a revealed the limnological characteristics and the relationship between in-lake nutrients and external nutrient loadings. Besides, the distribution of Chl-a and nutrients under the effect of physical processes was the first time discussed. The detailed results were shown as below:

1. The external nutrient loading including groundwater to Lake Biwa was estimated using a hydrological tank model and loading-discharge curve in chapter 2. Average PO_4-P loading was 273 tons $year^{-1}$ in the North Basin and 63 tons $year^{-1}$ in the South Basin, while average SiO_2 loading was 24,754 tons $year^{-1}$ and 5,490 tons $year^{-1}$ in the North and South Basins, respectively. The groundwater to river discharge ratio was from 0.2 to 0.28. The evapotranspiration rate was from 0.31 to 0.4. Nutrient loading in Hikone (western side) was the highest, while PO_4-P loading in Imazu (eastern side) was lowest and SiO_2 loading was lowest in Otsu (southern side). Loadings increased from March to June and reached a maximum in July, then decreased in winter and possibly affected to in-lake nutrients. However, the seasonal relationship between external nutrient loading and nutrient concentration in Lake at 17B point is not high. The vertical water quality would be analyzed by the flux profile to understand the process of seasonal change in chapter 3.

2. The monthly gradient change of nutrients and Chl-a has been analyzed in chapter 3. The accumulation of TP was observed in the hypolimnion from August to November while TN was high in the metalimnion and the hypolimnion but low in the epilimnion in autumn. Chl-a is high in summer and autumn. The flux profiles provide the information of nutrient and Chl-a cycle in Lake Biwa (loss or gain mechanism). From the flux, we suggest converting the flux to nutrient mass and biomass to find the remaining budget in the water column. The remaining mass was calculated based on fluxes profiles. However, it needs more further analysis in the future to identify

the quantifying dynamics of nutrients and biomass through production and metabolic rate, input, output factors. The change in gradient of nutrients and Chl-a may be affected by physical activities in the Lake in summer and autumn. The seasonal physical processes assessment is necessary to examine the hypothesis in chapter 4.

3. Time interval of internal Kelvin waves and gyre velocity, buoyancy fluxes of temperature have been found in chapter 4. Buoyancy flux and Gyre velocity are the highest value in June and July (summer) while internal wave periods are longer in October and November (autumn). The variation patterns of surface buoyancy flux were opposite between the Gyre-affected region and the less-affected region. The horizontal advection that occurred is the reason for the concentration of Chl-a was lower in offshore areas than in inshore areas. The concentration of Chl-a in C and A stations were higher than station B in the area of strong Gyres activity in summer. The horizontal fluxes are stronger than the seasonal-vertical fluxes of heating or cooling caused not only advection but also rotating from the south to the north. The gradient of Chl-a change was affected by biological and physical processes. The distribution of Chl-a in the surface layer is not only relying on horizontal transport from inshore to offshore but also from the south to the north of the North basin of the lake.

4. From the result in chapter 2,3 and 4, the BSMS (Blooming – Sustaining (Gyre) – Mixing (Internal waves) – Sedimentation) processes with the concept as blooming in spring, sustaining in summer, mixing in autumn, and sedimentation in winter for seasonal and vertical dynamics of the nutrient cycle were introduced. In a wider context, further examination of the long–term interactions between biological, physical and chemical processes that regulate nutrient bioavailability is an important and interesting topic. For future studies, the relationship of external loadings - in-lake nutrients - phytoplankton can be quantified by the ecological models. The vertical-horizontal model of the gyre and internal waves could be continuously analyzed based on the present results.

ACKNOWLEDGMENTS

During my study at Okayama University, I could not count on all the valuable help and sincere support from everyone. I am heartily grateful to my first supervisor, Prof. Kenji Okubo, for his tireless constructive critics and advice, he gave me the courage and strength to accomplish my thesis. Although he retired after 2.5 years of my studying period, he still has given me enthusiastic guidance. I gratefully acknowledge my second supervisor, Assoc. Prof. Mitsuyo Saito. She has been there always whenever I needed her guidance and her brilliant opinions throughout the academic degrees.

I extend my huge thanks to my co-supervisors, Assoc. Prof. Hideaki Nagare, Prof. Morihiro Maeda, and Prof. Katsuya Kawamoto for their useful advice and recommendations on my dissertation.

I would like to express my gratitude to Prof. Shin-Ichi Onodera (Hiroshima University) for his comments and suggestions. Besides, I was so lucky to stay at Assoc. Prof. Toru Iwata's laboratory with the best conditions in a friendly atmosphere. He brightly advised and commented on my work in many seminar presentations and made it possible to reach this stage. Thanks to all my laboratory members who have been together throughout these challenging and tough times. Particularly, I would like to say thank you so much to Japanese lab-mates and other people for greater support in field-work.

This thesis would not have been possible without the sponsorship of my studies by Mr. Tomio Kanemitsu for the master course, the Ministry of Education, Culture, Scientific, and Technology (MEXT) for a doctoral scholarship, Lake Biwa Environmental Research Institute and Shiga Prefecture for data providing. I would like to express my deep thankfulness for their support. Also, I am indebted to Okayama University, Graduate school of Environmental and Life Science. I have a total of 4 years to be educated by this great University and get a chance to enjoy a beautiful city, I will never forget the time I have been living here.

Furthermore, I would like to thank my colleagues at Hue University, the Union of Vietnamese Student Association in Okayama, and friends who greatly support me during the study period.

Last but not least, my deepest gratitude to my family, my wife, and my beloved little girl for their distant support and courage, patience, and understanding. They made me stronger and focused, they have been a reason to keep me moving on and reach this point.

REFERENCES

Akitomo K., Kurogi M., Kumagai M. (2004). Numerical study of a thermally induced gyre system in Lake Biwa. *Limnology*, *5*(2), 103–114. https://doi.org/10.1007/s10201-004-0122-9

Akitomo K., Tanaka K., Kumagai M., Jiao C. (2009a). Annual cycle of circulations in Lake Biwa, part 1: model validation. *Limnology, 10*(2), 105-118.

Akitomo K., Tanaka K., Kumagai M. (2009b). Annual cycle of circulations in Lake Biwa, part 2: mechanisms. *Limnology, 10*(2): 119-129.

Alexander R., Elliott A., Shankar U., McBride, G. (2002). Estimating the sources and transport of nutrients in the Waikato River Basin, New Zealand. *Water Resources Research*, *38*(12), 4-1-4–23. https://doi.org/10.1029/2001wr000878

Amano A., & Kazama S. (2012). Relationship between Discharge and Nutrient Concentration in Inundation Areas in Cambodia. *Journal of Water and Environment Technology*, *10*(2), 165–175. https://doi.org/10.2965/jwet.2012.165

Antenucci J., & Imberge J. (2003). The Seasonal Evolution of Wind/Internal Wave Resonance in Lake Kineret. *Limnol. Oceanogr. 48*(5), 2055-2061.

Arifjaya N., Kusmana C., Abdulah K., Prasetyo L. (2012). Application of Tank Model for Predicting Water Balance and Flow Discharge Components of Cisadane Upper Catchment. *Jurnal Manajemen Hutan Tropika*, *17*(2), 63–70. https://doi.org/10.7226/jmht.17.2.63-70

Boon A., & Duineveld G. (1998). Chlorophyll-a as a marker for bioturbation and carbon flux in southern and central North Sea sediments. *Marine Ecology Progress Series*, *162*, 33–43. https://doi.org/10.3354/meps162033

Bulgakov N., & Levich, A. (1999). The nitrogen:phosphorus ratio as a factor regulating phytoplankton community structure. *Arch. Hydrobiol.*, *146*, 3–22.

Canfield D., Linda S., Hodgson L. (1985). Chlorophyll-Biomass-Nutrient Relationships for Natural Assemblages of Florida Phytoplankton. *JAWRA Journal of the American Water Resources Association*, *21*(3), 381–391. https://doi.org/10.1111/j.1752-1688.1985.tb00148.x

Clarke R. (1990). Statistical characteristics of some estimators of sediment and nutrient loadings. *Water Resources Research*, *26*(9), 2229–2233. https://doi.org/10.1029/WR026i009p02229

Chen Y., Qin B., Teubner K., Dokulil M. (2003). Long-term dynamics of phytoplankton assemblages: Microcystis-domination in Lake Taihu, a large shallow lake in China. *Journal of Plankton Research*, *25*(4), 445–453. https://doi.org/10.1093/plankt/25.4.445

Ding Y., Xu H., Deng J., Qin B., He Y. (2019). Impact of nutrient loading on phytoplankton: a mesocosm experiment in the eutrophic Lake Taihu, China. *Hydrobiologia*, *829*(1), 167–187. https://doi.org/10.1007/s10750-018-3830-6

Downing A., & McCauley E. (1992). The nitrogen:phosphorus relationship in lakes. *Limnol.Oceanogr.*, *37*, 237-252.

Elser J., & Hasset R. (1994). A stoichiometric analysis of zooplankton-phytoplankton interaction in marine and freshwater ecosystem. *Science*, *370*, 211-213.

Endoh S. (1978). Diagnostic analysis of water circulations in Lake Biwa. *Journal of the Oceanographical Society of Japan, 34*(6)*,* 250–260.

Endoh S. (1986). Diagnostic study on the vertical circulation and the maintenance mechanism of the cyclonic gyre in Lake Biwa. *J. Geophys. Res. 91*, 869–876.

Endoh S. & Okumura Y. (1993). Gyre system in Lake Biwa derived from recent current measurements. *Jpn. J. Limnol. 54*, 191–197.

Endoh S., Okumura Y., Okamoto I. (1995). Field Observation in the North Basin, 15–29. In Okuda, S., J. Imberger and M. Kumagai [eds.], Physical processes in a large lake: Lake Biwa, *Japan. American Geophysical Union*.

Ferguson R. I. (1986). River Loads Underestimated by Rating Curves. *Water Resources*, *22*(1), 74–76.

Filstrup C. T., & Downing J. A. (2017). Relationship of chlorophyll to phosphorus and nitrogen in nutrient-rich lakes. *Inland Waters*, *7*(4), 385–400.

Fujino Y. (1980). Water budget. “An introduction to Limnology of Lake Biwa” (ed. Mori, S.),. *Kyoto*, 19–26.

Galat D. L. (1990). Seasonal and long-term trends in truckee river nutrient concentrations and loadings to pyramid lake, nevada: a terminal saline lake. *Water Research*, *24*(8), 1031–1040. https://doi.org/10.1016/0043-1354(90)90126-Q

Goto N., Azumi H., Akatsuka T., Kihira M., Ishikawa M., Anbutsu K., Mitamura O. (2013). Highly efficient silica sink in monomictic lake biwa in Japan. *Annales de Limnologie*, *49*(2), 139–147. https://doi.org/10.1051/limn/2013045

Goto N., Iwata T., Akatsuka T., Ishikawa M., Kihira M., Azumi H., Anbutsu K., Mitamura O. (2007). Environmental factors which influence the sink of silica in the limnetic system of the large monomictic Lake Biwa and its watershed in Japan. *Biogeochemistry*, *84*(3), 285–295. https://doi.org/10.1007/s10533-007-9115-1

Grzetic I., & Camprag N. (2009). The evolution of the trophic state of the Palic Lake (Serbia). *Journal of Serbian chemical society*, *75*(5), 717-732

Gupta H. V., & Sorooshian S. (1998). Toward improved calibration of hydrologic models: Multiple and noncommensurable measures of information. *Water Resources Research*, *34*(4), 751–763.

Gupta H. V., Kling H., Yilmaz K. K., Martinez G. F. (2009). Decomposition of the mean squared error and NSE performance criteria: Implications for improving hydrological modelling. *Journal of Hydrology*, *377*(1–2), 80–91. https://doi.org/10.1016/j.jhydrol.2009.08.003

Harashima A., Kimoto T., Wakabayashi T., Toshiyasu T. (2006). Verification of the silica deficiency hypothesis based on biogeochemical trends in the aquatic continuum of Lake Biwa-Yodo River-Seto Inland Sea, Japan. *Ambio*, *35*(1), 36–42.

Hartmann J., Jansen N., Dürr H. H., Harashima A., Okubo K., Kempe S. (2010). Predicting riverine dissolved silica fluxes to coastal zones from a hyperactive region and analysis of their first-order controls. *International Journal of Earth Sciences*, *99*(1), 207–230.

Hayami Y., Fujiwara T., Kumagai M. (1996). Internal surge in Lake Biwa induced by strong winds of a typhoon. *Jpn. J. Limnol.*, *57*(4), 425-444.

Hellström T. (1996). An empirical study of nitrogen dynamics in lakes. *Water Environ Res*. *68*, 55–65.

Howarth R. W. (1988). Nutrient limitation of net primary production in marine ecosystems. *Ann. Rev. Ecol.*, *19*, 89–110.

Hsieh C. H., Ishikawa K., Sakai Y., Ishikawa T., Ichise S., Yamamoto Y., Kuo T.C., Park H. D., Yamamura N., Kumagai M. (2010). Phytoplankton community reorganization driven by eutrophication and warming in Lake Biwa. *Aquatic Sciences*, *72*(4), 467–483. https://doi.org/10.1007/s00027-010-0149-4

Hsieh C. H., Sakai Y., Ban S., Ishikawa K., Ishikawa T., Ichise S., Yamamura N., Kumagai M. (2011). Eutrophication and warming effects on long-term variation of zooplankton in Lake Biwa. *Biogeosciences*, *8*(5), 1383–1399. https://doi.org/10.5194/bg-8-1383-2011

Ichise S., Wakabayashi T., Fujiwara N., Mizushima K. Nomura K. (1999). Yearly change in predominant species of phytoplankton and water quality in Lake Biwa, *Water Waste*, *41*, 582-591. (in Japanese)

Ichise S., Wakabayashi T., Fujiwara N., Mizushima K., Ito M. (2001) Long-term changes of biomass of phytoplankton in Lake Biwa. 1978–2000 (in Japanese). *Rep Shiga Pref Inst Pub Health Environ Sci., 36*, 29–35.

Ichise S., Ikegaya H., Furuta S., Fujiwara N., Ikeda S., Kishimoto N., Nishimura O. (2013). Analysis of long-term variation of Phytoplankton Biovolume and Gelatinous Sheath Volume in Lake Biwa. *Japanese Journal of Water Treatment Biology*, *49*(2), 65–74.

Ishikawa K., Kumagai M., Nakano S., Nakahara H. (1999) Influence of Wind on the Horizontal Distribution of Bloom-forming Cyanobacteria in Akanoi Bay, Lake Biwa. *Japanese Journal of Limnology (Rikusuigaku Zasshi), 60*(4)*,* 531–538.

Ishikawa K., Kumagai M., Vincent W. F., Tsujimura S., Nakahara H. (2002). Transport and accumulation of bloom-forming cyanobacteria in a large, mid-latitude lake: The gyre-Microcystis hypothesis. *Limnology*, *3*(2), 87–96. https://doi.org/10.1007/s102010200010

Jeppensen E., Torben L., Stuart F., Kirsten C., Carolyn W. (2000). Trophic structure in the pelagial of 25 shallow New Zeand lake: changes along nutrients and fish gradients. *Journal of Plankton Research*, *22*(5), 951-968.

Kamitani T. (1988). Grain size distribution of muds and its depositional process in Lake Biwa. *J.Res. Gr. Clas. Sed. Japan*, *5*, 23-33. (in Japanese)

Kishimoto N., Ichise S., Suzuki K., Yamamoto C. (2013). Analysis of long-term variation in phytoplankton biovolume in the northern basin of Lake Biwa. *Limnology*, *14*(1), 117–128. https://doi.org/10.1007/s10201-012-0390-8

Kishimoto N., Yamamoto C., Suzuki K., Ichise S. (2015). Does a decrease in Chlorophyll-a concentration in Lake Biwa mean a decrease in primary productivity by Phytoplankton? *Journal of Water and Environment Technology*, *13*(1), 1–14.

Kowalczewska-Madura K., Dondajewska R., Gołdyn R., Kozak A., Messyasz B. (2018). Internal Phosphorus Loading from the Bottom Sediments of a Dimictic Lake During Its Sustainable Restoration. *Water, Air, and Soil Pollution*, *229*(8). https://doi.org/10.1007/s11270-018-3937-4

Kronvang B. & Bruhn A. J. (1996). Choice of sampling strategy and estimation method for calculating nitrogen and phosphorus transport in small lowland streams. *Hydrological processes. 10*(11),1483-1501.

Kuczyńska-Kippen N., Joniak T. (2010). Chlorophyll-a and physical-chemical features of small water bodies as indicators of land use in the Wielkopolska region (Western Poland). *Limnetica*, *29*(1), 163–170.

Kumagai M., Asada Y., Nakano S. (1998). Gyres measured by ADCP in Lake Biwa, 199–208. In J. Imberger [eds.], Physical processes in lakes and oceans. *American Geophysical Union.*

Kumagai M. (2008). Lake Biwa in the context of world lake problems. *SIL Proceedings, 1922-2010*, *30*(1), 1–15. https://doi.org/10.1080/03680770.2008.11902076

Kunimatsu T., & Kitamura G. (1981). Phosphorus balance of Lake Biwa. *Verb. Internat. Verein. Limnol.*, *21*, 539–544. https://doi.org/https://doi.org/10.1080/03680770.1980.11897038

Lemmin U., Mortimer C., Bäuerle E. (2005). Internal seiche dynamics in Lake Geneva. *Limnol. Oceanogr.*, *50*(1), 207–216.

Longley K., Huang W., Clark C., Johnson E. (2019). Effects of nutrient load from St. Jones River on water quality and eutrophication in Lake George, Florida. *Limnologica*, *77*, 125687.

Maeda H., Kawai A., Tilzer M. M. (1992). The water bloom of Cyanobacterial picoplankton in Lake Biwa, Japan. *Hydrobiologia*, *248*(2), 93–103. https://doi.org/10.1007/BF00006077

McCauley, E., Downing, J., Watson, S. (1989). Sigmoid Relationships between Nutrients and Chlorophyll among Lakes. *Canadian Journal of Fisheries and Aquatic Sciences*, *46*, 1171–1175. https://doi.org/10.1139/f89-152

Moriasi D. N., Arnold J. G., Liew M. W, Bingner R. L., Harmel R. D., Veith T. L. (2007). Model evaluation guidelines for systematic quantification of accuracy in watershed simulations. *The American Society of Agricultural and Biological Engineers*, *50*(3), 855–900.

Morii F., T., Matsumura-Inoue I., Tanaka Y. (1993). Relationship between the Water Quality of River Waters Flowing into Lake Biwa and the Geological Environment of the Riverheads. *Japanese Journal of Limnology (Rikusuigaku Zasshi)*, *54*(1), 3–10.

Nagata T. (1990). Contribution of Picoplankton to the Grazer Food Chain of Lake Biwa. *In Large Lakes: Ecological Structure and Function (M.M. Tilzer and C. Serruya Eds.)*, 526–539. https://doi.org/10.1007/978-3-642-84077-7_28

Nagare H., Somiya I., Fujii S., Morita M. (2001). Phosphorus mass-quantity change in Lake Biwa. *Water Science and Technology: Water Supply*, *1*(2), 49–56.

Nakanishi M., Nozaki K.,Kagami M, Kohmatsu Y. (2011). *Trans.Res.Inst.Oceanochem.*, *14*, 104-111.

Nishimura S., Okubo K., Morita H., Koskiaho J., Tattari S. (2014). Simplified approach to evaluate total external loading to Kojima Lake. SYKE-OU Project Report, Okayama University, Japan.

Okamoto I., Morikawa M. (1961). Water circulation in Lake Biwa-ko as deduced from the distribution of water density. *Jap. Jour. Limnol. (Rikusuigaku Zasshi)*, *22*(4),193-200. https://doi.org/10.3739/rikusui.22.193

Okubo A. (1978). Horizontal Dispersion and Critical Scales for Phytoplankton Patches. In *In: Steele J.H. (eds) Spatial Pattern in Plankton Communities* (21–42).

Okubo K., Muramoto Y., Onishi Y., Kumagai M. (1984). Laboratory Experiments on Thermally Induced Currents in Lake Biwa. *Bulletin of the Disaster Prevention Research Institute*, *34*(2), 19–54.

Okubo K., Koskiaho J., Ventela A., Huttula T. (2014). Total loading curves applied to Lake Pyhäjärvi. SYKE-OU Project Report, Okayama University, Japan.

Okubo K., Inoue E., Iwata T., Huu L.T. (2021). Inertial internal waves and thermal gyres in monomictic Lake Biwa. *Limnology and Oceanography*. (submitted)

Onodera S., Saito M., Ban S., Jin G., Tomozawa Y., Okuda N. (2018). Estimation of Lacustrine Groundwater Discharge (LGD) via two paths in Lake Biwa, Japan. *Japan Geoscience Union*.

Oonishi Y., & Imasato N. (1975). Study on the currents in Lake Biwa (II), *Jap. J. Oceanogr. 31*(2), 53–60.

Phuong H. T., Tien N. X., Chikamori H., Okubo K. (2018). A hydrological tank model assessing historical runoff variation in the Hieu River Basin. *Asian Journal of Water, Environment and Pollution*, *15*(1), 75–86. https://doi.org/10.3233/AJW-180008

Peters R. H. (1986). The role of prediction in limnology. *Limnology and Oceanography*, *31*(5), 1143–1159. https://doi.org/10.1192/bjp.111.479.1009-a

Pierson D. C., & Weyhenmeyer G. A. (1994). High resolution measurements of sediment resuspension above an accumulation bottom in a stratified lake. *Hydrobiologia*, *284*(1), 43–57. https://doi.org/10.1007/BF00005730

Quiros R. (1990b). Factors related to variance of residuals in chlorophyll - total phosphorus regressions in lakes and reservoirs of Argentina. *Hydrobiologia*, *200/201*, 343-355

Rabemanolontsoa H. & Saka S. (2012). Characterization of Lake Biwa macrophytes in their chemical composition. *Journal of the Japan Institute of Energy, 91*(7), 621-628.

Rolle L. K., Huang W., Clark C., Johnson E. (2019). Effects of nutrient load from St. Jones River on water quality and eutrophication in Lake George, Florida. *Limnologica*, *77*, 125687. https://doi.org/10.1016/j.limno.2019.125687

Sakai Y., Murase J., Sugimoto A., Okubo K., Nakayama E. (2002). Resuspension of bottom sediment by an internal wave in Lake Biwa. *Lakes and Reservoirs: Research and Management*, *7*(4), 339–344. https://doi.org/10.1046/j.1440-1770.2002.00200.x

Sakamoto M. (2011). Limnological responses to changes in the thermal mixing regime in Lake Biwa associated with global warming. *Aquatic Ecosystem Health and Management*, *14*(2), 214–218. https://doi.org/10.1080/14634988.2011.577717

Saijo Y. & Sakamoto M. (1970). Primary production and metabolism of lakes, 208-225. In Yukawa H. (ed.), *Profiles of Japanese Science and Scientists*, Kodansha Ltd., Tokyo

Salvia-Castellví M., Iffly J. F., Vander Borght P., Hoffmann L. (2005). Dissolved and particulate nutrient export from rural catchments: A case study from Luxembourg. *Science of the Total Environment*, *344*(1-3 SPEC. ISS.), 51–65. https://doi.org/10.1016/j.scitotenv.2005.02.005

Schoelynck J., Bal K., Backx H., Okruszko T., Meire P., Struyf E. (2010). Silica uptake in aquatic and wetland macrophytes: a strategic choice between silica, lignin and cellulose?. *The New phytologist*, *186*(2), 385–391. https://doi.org/10.1111/j.1469-8137.2009.03176.x

Serra T., Granata T., Colomer J., Stips A., Møhlenberg F., Casamitjana X. (2003). The role of advection and turbulent mixing in the vertical distribution of phytoplankton. *Estuarine, Coastal and Shelf Science*, *56*(1), 53–62. https://doi.org/10.1016/S0272-7714(02)00120-8

Shiga Prefecture. (2020). Environmental White Paper Material in Water quality monitoring. Data collection from 1980 to 2020.

Shimizu K., Imberger J., Kumagai M. (2007). Horizontal structure and excitation of primary motions in a strongly stratified lake.) *Limnol. Oceanography. 52*, 2641-2655.

Shrivastava A. (2014). Major Nutrients and Their Stoichiometry over 45 Years (May 1963-May 2008) at the Northern and Southern Basin of Lake Biwa, Japan. *World Journal of Environmental Engineering*, *2*(1), 6–11. https://doi.org/10.12691/wjee-2-1-2

Sohrin Y., Tateishi T., Mito S., Matsui M., Maeda H., Hattori A., Kawashima M., Hasegawa H. (1996). Nutrients of Lake Biwa in the unusually cool and hot summers of 1993 and 1994. *Lakes and Reservoirs: Research and Management*, *2*(1–2), 77–87.

Søndergaard M., & Jensen P. J.(2001). Retention and internal loading of phosphorus in shallow, eutrophic lakes. *Scientific World Journal*, *1*, 427–442.

Søndergaard M. (2007). Nutrient dynamics in lakes – with emphasis on phosphorus, sediment and lake restoration. *Doctor's dissertation (DSc).* Aarhus University, Denmark

Sugawara M., Watanabe E., Ozaki E. (1984). Tank model with snow component. In *The National Research Center for Disaster Prevention, Science and Technology Agency, Japan*.

Sugawara M. (1979). Automatic calibration of the tank model. *Hydrological Sciences Bulletin*, *24*(3), 375–388. https://doi.org/10.1080/02626667909491876

Taniguchi M., & Tase N. (1999). Nutrient discharge by groundwater and rivers into Lake Biwa, Japan. *IAHS-AISH Publication*, (257), 67–73.

Tezuka Y. (1986). Does the seston of Lake Biwa release dissolved inorganic nitrogen and phosphorus during aerobic decomposition?: Its implication for eutrophication. *Ecological Research*, *1*(3), 293–302. https://doi.org/10.1007/BF02348686

Tezuka, Y. (1992). Recent Trend in the Eutrophication of the North Basin of Lake Biwa. *Japanese Journal of Limnology (Rikusuigaku Zasshi)*, *53*(2), 139–144.

The Ministry of Land, Infrastructure, Transport and Tourism. (2020). Water information system-Observatory search from map. http://www1.river.go.jp/cgi-bin/SelectMapSite.exe. Last access: May 28, 2020.

Tilman D. (1982). Resource competition and community structure. *Princeton Univ Press, Princeton, NJ*.

Toda T. (2013). A history of research into the geostrophic gyres of Lake Biwa. *Japanese Journal of Limnology (Rikusuigaku Zasshi), 75*(1)*:35-48.*

Tsugeki N. K., Urabe J., Hayami Y., Kuwae M., Nakanishi M. (2010). Phytoplankton dynamics in Lake Biwa during the 20th century: Complex responses to climate variation and changes in nutrient status. *Journal of Paleolimnology*, *44*(1), 69–83. https://doi.org/10.1007/s10933-009-9386-8

Tsunogai U., Miyauchi T., Ohyama T., Komatsu D., Ito M., Nakagawa F. (2018). Quantifying nitrate dynamics in a mesotrophic lake using triple oxygen isotopes as tracers. *Limnol. Oceanogr. 63*, S458–S476

Tsurumaki M., & Kobayashi M. (1989). Interaction of Lake and groundwater case study of Lake Biwa. *Journal of Geography (Chigaku Zasshi)*, *98*(2), 139–163.

Ulén B. (1978). Seston and sediment in Lake Norrviken I. Seston composition and sedimentation. *Schweiz Z Hydrol. 40*, 262–286.

Yoshimizu C., Urabe J., Sugiyama M., Maruo M., Nakayama E., Nakanishi M. (2002). Carbon and phosphorus budgets in the pelagic area of Lake Biwa, the largest lake in Japan. *SIL Proceedings, 1922-2010*, *28*(3), 1409–1414.